Dissertation

"ULTRASOUND MEASUREMENT OF SUBCUTANEOUS ADIPOSE TISSUE THICKNESS: METHODICAL IMPROVEMENTS, INTRA-OBSERVER RELIABILITY IN OVERWEIGHT AND OBESE PERSONS, AND FAT PATTERNING ANALYSES"

submitted by

Mag. rer nat. / Bakk. rer nat.

Paul STÖRCHLE

for the Academic Degree of

Doctor of Medical Science

(Dr. scient. med.)

at the

Medical University of Graz

Institute of Biophysics

under the Supervision of

Univ.-Prof. Mag.rer.nat. Dr.phil. Wolfram MÜLLER

Ao.Univ.-Prof. Mag. Dr.rer.nat. Helmut AHAMMER

Assoz. Prof.in Priv.-Doz.in Mag.a Dr.in rer.nat. Sandra Johanna HOLASEK

2019

Statutory Declaration

"Declaration I hereby declare that this thesis is my own original work and that I have fully acknowledged by name all of those individuals and organisations that have contributed to the research for this thesis. Due acknowledgement has been made in the text to all other material used. Throughout this thesis and in all related publications I followed the "Standards of Good Scientific Practice and Ombuds Committee at the Medical University of Graz".

Date: 15.11.2019

Disclosures

Part of this thesis has been published in Störchle et al., 2017 "Standardised ultrasound measurement of subcutaneous fat patterning: high reliability and accuracy in groups ranging from lean to obese", Ultrasound in Medicine & Biology (1) DOI: http://dx.doi.org/10.1016/j.ultrasmedbio.2016.09.014, and in Störchle et al., 2018 "Measurement of mean subcutaneous fat thickness: eight standardised ultrasound sites compared to 216 randomly selected sites", Scientific Reports (2) DOI:10.1038/s41598-018-34213-0).

List of co-authors (in alphabetic order) and institutions:

Helmut Ahammer[1], Norbert Bachl[2], Sandra Holasek[3], Sonja Lackner[3], Sabrina Mörkl[4], Wolfram Müller[1], Alfred Fürhapter-Rieger[1], Marietta Sengeis[1]

[1]Medical University of Graz, Institute of Biophysics, Graz, Austria

[2]University of Vienna, Centre of Sports Science, Department of Sports and Physiological Performance, Vienna, Austria

[3]Medical University of Graz, Institute of Pathophysiology and Immunology, Graz, Austria

[4]Medical University of Graz, Department of Psychiatry and psychotherapeutic medicine, Graz, Austria

All co-authors have approved the use of the data of this publication in this thesis.

The original articles have been published in the journals Ultrasound in Medicine & Biology published by Elsevier, and Scientific Reports published by the Nature Publishing Group. According to the copyright agreements, the right to include the data in a thesis or dissertation retains by the author. Thus, the permission for reproduction of figures and tables has been obtained.

Acknowledgements

I would like to take this opportunity to thank the people who supported me during my studies.

First of all, I would like to thank my first supervisor and mentor Prof. Wolfram Müller for giving me the opportunity to be involved in this project, for continuously teaching me with remarkable commitment how to write scientific articles, and most importantly, for being available and giving me advice whenever needed.

Further, I would like to thank Prof. Norbert Bachl who sparked my passion for science and without whom I would never have made the decision to start the Ph.D.

I am grateful for my second supervisor Prof. Helmut Ahammer for his valuable comments and support during various manuscript preparations, particularly in statistical concerns.

I want to thank Alfred Fürhapter-Rieger for all his support in those years. No matter which requests I had, you helped me.

Special thank goes to Marietta Sengeis with whom I went through my studies together. You have introduced me into the field of anthropometry, enabled exciting collaborations, and always encouraged me. I could not imagine a better colleague.

I would like to express my gratitude to all co-authors of the articles related to this thesis and want to thank my colleagues of the AKA St. Pölten for their understanding and support.

I thank the Doctoral School for Lifestyle-Related Diseases (LIFEMED) and the Institute of Biophysics for financial support.

Of course, I have to thank my friends and companions, especially Gabriel Berkes, Martin Komar, and Jürgen Ratheyser, who literally forced me to graduate from university.

I want to thank my partner Elena Peischl, particularly for the intensive support during the last months. You have always managed to put a smile on my face.

Finally, all of this would not have been possible without the intense support of my family. Especially, I would like to thank my parents Rainer and Regina for encouraging me in all of my pursuits and inspiring me to follow my dreams. You believed in me, supported me emotionally as well as financially, and were always willing to listen to my problems. For that I am infinitely grateful.

Table of Contents

Abbreviations

E	Excluded; indicates that the fibrous structures embedded in the SAT are not included in the thickness value.
F	Thickness of embedded fibrous structures
I	Included; indicates that the fibrous structures are included
ROI	Region of interest
SAT	Subcutaneous adipose tissue
US	Ultrasound
BS	Body segments
S	Surface area
T	Total
V	Volume
HE	Head
NE	Neck
AT	Anterior trunk
PT	Posterior trunk
BU	Buttocks
AU	Upper arms
FA	Forearms
HA	Hands
TH	Thighs
LE	Legs
FE	Feet

Parameters and variables:

b	Biceps girth flexed and tensed, in m
g	Gluteal (hip) girth, in m
h	Stature, in m
m	Body mass, in kg
s	Sitting height, in m
t	Thigh girth at the site front thigh, in m
w	Waist girth, in m

d	SAT thickness at a given site, in mm (this is the average of the distances measured in the US image within the region of interest)
D	Sum of SAT-thicknesses at all eight sites in a given participant, in mm
ρ	Density kgm^{-3}
k	Calibration factor: k = k (D); $k= d_{M216}/d_{M8}$
f	Normalisation factor $f = 100/d_{M2160}$

BMI	Body mass index: $BMI=m/h^2$, in kgm^{-2}
C	Cormic index: s/h
MI_1	Mass index: $MI_1=0.53 \cdot m/(hs)$, in kgm^{-2}
W	Waist to height ratio W=w/h

Statistics:

M	Mean value
MD	Median
N	Number of values
SD	Standard deviation
SEE	Standard error of estimate

US Sites:

UA	Upper abdomen
LA	Lower abdomen
EO	External oblique
ES	Erector spinae
DT	Distal triceps
BR	Brachioradialis
LT	Lateral thigh
FT	Front thigh
MC	Medial calf

Groups used:

Skin patterning	N=100 (50 men and 50 women)
Mean SAT thickness	N=10 (all male)
Intra-observer	N=39 (26 men and 12 women)
Group 1 (G1)	N=19 (12 men, and 7 women) BMI ≤24.9 kgm^{-2}
Group 2 (G2)	N=19 (14 men, and 5 women) BMI ≥25 kgm^{-2}

Fat patterning, fibrous structures, and SAT correlations with anthropometric indices

	N=153 (82 men and 71 women)
Group 3	N=57 (men) BMI ≤24.9
Group 4	N=25 (men) BMI ≥25
Group 5	N=65 (women) BMI ≤24.9
Group 6	N=6 (women) BMI ≥25

List of Figures

List of tables

Zusammenfassung

Hintergrund: Die menschliche Körperkomposition ist eng mit der Gesundheit und der körperlichen Leistungsfähigkeit verbunden. Eine, vor kurzem entwickelte, standardisierte Ultraschalltechnik (US) stellt die genaueste und zuverlässigste Methode zur Messung des subkutanen Fetts (SAT) dar. Die Methode wurde bisher nur bei SportlerInnen und normalgewichtigen Personen getestet, jedoch nicht bei Gruppen mit Übergewicht bzw. Fettleibigkeit.

Ziele: (a) Optimierung der US: Anwendung bei übergewichtigen und adipösen Personen, Untersuchung der Hautdicken an den standardisierten Stellen, Vergleich der mittleren SAT-Dicken zwischen den acht und 216 Messstellen.

(b) Intra-Observer-Reliabilitätsuntersuchung mit einem breiten Spektrum von schlanken bis adipösen Personen.

(c) Untersuchung der Eigenschaften der Körperkomposition: Fettverteilung, Menge der eingebetteten Faserstrukturen, mögliche Korrelationen der SAT-Dicken mit ausgewählten anthropometrischen Parametern.

Methoden: 82 Männer und 71 Frauen mit einem BMI zwischen 17 und 40 kgm^{-2} und einem breiten Spektrum an SAT-Dicken wurden untersucht. Die eingesetzte Bildauswertesoftware ermöglichte halbautomatische Mehrfachdickenmessungen im SAT und die Quantifizierung der eingebetteten Faserstrukturen (Faszien). Die US enthält folgende Messstellen: Oberbauch (UA), Unterbauch (LA), Erector Spinae (ES), distaler Trizeps (DT), Brachioradialis (BR), lateraler Oberschenkel (LT), vorderer Oberschenkel (FT) und mediale Wade (MC). Die früher gemessene Stelle External Oblique (EO) wurde in dieser Dissertation durch die Stelle LT ersetzt. In einer Subgruppe von zehn Teilnehmern wurden SAT-Dickenmessungen an 216 randomisierten Stellen durchgeführt. Die Hautdicken wurden aus den zur Fettbestimmung aufgenommen Ultraschallbildern ausgewertet. Die Genauigkeit der US lag im Bereich von etwa 0,1 mm (bei 18 MHz Sondenfrequenz) bis etwa 0,3 mm (bei 6 MHz).

Ergebnisse: Die Stelle EO verursachte große Probleme bei übergewichtigen und adipösen Personen, weshalb die neue Stelle LT verwendet wurde. Die Hautdicken waren an allen Stellen, mit Ausnahme von ES, in der männlichen Gruppe signifikant höher als in der Weiblichen. Alle Hautstellen unterschieden sich signifikant voneinander ($p < 0.05$). Die Mittelwerte der acht Stellen überschätzten die Mittelwerte der 216 randomisierten Stellen,

da typische Fettdepotstellen überrepräsentiert darin vorkommen. Die mittlere Dicke der 216 Stellen ergab das 0,65-fache (SD 0.05) des Mittelwerts der acht Stellen (Mittelwerte der acht Stellen lagen zwischen 3 und 10 mm). Der Korrelationskoeffizient (ρ) der Intra-Observer-Studie betrug 0,999, der Standardfehler der Schätzung war 1,1 mm und 95% der Messungen lagen innerhalb von ± 2,2 mm. In der Subgruppe mit Summen der SAT-Dicken unter 77 mm lagen 95% der Messungen innerhalb von ± 1,4 mm. Mit Ausnahme von BR zeigten alle Stellen signifikante Unterschiede in der mittleren SAT-Dicke zwischen den Geschlechtern. Die SAT-Dickensummen unterschieden sich ebenfalls signifikant, wenn Männer (Median 40,3 mm) und Frauen (Median 76,0 mm) verglichen wurden. An den Stellen ES, DT, LT, FT, MC und in der Summe der acht Stellen (15% bzw. 9%) wurden signifikante geschlechtsspezifische Unterschiede in der Menge der Faserstrukturen festgestellt.

Conclusio: Eine hohe Reliabilität der US zur Bestimmung von SAT-Dicken kann von sehr schlanken bis zu adipösen Personen erwartet werden. Es wurde gezeigt, dass die Abweichungen bei der Fettschichtdickenmessung mit steigender SAT-Dicke zunehmen, die prozentualen Abweichungen (in Bezug auf die gegebene SAT-Dicke) jedoch abnehmen. Ein ausgeprägter Dimorphismus zwischen Männern und Frauen wurde für die folgenden Variablen gefunden: Summen der SAT-Dicken, Hautdicken, Menge der Faserstrukturen und in der Fettverteilung. Es ist daher von Bedeutung bei der Erstellung von Referenzdaten und bei der Suche nach Grenzwerten für medizinische Diagnosen zwischen den Geschlechtern zu differieren.

Abstract

Background: Body composition, health and physical performance are closely related. The most accurate and reliable method for measuring subcutaneous adipose tissue (SAT) thickness is the recently developed and standardised brightness mode ultrasound (US) technique; however, the application of this method has not been tested in overweight and obese people before.

The aims of this thesis were:

(a) to contribute to the methodical developments of the standardised US technique by testing the applicability of the method in overweight and obese persons, by investigating the skin thicknesses at the eight standardised sites, and by comparing mean SAT thicknesses of eight sites to means of 216 randomly distributed sites.

(b) to conduct intra-observer reliability tests in all groups from lean to obese.

(c) to analyse the participants' body composition characteristics in terms of fat patterning, amounts of fibrous structures embedded in the SAT, and correlations of SAT with anthropometric indices.

Methods: The 82 men and 71 women investigated covered a wide range of SAT thicknesses, and BMI ranged from 17 to 40 kgm^{-2}. The image evaluation software enabled semi-automatic multiple thickness measurements in SAT and quantification of the embedded fibrous structures (fasciae). US measurements were made in accordance with the standardised method at the eight sites: upper abdomen (UA), lower abdomen (LA), erector spinae (ES), distal triceps (DT), brachioradialis (BR), lateral thigh (LT), front thigh (FT) and medial calf (MC). The previously used site external oblique (EO) was replaced by LT. Additionally, in a subset of ten participants, SAT thickness measurements were performed at 216 randomly distributed sites. Skin thicknesses were also measured. Obtainable accuracy of US measurements ranged from about 0.1 mm (at 18 MHz probe frequency) to about 0.3 mm (at 6MHz).

Results: The site EO caused major problems in overweight and obese persons, therefore, the new site LT was introduced instead. Mean skin thicknesses were significantly higher in men compared to women at all sites, except for ES, and the thicknesses were also significantly different at all sites ($p<0.05$). The means from the eight sites (means of SAT thicknesses ranged from 3 to 10mm) overestimated the means obtained from 216 sites because typical

fat depot sites are overrepresented in the set of the eight sites. Within this range of SAT thicknesses, the 216-site mean was 0.65 (SD 0.05) times the mean of the eight sites.
The intra-observer study resulted in a correlation coefficient of ρ=0.999, the standard error of the estimate (SEE) was 1.1 mm, and 95% of measurements were within ±2.2 mm. In the subgroup with sums of SAT thicknesses below 77mm, 95% of measurements were within ±1.4mm. Except for BR, all sites showed significant differences in median SAT thicknesses between men and women. SAT thickness sums differed significantly when men (median 40.3mm) and women (median 76.0 mm) were compared. Significant sex differences in the amounts of fibrous structures were found at the individual sites ES, DT, LT, FT, MC, and also for the sums of the eight sites (15%, and 9%, respectively).

Conclusion: In a wide range of body fatness from extremely lean to obese, high reliability can be expected when using the standardised US method for measuring SAT. The thickness measurement deviations increased with increasing SAT thickness, but the percentages of deviations (with respect to the given SAT thickness) decreased. Pronounced dimorphisms between men and women was found for the following variables: sums of SAT thicknesses, skin thicknesses, amount of fibrous structures embedded in SAT, and in the fat patterning. Therefore, it is of predominant importance to distinguish between men and women when normative datasets are collected, and when searching for cut-off values for medical diagnoses.

Keywords: Body composition, Subcutaneous adipose tissue, Overweight, Obesity, Ultrasound measurement precision.

1. Introduction

1.1 Anthropometry, body composition and physical performance

Body composition is an important determinant of both health and physical fitness. Body mass or composition, size and shape are important to enhance performance in many sports (3). It is common practice to monitor anthropometry and body composition amongst athletes which provides insights into growth, diet and training adaptions which would otherwise not be available (4). The impact of physical morphology or physique varies across sports and competition levels. At elite level, specific and often extreme morphological characteristics are critical for success e.g. in professional bodybuilders or sumo wrestlers, whereas a wider range of morphologies are acceptable in other sports such as football, netball, softball etc. Often, this phenomenon can be explained by special positions in team sports such as a centre back versus a winger in football, or competition rules in weight category sports. In individual sports with diverse physique characteristics (e.g. golf, archery etc.), success can be connected more closely to skill or psychological attributes rather than anthropometric attributes (3).

Especially weight-sensitive sports are affected by extreme methods to reduce body mass rapidly or maintain a low body mass to gain competitive advantages (5). According to Ackland et al. (6), weight-sensitive sports, which are associated with low percentage of body fat, frequent mass fluctuation and eating disorders, can be summarised into three groups: gravitational sports, weight class sports, and aesthetic sports.

In gravitational sports, mass restricts performance due to mechanical and gravitational reasons. For example, in endurance sports body weight is carried over a distance and this results in a significant energy cost and increased heat production (3). Low body mass, a smaller stature and lean mass is a noticeable advantage as it minimises heat production (7) and reduces the energy cost of locomotion (8). Sports in which the power to weight ratio is important, as gravity has to be "overcome" (ski jumping, high jumping), are another example of gravitational sports.

In weight class sports, unhealthy body mass reductions can be observed, because of possible advantages gained when competing in a lower weight category (6). Reale et al. (9) and Wroble & Moxley (10) showed some evidence that heavier athletes are more successful within a specified weight category, but *this remains a contentious issue* and can vary

depending on the sport discipline and level of competition (3,10-13). Weight class sports are wrestling, judo, boxing, taekwondo, weight lifting, and light weight rowing.
In aesthetic sports higher scores are expected when the body shape matches a perceived ideal (6). Coaches and athletes know, *that failure to attain the right appearance will result in lower scores for artistic impression* (3). This concerns judged and particularly female sports of rhythmic and artistic gymnastics (14-16), diving (17), figure skating, and synchronised swimming (6). According to O´Connor & Catterson the desired physique can be dictated by social attractiveness more than athletic performance (18).

In biomechanical terms, body fat can be seen as ballast, but adipose tissue also functions as an endocrine organ and is important for health (5,6). Team doctors and other healthcare professionals are confronted with the difficult question of how to minimise health and performance risks for athletes (19,20). The popularity of rapid weight loss and dieting among athletes *seems to be as common and inappropriate today as it was many years ago* in weight-sensitive sports (20,21). Referring to Sundgot-Borgen et al. (20,22), up to 94% of elite athletes who compete in weight-sensitive sports, *report dieting and the use of extreme weight control measures* in order to accomplish their target weight prior to competitions. In all three groups of weight-sensitive sports (as described above), a high prevalence of *disordered eating and eating disorders* has been reported in female athletes. In male athletes, the highest values can be found in gravitational sports. For female athletes in aesthetic sports, the prevalence is estimated to be about 40% and in weight class sports approximately 30%. For male elite athletes the values are 18% in weight class sports and 24% in gravitational sports (20). Corresponding values in team sports are 5% in male and about 15% in female elite athletes and in technical sports 4% and 17%, respectively (23,24). Various methodological factors may explain the dispersion of the reported prevalence e.g. differently used definitions and assessment tools, different sport disciplines, and different examined athlete groups (performance level, age etc.). The reports show a higher prevalence in elite athletes than in athletes at a lower competitive level and the control group (20,23,25,26).

Overall, characteristics such as stature, skeletal lengths and breadth are not adaptable, but body mass, lean and fat mass are adaptable. According to Slater, O´Connor & Kerr (3), practitioners who work with athletes and want to change the morphology of the athletes, should always be motivated by performance improvements. They have to consider the influence of variance in physique traits on competitive success. On the one hand, it is

necessary to understand, that *physique is just one of an array of fitness traits* that can contribute to the success of athletes, and that the link between physique traits and competitive success should not be over emphasised. On the other hand, the routine monitoring of physique traits can offer insights into adaptions of training or dietary interventions. This allows the practitioner to create an individual database to make an informed opinion on what can be considered on morphological optimisation for the individual athlete within their respective sport (3).

1.2 Body composition and health

The World Health Organization (WHO) defines health as:"*...a state of complete physical, mental, and social wellbeing and not merely the absence of disease or infirmity"* (27). Health is an indispensable factor for growth, daily living, improved productivity and quality of life. The double burden of malnutrition, that includes both under- and over-nutrition, is a significant global health problem (28). The WHO reported the worldwide prevalence of obesity nearly doubled between 1980 and 2014. More than 1.9 billion adults are overweight, and more than half a billion of them are obese (29). In 2010, overweight and obesity were estimated to account for 3.4 million deaths per year and 93.6 million disability-adjusted life years (29,30). At the same time, eating disorders are increasingly recognised as an important cause of morbidity and mortality in young individuals (31). Malnutrition and eating disorders can cause underweight and body composition disturbances that may lead to severe diseases like anorexia nervosa, which is associated with alarming mental and physical implications and a high mortality rate (32-35). Data of Lackner et al. 2019 showed that body composition assessment in this group can be essential to choose treatment (36).

To optimise performance in physical activity, exercise, and sport settings maintenance of health is crucial. An increased risk of developing numerous health problems can be caused by a severely malnourished status (28). As described in chapter 1.1, this phenomenon is common especially among female athletes in weight-sensitive sports and is known as Female Athlete Triad (Triad). According to Mallinson and De Souza (37):" *Triad represents a syndrome of three interrelated conditions that originate from chronically inadequate energy intake to compensate for energy expenditure"*. This circumstance leads to insufficient stored energy to maintain physiological processes, which is known as *low energy availability*. Associated with low energy availability, physiological adaptions in turn contribute to menstrual cycle disturbances or Amenorrhoea. Further, bone health is affected by the synergistically working downstream effects of low energy availability and suppressed

oestrogen concentration, leading to low bone mineral density, compromised bone structure and microarchitecture, and a decrease in bone strength. Often poor bone health does not have obvious symptoms and develops silently, incomprehensibly to athletes. Highlighting the long-term health consequences of Triad, compromised bone health among female athletes raises the risk of fractures throughout the lifespan (37).

1.3 The development of a novel approach to measure body composition

The impact to develop a new body composition measurement approach, which is designed for applications in all persons or patients, came out of problems concerning body composition disturbances and low weight problems or rapid weight changes found in many sports. The starting point was ski jumping in which low weight and associated body composition problems caused severe health problems and several cases of anorexia nervosa (19,38-43). Within the framework of the International Olympic Committee (IOC) Award, for a project during the Olympic Winter Games 2002 in Salt Lake City, USA, a field study on low weight and body composition problems in sports was conducted by Wolfram Müller. This research led to changes of the ski jumping regulations for the health benefit of the athletes. The body mass index (BMI)-rule in ski jumping was introduced as well as an improved measure for the relative body weight termed mass index (MI) (40). It was during the course of this project that it became obvious that body composition assessment approaches which are applicable in the field are not as precise and accurate as necessary for investigations of athletes (19,20). This also holds true for many fields of medical diagnoses, particularly in diseases which are caused by eating disorders and/or underweight (6,19,20,34,35).

Based on the success in improving severe health problems in ski jumping, the International Ski Federation (FIS) has changed the ski jumping regulations, W. Müller was invited to join another IOC research group and to contribute to the Consensus Statement on *the Female Athlete Triad*. In a following step (2009), the IOC Medical Commission (Arne Ljundquist, President; Lars Engebretsen, Scientific Director; Patrick Schamasch, Medical Director) appointed W. Müller to coordinate and lead a Working Group on *Body Composition, Health, and Performance in Sports* (44). In accordance with the primary concern of the IOC Medical Commission, *the protection of the athlete's health must have precedence over all other perspectives* (44). Research projects in the field of Body Composition, Health and Performance were given prime importance and supported by the IOC Medical Commission in order to further develop this trans-disciplinary field of research, which is of high

importance for both sports practice and basic medical research. Most recently, a publication on *relative body weight and standardised ultrasound measurement of subcutaneous fat in athletes* has been published by this research group (45).

1.4 Considerations for physique assessment in athletes

Particularly in athletes, preliminary considerations must be done before measurements are taken. According to Slater, Shaw & Kerr (46), a range of factors have to be considered to select the most appropriate technique including technical issues of safety, validity, precision, and accuracy of measurement. Further, practical issues have to be considered such as availability, financial implications, portability, invasiveness, time effectiveness, and technical expertise necessary to conduct the procedures. The ability of body composition methods *to accommodate the unique physique trait characteristics of some athletes* also must be considered. For many reasons, special body types e.g. tall, broad, very muscular, or extremely low body fat levels, can be more challenging to assess. It is important to understand the variables of interest to be assessed and have an understanding of whether the assessment is an one-off measure, or a measure to track changes longitudinally, which most often occurs in athletic groups (4). Finally, when collecting data, the highest priority should always remain the physical and emotional well-being of the athlete (46).

1.5 Body Composition assessment methods

The assessment of human body composition has played an important role in various fields of medicine and over the past century a great number of techniques and equations have been proposed. But each method has its advantages as well as limitations. According to the Position Statement of the IOC Medical Commission Working Group on Body Composition, Health, and Performance (6), *there is no universally applicable criterion or "gold standard" methodology* to quantify body composition at the moment. To better deal with the wide variety of methods, Lohman, Milliken & Sardinha (47) categorised all methods by level of accuracy in estimating body fatness (see table 1).

Table 1: Body composition methods by level of percent fat accuracy.
Adapted with permission from T.H. Lohman, L.A. Milliken, and L.B. Sardinha, "Introduction to Body Composition and Assessment," in *ACSM's Body Composition Assessment*, edited by T.H. Lohman and L.A. Milliken for the American College of Sports Medicine (Champaign, IL: Human Kinetics, 2020), 2.

Level 1 Reference methods (1%-2%)	Level 2 Laboratory methods (2%-3%)	Level 3 Field methods (3%-4%)	Level 4 Field methods (5%-6%)
Multicomponent models	Dual-energy X-ray absorptiometry (DXA)	Skinfolds	Body mass index (BMI)
Magnetic resonance imaging (MRI)	Densitometrie: Water displacement densitometry, or air displacement plethysmography	Bioelectrical impedance analysis (BIA)	Body size indexes
Computed tomgraphy (CT)	Body water (Hydrometry)	Cirumferences	
Cadaver dissection	Ultrasound *		
	Three-dimensional scanning combined with US		

* Remark: Ultrasound is also applicable in the field. Concerning the accuracy, image resolution of today's B-mode US systems (probe frequencies 12- 18 MHz) for measuring thicknesses of SAT layers is app. 0.1 to 0.2 mm, and reliability was found to range from ± 1.1 mm to ± 1.2 in athletes, and from ± 2.2 to ± 2.9 in persons with larger fat amounts

The level 1 category includes the reference methods which are the most accurate. Level 2 contains the laboratory methods and the third and fourth levels the field methods, where the third level is more accurate than the fourth level (47). The different methods (reference, laboratory and field) are described in the following chapters (1.5.1 to 1.5.3). All categorised methods (see table 1) are introduced in this thesis, and at the end of each section a table summarises the characteristics.

It also has to be mentioned that within the molecular and anatomical approaches body composition methods can be further classified as direct, indirect or doubly indirect (6). Direct methods measure the specific/targeted aspect or process, e.g. cadaver dissection, total body water (TBW), isotope dilution, and neutron activation etc.(48). Indirect methods measure a surrogate parameter to estimate tissue or molecular composition. Doubly indirect methods use one indirect measure to predict another indirect measure (e.g. via regression equations). Using regression equations also means that these approaches are sample specific (6). According to Hawes and Martin (49) these categories can be classified as levels of validation.

1.5.1 Reference methods

Reference methods are the most accurate techniques for assessing body composition. They have often been employed as criterion method to validate other techniques. Reference methods presented in this thesis are multi-component models, medical imaging (magnetic

resonance imaging, MRI; computer tomography, CT), and cadaver dissection. As described in chapter 1.4 also in reference methods, considerations have to be made based on limited applicability for monitoring athletes. These limitations include feasibility (cadaver dissection), time and financial costs involved (MRI), a lack of published normative data (multi-component models), and unnecessary radiation exposure (CT). Also, sensitivity (acuteness) of some of the accepted reference methods is not completely clear (6). For a better understanding of body composition, the following part gives a brief description of human body composition analysis approaches and the different models (50-52).

Human body composition analysis approaches:

In 1992, Wang, Pierson & Heymsfield. (52) proposed a five-level model for organising body composition research (53).

Aragon et al. (48) summarised the work of Lee (53) in their review, regarding the five levels of human body composition and their assessment methods as follows: *"Each level has different components, eventually deemed compartments, and have undergone further organization to include two (2C), three (3C) and four (4C) compartments*".

This organisational structure is listed below, and additionally to these chemical (molecular) approaches, the anatomical 4C model (tissues) is added (6):

1. Atomic level: hydrogen, oxygen, nitrogen, carbon, sodium, potassium, chloride, phosphorus, calcium, magnesium, sulfur
2. Molecular level: Fat mass (FM), (TBW), total body protein, and bone mineral content are included in the 4C model. The 3C model contains either FM, TBW, and nonfat solids or an alternate model FM, bone mineral, and residual mass. In the 2C model FM and fat free mass (FFM) are included.
3. Cellular level: In the 3C model cells, extracellular fluids (ECF), and extracellular solids (ECS) are included. In the 4C model body cell mass, FM, ECF, and ECS are included.
4. Tissue-organ level: 4C model includes adipose tissue, skeletal tissue, muscle and connective tissue, and other (e.g. visceral organs)(6).
5. Whole body level: head, trunk and appendages.

Models of human body composition:

This part of the thesis is dedicated to the different models of human body composition. First, the simpler models with more assumptions are introduced followed by the more complex and accurate multicomponent models (several methods are involved) with viewer assumptions.

Two-component model

The two-component model (2C) estimates FM and FFM on the chemical level. FM includes all ether-extractable lipid in the body and FFM all other tissues (54). Methods using the 2C model are hydrodensitometry (under water weighing - UWW), air displacement plethysmographie (ADP/Bod Pod), body water, skinfold thickness, and bioelectrical impedance analysis (BIA). The 2C model operates under the assumption that water, protein, and mineral content of FFM are constant. E.g. when estimating body fatness via densitometry by UWW in adults it is usually assumed that the density of fat is 0.90 g/cm³, the density of FFM is 1.1 g/cm³ and that FFM contains 73.8% water, 19.4% protein, and 6.8% mineral (54). Using the hydrometry method, it is assumed that water makes up a constant fraction of the FFM (54-56). Although methods using the 2C model are reasonably accurate in most people, variability among individuals in the assumed parameters results in considerable errors in the assessment of body composition. (54,57). In some subgroups (children (58), diseased subjects (59), and athletes (60,61)), systematic errors exists as the makeup of the FFM is different than assumed. According to Bea et al. (54), in these groups different constants have to be used for accurate body composition assessment when using a 2C model.

Because of their relatively low cost, non-invasiveness, and ease of operation, 2C model-based methods are common in clinical practice, and sports settings and represent the most commonly used approach for adults (48).

Three-component model

The first of the multi-component models adds an additional estimate of some component of FFM like TBW (i.e., fat, water, residual), using tritium- or deuterium-labelled water dilution techniques (54). According to Ackland et al. (6), it is the most practical multi-component model and can estimate fatness within standard errors of estimate of 2.0-2.5%. The measured components are body weight, TBW, and body volume to get FM, TBW, and dry FFM (mineral and protein) (54). Specific hydration levels are assumed using this assessment of body composition (55). *It is still subject to confounding from inter-assessment differences in*

hydration, glycogen, and muscle creatine levels that can be significant in athletic groups *with distinct exercise and recovery cycles* (48,62,63). Additionally, other 3C model exist where other components of FFM are measured directly (54) (e.g. bone mineral content, FFM, and FM based on DXA).

Four-Component Model

The 4C model adds an estimate of mineral (i.e. fat, water, mineral, and residual) to the 3C model. Due to the comprehensiveness and accuracy, the 4C model is the state of the art method, to which all other models should be compared (48,64,65). But logistical challenges limit the method to occasional use in primary research (48). It determines the total body fat content measuring the hydration status (D_2O-diliution method), density (UWW or ADP), bone mineral density (DXA), and body mass (scale), (2).

The 4-component equation is always in the form of:

$$\text{Fat mass} = C_1\ \mathbf{BV}\text{-}C_2\ \mathbf{TBW}\text{+}C_3\ \mathbf{M}\text{-}C_4\ \mathbf{BM}$$

where components (C) 1 to 4 are body volume (BV), total body water (TBW), bone mineral (M) and body mass (BM) (6).

Five Component Model

Streat, Beddoe & Hill (66) tried to improve the 4C model by using a five-component model in which the body is conceived as consisting of water, protein, mineral, glycogen, and fat. In this model, neutron activation analysis (NAA) is used to measure total body protein (TBP) and tritium dilution is used to measure TBW. Total body mineral (TBM) and TBP are assessed by assuming a constant relationship to TBW: The FFM is the sum of the first four components. The difference of BM and FFM yield to the fat component. On the one hand, the advantage of this model compared to the ones described above is that TBP is measured directly. On the other hand, body mineral and glycogen are not directly measured (54).

Six-Component model

Heymsfield et al.(67) proposed a 6-component chemical model in the search of a more refined, definitive reference method. In this model, the body consists of water, protein, glycogen, osseous bone mineral, non-osseous bone mineral, and fat. Neutron activation methods are used to measure total body nitrogen, calcium, chloride, sodium, and carbon. Whole-body potassium-40 counting to measure total body potassium and tritium dilution method for assessing TBW are used. All components in the model are measured directly,

accounting for over 97.5% of body weight. Compared to the 4C and 5C model, the 6C model has the advantage that TBF is directly measured from total body carbon and not calculated (54). In the study of Heymsfield et al. (67) a high correlation between body weight and calculated body weight, and density and calculated density from the 6C model existed. Therefore, this approach seems to be very accurate. Wang et al. (68) used a slightly modified approach and compared the fat content from the 6C model with estimates from 16 other laboratory and field methods. The results showed very high agreement between the estimates of the 6C model and the estimates from the 3C and 4C models, which included measurement of TBW. When using a 3C model based on DXA or a 2C model based on UWW slightly less agreement was found. Bea et al. (54) consider the 6C model to be the most accurate method for measuring body composition in living humans, but access to the appropriate measurement techniques limits its applicability.

1.5.1.1 Multi-component models

Multi-component models are the best reference methods for estimation of total body fat (6,51,64,65,69). Their precision and accuracy are both in the order of 1–2% (6). Multi-component models measure TBF on the molecular level (which is not identical with total adipose tissue on the tissue-organ level). As described above there are 6-, 5-, 4-, and 3- multi-component models available for body-fat estimation (50,70). However, multi-component models require access to expensive and sophisticated technology and are time consuming. This often places them out of reach for practical applications in sport (6).

Table 2: Features of Multi-component models

Advantages	Limitations	Cautions and Assumptions
- Currently most appropriate reference method - Considers variability of water and bone mineral content and in this way invalidates the 2-component model	- Long analyses process (depending on the number of compartments from one to more than six hours) - Expensive technology - Lack of published normative data	- Bone mineral includes other mineral in other tissues - Constant proportion of protein to water - Constant densities of each component were assumed

Cited from Ackland et al. (6)

1.5.1.2 Medical imaging: magnetic resonance imaging and computed tomography

MRI and CT are imaging techniques which provide highly accurate measurements of human body composition at the tissue-organ level (52,71-73). Due to the high precision and validity of both methods, they are considered as reference methods (6,72). According to Heymsfield et al. (73), the techniques provide high image resolutions of body tissues (adipose tissue, connective tissue, vessels, skeletal muscle and organs) in the sagittal, coronal and axial anatomic planes.

MRI uses a strong magnetic field (1.5-3.0 TESLA) to align positively charged protons in the body´s tissues (72). A radio frequency system is used for signal generation and processing (6). The system sends a radio frequency wave which activates the protons and they absorb the wave until the pulse ceases at which time the protons release energy. Depending on the water content, different tissues contain different amounts of hydrogen. The properties of the protons (alignment, relaxation time and density) in different body tissues are determined. The data is digitised to provide a grey scale image which quantifies the different body tissues (72). Detailed information on MRI can be found in Runge et al. (74) or in Liang & Lauterbur (75).

MRI is on the one hand a safe and non-invasive method using magnetic fields. On the other hand, it is a very costly technique that requires powerful software for analysis involving setting thresholds for different tissues. The used software packages are not designed for quantifying tissue dimensions beyond the organ level (6). Ross showed that whole body scans are possible but take about 30 minutes in total, depending on the used machine and technique (76). Full body composition assessments by MRI are limited by the accuracy of measurement due to the pixel size of about 2x2 mm^2 commonly used for these scans. This problem especially affects measurements in lean athletes. Further, there are difficulties in the selection process of boundaries between tissue layers which limits sensitivity (6). To address some of these limitations, a new technique named quantitative magnetic resonance (QMR) has been developed. QMR measurements take from 0.5-3.0 minutes for a whole-body scan, but more validation work in humans is necessary (72).

The CT process measures the attenuation of X-rays through the tissues of the body and are shown as cross-sectional images. They are displayed by a two-dimensional map of pixels and given a numerical value. These numerical values are called Hounsfield Units (HU) related to the electron density. The HU ranges of different tissues (e.g. skeletal muscle, bone, visceral organs and brain) are known and represented by different shades. The shades range

from most dense (white, water) to least dense (black, air) (72,77). To get the tissue area, the pixels of known depth and the number by the width of the cross-sectional image are multiplied. This allows the creation of a three-dimensional image. Software's of CT-machines are able to automatically analyse the tissue type based on HUs and provide summary information (72). For further detailed information on CT the readers are referred to Heymsfield et al. (73), Silver et al.(78), and Prado & Heymsfield (79)

Due to an unjustifiable high radiation dose, full body composition assessment is not feasible (6). According to MacKenzie-Shalders (72) CT can ethically not be supported for individual or repeat body composition assessments. Especially the latter would be necessary for athletes.

All in all, the techniques are generally only used for athletes as part of a research project or for clinical purposes due to constraints in cost and availability (72).

Table 3: Features of MRI and CT

Advantages	Limitations	Cautions and Assumptions
- High accuracy and reproducibility - MRI is a safe method using magnetic fields - Clear compartmental tissue data (bone, subcutaneous, regional and visceral adipose tissue, connective tissue, vessels, skeletal muscle and organs)	- Expensive and long analysis procedure - Cannot accommodate large body size (e.g. BMI > 40) - High radiation exposure with CT - Slight movement can impact measurement and require a re-measurement - Missing reference ranges for body composition assessment	- MRI and CT are designed primarily for diagnostic use rather than quantifying tissue dimensions - Assumptions about tissue densities are necessary relating anatomical dimensions to tissue masses - For assessing deep fat depots more assumptions and vast computing power are required

Cited from Ackland et al. (6), Aragon et al. (48), Lee & Gallagher(53), and MacKenzie-Shalders (72)

1.5.1.3 Cadaver dissection

Cadaver dissection provides the best data on human body composition (80). Although body composition is popular, there are only a few dissection data (81). Despite the obvious limitations (time, costs, and ethical barriers) cadaver studies were important to test several assumptions related to body composition assessment (81-83). As individual analyses cannot

be utilized with the dissection method, practitioners have turned to other reference, laboratory and field methods to estimate body composition (6).

Table 4: Features of cadaver dissection

Advantages	Limitations	Cautions and Assumptions
- Can be used to validate other indirect methods	- Small number of cadavers and none were athletic - Limited range of structures - Tedious method - Body fluid gets lost - Cannot be used for individual analysis	- Due to the limited number of dissected specimens, these cannot be representative for the range of different body types and compositions, especially among athletes

Cited from Ackland et al. (6)

1.5.2 Laboratory Methods

Nowadays laboratory methods (particularly for the assessment of athletes) have a higher status in practice as the availability has increased, and the costs have dropped.

1.5.2.1 Dual Energy X-Ray Absorptiometry

About 30 years ago DXA was developed (84). It has been historically used to assess bone mineral content and density to diagnose osteoporosis and osteopenia and considered to be the reference method for such assessments (85-87). However, in recent years DXA has been used increasingly in the quantification of soft tissue. DXA allows whole body measurements of fat and lean mass and can be used to get information on regional body composition including visceral adipose tissue (87,88).

The DXA method uses filtered x-ray beams at two different photon energies. They were transmitted through the body which are attenuated differentially by bone, fat and lean tissue (6). In theory, to assess all three components, measurements of three different photon energies would be necessary. Therefore, the DXA technology can *only be used to estimate the fractional masses of two components in any one pixel* (87,89). In non-bone containing pixels, fat and bone mineral free lean can be measured and in bone containing pixels, bone mineral and soft tissue can be measured. In bone containing pixels the proportion of fat and bone mineral free lean is assumed to be the same as the neighbouring non-bone containing pixels (segment constancy is assumed). The software automatically integrates single pixel

data into a whole-body output (87,89). In a whole-body scan, this assumed ratio (fat to bone mineral free lean) in soft tissue is applied to upwards of one-third of pixels. Lands et al.(90) and Roubenoff et al. (91), showed that the identification of composition changes in regions of low bone-free pixels like thorax, arm or head are less reliable. At the moment, there are three different types of beam technologies in use: pencil-, fan-, and narrow-fan beams. Depending on the particular type that is used differences in scanning time, radiation exposure and potentially the accuracy of the estimates occur (87,92).

The radiation exposure to participants and technicians is one of the concerns with DXA. Although the dose from one whole-body scan is small, cumulative exposure from serial scanning as normally used in athletes could be significant (87,93,94). Ackland et al. (6) recommends using not more than four measurements per annum. This is firstly because of the cumulative radiation dose and secondly, due to the error of measurement. The error of measurement affects the ability to detect small changes in body composition over time.

DXA has been validated against the four-compartment model. While the data of Prior et al. (61) suggests a good agreement in healthy, young males and females, other studies came to the conclusion that DXA underestimates body fat (95), especially among leaner individuals (96,97). Stewart et al. (98) even described negative fat values on the torso in an athletic population. Possible reasons could be individual variation in fat free mass hydration (95) or differences in anterior-posterior tissue thickness (97). Further validation studies concluded that DXA can predict regional (99) and whole-body (100) skeletal muscle mass accurately.

Ackland et al. (6) summarised the DXA method in his review as follow: ”*DXA, though a reasonably precise whole-body method, is not reliable in producing accurate fat estimates of lean athletes, although its assessment of total and regional FFM is generally acceptable if total scanned mass equates to scale mass.*”

Table 5: Features of dual energy x-ray absorptiometry (DXA)

Advantages	Limitations	Cautions and Assumptions
- High accuracy and reproducibility - Whole body approach - Regional compartment analysis possible - Valid measure of visceral adipose tissue	- Small amount of radiation exposure - Not portable - Expensive equipment - Limited scan bed size (especially athletes)	- Soft tissue gets interpolated where bone is detected - Magnification errors and beam hardening are assumed to be insignificant

- Cost and time efficiency - Independent of hydration status - Non-intrusive - Gold standard for diagnosing osteopenia and osteoporosis	- Trained technician required - Different calculation algorithms are used from manufacturers and are not published - Accuracy differences in pencil- vs fan-beam - Cannot scan if pregnant - Lack of comprehensive normative data for athletes	- Estimation of fat mass is confounded by trunk thickness (error increases alongside degree of trunk thickness) - DXA may be unreliable for longitudinal studies of subjects who undergo major changes in glycogen or hydration status between measurements, when compared to 4 component model

Cited from Ackland et al. (6), Aragon et al. (48), and Slater, Nana & Kerr (87)

1.5.2.2 Densitometry

The term densitometry refers to the general method of determining body composition through body density (101). Body density is the body mass divided by the body volume. The mass is first determined via a calibrated scale. There are two ways to get the volume: hydrodensitometry (UWW) or air displacement plethysmography (ADP). Both methods are based on the 2-component model. As described in point 1.5 the 2C model estimates FM and FFM. Therefore, a constant density of each component is assumed and then relates the measured whole-body density to a percentage of body fat (6,56,102). The specific gravity of water is 1000 kg/m³. Lipid is the only constituent of the body which has a lower one, and *its buoyant force is opposed by all other, denser constituents* (6). According to Going, (101) the utility of this approach as a reference method is limited, as the variations in water and bone mineral content of the FFM among populations and individuals affect its density.

Traditionally, UWW has estimated total body volume via Archimedes' principle. ADP follows a similar approach, but the participants are placed in a sealed air capsule with two chambers instead under water. Previous attempts, using Boyles Law which states that the product of density (P) and volume (V) of the two chambers is equal ($P_1V_1 = P_2V_2$), had shown the principles of ADP (103). However, Gnaedinger et al.(104) and others (105) reported significant errors using this approach. The errors resulted by violating the isothermal requirements of Boyle's Law due to the introduction of a participant in the

measurement chamber (103). In 1995, the Bod Pod (Life Measurement Inc., Concord, CA, USA) was introduced. The system comprises a sealed measuring chamber and a reference chamber (beneath the seat) linked by a flexible airtight diaphragm, which is perturbed to induce small pressure changes between both chambers (6,103). Using Poisson´s Law, the Bod Pod measures the inverse pressure-volume relationship between the chambers (at a fixed temperature), to calculate the volume of the participant (6,103,105). In both measurement techniques, the estimation of residual lung volume is necessary and needs additional equipment and expertise (6). The Bod Pod offers the possibility to estimate the thoracic gas volume by its in-built pulmonary plethysmography device (103). Clothing is also an important factor. Swimwear is recommended, as errors occurred in test retest reliability wearing gym apparel (106).

The Bod Pod has been shown to be a reliable device for fat measurements across different body types, ages and ethnicities (107-111). The technical error of measurement for percent body fat is between 0.4 and 1.24% (112,113) and the coefficient of variation between 2.0 and 5.3% (107,110). ADP has been shown to underestimate fat mass when compared to MRI (114) , DXA (115), 3C (115) and 4C (116,117) methods. Differences in the percentage of body fat have been shown between sexes for UWW and ADP (118). Comparisons between UWW and ADP showed that ADP underestimated body fat in absolute terms by 8% in lean female athletes (119), underestimated TBF at lower fat values as well as overestimated TBF at higher fat values in male children (120), and mostly underestimated fat mass (average of 2%) due to a higher measured body density in male college football players (115).

Despite their popularity both techniques (UWW and ADP) adopt the 2C model and therefore assume density of FFM to be constant. In many groups of athletes, this assumption is violated. Hence, caution is necessary when interpreting body-fat results from these approaches (6).

Table 6: Features of densitometry

Advantages	Limitations	Cautions and Assumptions
UWW		
- Whole body approach - Simple calculation - Good test-retest reliability - Accurate in determining body density	- UWW requires considerable participant involvement (completely exhaled, submerged)	- UWW requires estimation of residual volume and other entrapped air spaces

- Many reference data are available (also for athletic populations)	- Errors in measurement of thoracic gas volume can confound the assessment of body composition - The density of FFM is assumed as constant, but can vary within age, sex, race and training status - Individual tissue components can not be deduced by the density - The method does not support strength trained individuals, children and people with osteoporosis	- UWW uses invalid assumptions regarding the density of fat-free tissue
ADP		
- High reliability for body fat percentage, body density and thoracic gas volume in adults - Non-invasive - Quick - Same-day test-retest reliability has been shown to be slightly better than UWW - ADP is easier to administer, more time efficient and requires less participant involvement and/or discomfort than hydrodensitometry	- Tends to underestimate FM compared to MRI, DXA, the 3C and the 4C model - Disease states can reduce accuracy - Errors can occur in reliability due to clothing, facial/body hair and exercise prior testing - Expensive - The method does not support strength trained individuals, children and people with osteoporosis	- Assumptions about the thermal air properties within the measurement chamber are made by ADP - Estimation of other entrapped air spaces are necessary using ADP. Therefore, invalid assumptions regarding the density of fat-free tissues are in use.

Cited from Ackland et al. (6), Aragon et al. (48), Going (101) Shaw & Kerr (103), and Davis et al. (121)

1.5.2.3 Hydrometry

Except in very obese people, water is the largest single component of the body comprising about 50-70% of body mass (6). The water content of different tissues varies. Water is mostly found in the fat-free body in a relatively constant amount of 70-80% (6,122). For adipose tissue different amounts of water content (10-20%) were found in the literature (123,124). Assuming a constant hydration (72-73%) TBW can be used to estimate both FM and FFM. Variations in hydration status is the main limitation of this approach related to athletes (6).

The doubly labelled water technique is a non-invasive technique to measure the rate of carbon dioxide production in participants over a period of 7-14 days. Doubly labelled water means water that contains higher concentrations of both deuterium (^{2}H) and oxygen-18 (^{18}O). They are stable and non-radioactive isotopes, which are naturally found in the human body, in water, and in other molecules which contain hydrogen and oxygen. Doubly labelled water is consumed by drinking. Timed samples of two body fluid samples from urine, blood or saliva are taken before (natural background level) and after consumption, allowing enough time for penetration of the isotope (122,125-127). The volume in which the isotope has been diluted can be calculated when the amount of isotope, the baseline, and equilibration concentrations are known (127).

Currently, deuterium is the most commonly used isotope for the measurement of TBW (6,122,125). According to Schoeller (127), oxygen-18 would have the advantage that its dilution space more closely approximates TBW, but it can only be measured adequately by isotope ratio mass spectrometry. Further, the costs of ^{18}O-labeled water are about 15 times higher than that of deuterium. Deuterium can be measured in two ways: infrared spectrometry and mass spectrometry. Mass spectrometry should be preferred as greater technical errors were found using the infrared approach (122).

The dose of the isotope that is being administered as well as the chosen analytical method are the depending factors for the precision of measuring TBW (127). The precision for the dilution method using mass spectrometry, particularly high-precision isotope ratio mass spectrometry is stated in the literature with 1-2% (122,127-130). According to Blew Sardinha & Milliken (122) the accuracy of dilution techniques to estimate TBW is excellent, but a bias in the estimation can occur if there is failure to reach equilibrium. As stated by Schoeller et al. (127) the accuracy of dilution techniques dependents on the estimate of nonaqueous exchange, corresponding to about 1%. In terms of body composition, the major source of error arises when using TBW to estimate FFM, as the use of 2C hydrometric models is necessary, which assume a constant hydration of 72.3% (122). The main limitation

of this method is the variation in hydration levels among participants particularly in athletes (water comprises about 74% of skeletal muscle (60)). According to Ackland et al. (6), body water can be used to determine fatness within 3% and when combined with body density, to within 2%.

All in all, TBW can be accurately and reliably measured but expenditure of time, cost, lack of availability and technical issues make it uncommon especially amongst athletic populations (122,125). The assessment of body fat is based on the 2C model and therefore, assumes a constant hydration. If a standardised protocol could be developed to manage the total water status to be constant between 72-73% 24h before the test, then TBW could become a reference method to estimate FM and FFM (122).

Table 7: Features of hydrometry

Advantages	Limitations	Cautions and Assumptions
- Whole body approach - Easy to administer - Minimal participant involvement - Urine, saliva or blood can be used to estimate the dilution	- Time consuming (~6h) - Expensive - The assessment is affected by a acute ingestion of a large bolus of fluid - Method do not support people with cardiac or kidney disease or those with oedema and other fluid retention problems	- The tracer is not metabolized and distributed homogeneously equally across all components - Invalid assumptions are used regarding the hydration of fat-free tissues

Cited from Ackland et al. (6), Blew Sardinha & Milliken (122), Rush (125), and Schoeller (127)

1.5.2.4 Three-Dimensional Scanning

Three-dimensional (3D) photonic scanning is used to measure surface anthropometry characteristics such as body volume, segment lengths, and girths in a time-saving way. Laser, light or infra-red technologies are used to acquire the shape. The most common devices use class 1 (eye safe) lasers or structured light projected onto the body surface. The position of the projected light is captured by multiple digital cameras (arranged in columns and measured from head-to-toe in a co-horizontal plane). A software reconstructs the body contour of the acquired image using a mathematical algorithm based on triangulation (131). Currently, there are only a few data of 3D anthropometry scanning for research purposes in health and sport science available (131,132). 3D scanning data have shown fundamental

differences between men and women in BMI-shape relationships (133), have investigated the effect of age in varying shape at a given body size (134), and have found out the contrasting shapes of different ethnicity with similar BMI levels (6,135). In 2006, Wang et al. (136) validated a 3D photonic scanner against UWW and tape measure for the measurement of body volumes, dimensions, and percentage body fat. The values obtained with a 3D scanner were significantly greater than those obtained by UWW for body volume, and then those obtained with a tape measure for circumferences. The values for percentage body fat were not significantly different between 3D scanner and UWW (136). Ryder and Ball (137) compared body fat percentage measured by DXA, Bod Pod and 3D scanning in 85 male participants and the results showed significant differences between the three methods.

On the one hand, the 3D scanning approach measures body volume with some accuracy but includes the same assumptions and limitations (constant density assumed, lung volume determination necessary) as the densitometry when estimating FM and FFM. On the other hand, the rapid profiling enables great numbers of participants to be measured within the limitations of time and cost. In future body composition research, the combination of 3D scanning with other methods like ultrasound or DXA could represent a major advance (6).

Table 8: Features of three-dimensional scanning

Advantages	Limitations	Cautions and Assumptions
- Minimum subject involvement - Rapid data acquisition (10-15 sec.)	- Clothing colours and textures can affect image quality - Hirsutism influences body volume - Method does not support strength trained individuals and other populations such as osteoporotic and children - Lack of data in athletic population (percentage fat)	- Clothing tightness does not influence the body´s profile - Overestimation of body volume due to hair or clothing - Uses invalid assumptions regarding the density of fat and fat free mass

Cited from Ackland et al. (6)

1.5.3 Field Methods

Many field techniques are in use to estimate body composition. They are used in sports as well as in health applications, but with varying degrees of validity (6). In this chapter, skinfolds, circumferences, bioelectrical impedance analysis (BIA), and different indexes of body size are covered.

1.5.3.1 Surface anthropometry

In 1921, Matiegka (138) introduced the *acquisition of surface dimensional measurements* as surrogate parameters of body composition. Many different approaches were developed and already in 1988 over 100 body-fat prediction equations had been developed from skinfold measurements (6,139). According to Lohman (6,139), the differences in sampled populations and lack of rigour in standardisation leaded to inconsistent outcomes. Therefore, *the Anthropometric Standardization reference Manuel (139)* was published. For the first time clinicians and researchers had a standardised set of anthropometric dimensions. In 1986, the International Society for the Advancement of Kinanthropometry (ISAK) was formed and established a carefully designed training and certification process for anthropometrists (140). In 2001, the first edition of the *International Standards for Anthropometric Assessment* (141) was published. To assess body size, shape and composition the ISAK protocols should be followed. For a restricted profile, this approach includes two basic measures, eight skinfolds, five girths, two breadths, and takes approximately 10 minutes. The full profile contains four basic measures, eight skinfolds thirteen girths, eight lengths and heights, nine breadths, and takes up to 30 minutes (142).

The skinfold approach assumes that a double layer of skin (fold) plus the underlying subcutaneous adipose tissue (SAT) are representative of overall body fatness, as over 50% to 70% of body fat is located subcutaneously (140). According to Brandon et al. (140) several skinfold thicknesses can be used to estimate total percent body fat with a SEE in the range of 3% to 4%. The methods are reliable and valid if ISAK training is undertaken (142) . Hume et al. (143), investigated the importance of accurate skinfold measurement site location using ISAK standardised sites. The study showed, that varying the site by as little as one centimetre produces significant differences in the majority of obtained values when experienced anthropometrists (ISAK Level 4) measure the same subject. No site was totally free from this variation. Therefore, it is essential to identify, mark and measure the defined sites correctly (142). Currently both, raw skinfold data and converted values to body density and

percent fat are in use (4). On the one hand Lohman (144) showed the well-established relationship of skinfolds to body fatness. On the other hand, a multitude of equations exist for predicting percent body fat and body density. Many of these equations have not been cross-validated or are sample specific (140). Sinning et al. (145,146) investigated the validity of generalised equations from Durnin and Womersley (147), Jackson and Pollock (148) and Lohman (144) for the use in male athletes and equations by Durnin and Womersley (147), Jackson, Pollock and Ward (149) for the use in female athletes. Of the 21 evaluated equations for male athletes only three had not significantly different values from UWW percentage of fat (146). In female athletes, only two equations were shown to be acceptable (145).

Data published by Kerr and Stewart (150) show that the average skinfold magnitude across sites assessed by qualified ISAK anthropometrists, is generally higher in females than in males and varies considerably by sport. In both, extreme obesity and extreme leanness, the sexual dimorphism becomes less apparent (fat patterning becomes similar) (6).

Circumferences also have been used to measure body fatness independently (SEEs 3% to 4%), or in combination with skinfolds to assess body composition (140). In the past decades, more than 17 circumferences have been used to calculate percent body fatness (abdomen, arm, waist, calf, and forearm are the most often used) (151-153). However, according to Thorland et al. (154) combining circumferences and skinfolds does not increase the body fat prediction compared to the skinfold approach alone. Skeletal breadths were also tested to estimate body fatness with a SEE of >4% and therefore offers no improvement over the skinfold approach (6). Waist circumference (WC) is often associated with abdominal adiposity. According to Brambilla (155), WC is a good predictor of visceral adipose tissue (VAT). However, Bouchard et al. (156) showed that WC is better correlated to TBF than to VAT and that body mass index, fat mass and WCs are equally correlated to VAT. Another approach to predict VAT are abdominal diameters. They have been associated as indicator for visceral fat (157) , metabolic syndrome (158), cardiovascular risk (159) and change of shape during weight loss (160). According to Ackland et al. (6), abdominal dimensions might not initially seem to be a strong candidate for the use in athletes, but it is possible that they could provide a framework for a normal anticipated shape, once normative data have been established.

On the one hand there is the advantage of a simple and highly portable field method with a big data pool available for comparisons of athlete measures for many sports. On the other hand, skinfold calipers compress the SAT and two times the skin resulting in variations of

the measurements. Skilled technicians and standardised equipment are needed for valid and reliable results (142).

Table 9: Features of surface anthropometry

Advantages	Limitations	Cautions and Assumptions
- Reliable values with trained technicians - Regional assessment possible - Many norm values available to compare - Legitimate for test -re-test on individuals - Low cost, easy data collection - Useful for monitoring fat changes in children because of their small body size and their fat stores are primarily subcutaneous	- Most skinfold calipers have an upper limit (45-60 mm). Therefore, the application is limited to moderately overweight and thin participants - Measurement reliability depends on the experience and skill level of the technician - Only samples the subcutaneous fat deposit - Can be intrusive for some individuals - Some sites are difficult to achieve - Standardisation of the method is essential - Numerous equations available and they are sample specific	- Consistent fat patterning - Fixed relationship of subcutaneous to internal fat - Constant skinfold compressibility - Constant ratio of skin to adipose tissue - Lipid fraction and water content of adipose tissue

Cited from Ackland et al. (6), Aragon et al. (48), Brandon et al. (140), and Hume et al. (142)

1.5.3.2 Bioelectrical impedance analysis

BIA uses the principle that the total volume of a conductor can be estimated from its length (L) and the resistance (R) to a single frequency electric current (L^2/R) and applied this approach to body composition (6). The method assumes that the human body consists of a series of cylinders which have equal resistivity to an electrical current that passes through

water-containing tissue (e.g. fat-free mass) and therefore, the current is distributed throughout the conductor uniformly (6,161,162). Once the current is measured, the used device calculates its impedance, resistance, and reactance (161). This is then converted into TBW, intracellular and extracellular water in the measurement results. Pre-programmed algorithms then estimate body composition via fat-free mass, fat mass and fluid distribution. BIA is a doubly indirect measurement and considered to be a safe, non-invasive and cost effective tool with instantaneous TBW results (161,163,164). Although, BIA is used widely to estimate body composition, its accuracy is limited in estimating body water and body fatness (162). As the conductivity of electrical current is related to body water, acute changes in hydration status (due to food or fluid ingestion or exercise) impact the results (161). Rodriguez-Sanchez and Galloway (165) showed an effect of exercise on body composition assessment due to hypo-hydration. Using BIA any fluid deficit resulted from exercise is identified as fat mass (161). Furthermore, as an effect of exercise, precision of BIA is influenced by increased cutaneous blood flow and skin electrolyte accumulation (166). Heiss et al. (167) showed significant differences in the percent body fat values after a one litre fluid load right before the measurements. Acute ingestion of fluid can overestimate fat mass by 3.2% (168). This shows the necessity of a standardised protocol in terms of fluid ingestion (169). Bosy-Westphal (170) showed that bioelectrical impedance consumer devices are inaccurate compared to whole body MRI and DXA. Another investigation of Lohman et al. (65) compared skinfolds and BIA measurements in wrestlers with a standardised measurement protocol. Both approaches predicted percentage of body fat from densitometry with a SEE of 3.5%. This shows the accuracy limits of these techniques, especially considering that the resulted SEE values are for a specific group, and not for mixed groups of athletes (6).

All in all, BIA is low in accuracy and reliability. Regional assessment is possible, but invalid. The method is athlete friendly and quick, but defined protocols have to be used due to the fluid dependence of the method (161). In general, BIA is capable of determining body composition of groups and monitoring changes within individuals over time (48). However, the use of this approach to make single measurements in individuals is not recommended (171).

Table 10: Features of bioelectrical impedance analysis

Advantages	Limitations	Cautions and Assumptions
- Economical - Safe (no radiation) - Quick - Minimum participant involvement - BIA is able of delineating TBW into intracellular and extracellular water and therefore allows an estimation of body cell mass	- Poor accuracy - Validity is population specific and influenced by sex, age, height, disease state, and race - Validity may be limited to healthy, young, euhydrated adults - Results affected by hydration status - Trunk is under-represented, and limbs are over-represented in value	- Assumes geometric similarity between individuals - Tissue resistivity is assumed to be similar between individuals - Input data (age, height, weight, athletic status) are responsible for high (up to 85%) of variance in the dependent variable - - Subject compliance to the testing prerequisites is assumed

Cited from Ackland et al. (6), Aragon et al. (48), Brandon et al. (140), and Kerr et al. (161)

1.5.3.3 Relative measurements (weight and height indexes)

The body mass index (BMI=m/h^2, m body mass; h body height) is widely used for distinguishing between underweight, overweight, and obesity. It is often used as a screening tool for interventions, but this approach is misleading because: (a) the BMI is only a rough measure for relative body weight (172) that does not considers the individual's sitting height, and (b) it is just a measure of ponderosity, but not of body composition, particularly not of body fat (5,6). This inability of BMI to assess adiposity has been reported by Nevill et al. (173).

When ponderosity is to be assessed, leg length or sitting height should also be measured (6). The mass index (MI) (19,41,174) is an extension of the BMI and *has the advantage of considering the individual´s sitting height*: MI = BMI $(\frac{\bar{C}}{C})^k$, with C being the Cormic index C = *s*/*h* (*s* = sitting height and *h* = height), and $\bar{C}$ with a value of 0.53, *which is a value in the middle of the Cormic index continuum*, *representing the "mean sitting height";* and k

weights the impact of the Cormic index (6). For k = 0 there is no consideration of the individual leg length, the MI_0 and the BMI are identic. For k = 2, the MI_2 is related to sitting height only, $MI_2 = 0.53^2\ m/s^2$. This measure ignores the contribution of the legs for assessing relative body mass (175). For a relative measure which considers both *s* and *h*, k = 1 should be chosen: $MI_1 = 0.53\ m/(hs)$.

Table 11: Features of weight and height indexes

Advantages	Limitations	Cautions and Assumptions
- High precision - Minimal subject participation - - Quick data acquisition	- High variability among individuals in fat content with the same BMI - Muscularity, proportions and frame size independently influence the BMI - - Diurnal variations to body height and body mass have to be considered	- Assumes constant fat-free mass to height proportions - Constant body segments are assumed - Weight changes are related solely to adiposity

Cited from Ackland et al. (6)

1.5.4 Ultrasound

Ultrasound (US) is a laboratory method, but also applicable in the field. The ability of US to measure fat thickness accurately was first investigated in the sixties of the last century (176,177). Since then, many studies have shown US to be an accurate and precise method to measure tissue thicknesses compared to more established laboratory techniques (178-184). But there were also studies concluding ultrasound to be less accurate and not better in assessing body fatness than commonly practiced field techniques, such as BIA or skinfold measurements (122,185-188) .

US imaging is based on the pulse-echo technique, whereby a probe/transducer comprises piezoelectric crystals which are producing high-frequency sound waves and transmits an ultrasound pulse through the skin (122). This pulse travels through the given tissue with the speed of sound (*c*). Conventional diagnostic US systems use a speed of sound of 1540 ms^{-1} to calculate the distance from the transducer to the boundary between two tissues (6). As

each tissue type (e.g. fat, muscle, bone) has a different density, it also has a specific resistance to the ultrasound beam passing through (acoustical impedance). Therefore, when the ultrasound beam crosses the interface between different tissues, the beam will reflect at different echo strengths. The detector converts these signals to images to provide depth and tissue-type information (122). To assess body composition, two different US modes are in use: amplitude mode (A-mode) and brightness mode (B-mode). US A-mode devices utilise a narrow beam to scan tissue borders, represented by a change in the amplitude of the signal (188). A validation study of Smith-Ryan et al. (188) showed high reliability, but questionable validity for A-mode ultrasound compared to a 3C model (>4% BF error). Wagner et al. (189) got similar results for women (5%) but only small mean differences between A-mode US and Bod Pod for men (1.5%). According to Ackland and Müller (190), several manufacturers distribute A-mode ultrasound equipment employing unknown algorithms to estimate subcutaneous adipose tissue (SAT). Serious errors can occur using A-mode devices, as fibrous structures embedded in the SAT cannot always be detected correctly (e.g. the automatic processing algorithm misleadingly perceives embedded fascia as muscle fascia).

In B-mode ultrasound, beams are sent sequentially into the tissue to create a two-dimensional image in which the brightness of the screen corresponds to the echo intensity in the plane of the scan (6). Due to diffraction and technically obtainable minimum pulse length, lateral and axial resolution is limited approximately to the wavelength used. Frequencies from 3 to 22 MHz are generally used in diagnostic US probes, which corresponds to a wavelength in soft tissue of 0.5–0.07 mm (6). B-mode ultrasound yields a clearer image of the SAT-layer compared to A-mode devices and provides real-time, two-dimensional images, where anatomical structures contained (e.g. fascia, blood vessels) in the SAT can be detected by the operator (122).

The ultrasound method to assess body composition is relatively simple but has been limited until recently by its lack of uniform guidelines (122). In the last view years, a standardised US method to measure SAT and embedded fibrous structures has been introduced (1,2,5,190-192). This approach developed by Müller et al. (192) offers image capture from any standard B-mode ultrasound device followed by a semi-automatic image analysis procedure and avoids tissue compression, which can lead to an error of up to 37% in SAT measurements (193). The method uses a newly developed software (191,192,194) to accurately detect the contour of the adipose layer. The procedure was shown to be highly correlated with vernier caliper measurements, using excised pig tissue (195). In this investigation, a linear probe (7.5 MHz) was used and positioned with its centre at a marked

position on the skin of the excised tissue. The US measurement was made without compression due to a thick layer of gel and the SAT was evaluated on the vicinity of the centre of the US image. SEE was 0.21 mm and the slope of the regression line was 0.98 using conventional speed of sound. The best fit for these data with a slope of 1.00 was found when using a lower sound speed of 1510 ms^{-1} in SAT (190,195). The technique was compared to skinfold thickness at the eight ISAK sites and found to be more accurate and reliable (194). During this study the authors discovered that several ISAK sites are not suited for US measurements. At these sites, complex structures surround the SAT and thickness changes in the SAT-layer can occur in the vicinity of the centre. To obtain maximum accuracy and reliability, a new set of sites and a standardised protocol for landmarking and the correct US measurement procedure were developed by Müller et al. (192), and are presented in the methods section of this thesis. The method was already applied in various groups including anorectic patients (36), overweight and obese (1) (results presented in this thesis), children (196,197), youth athletes (198), weight sensitive athletes (45), gymnasts and swimmers (192) , elite judokas (175), rowers (198), and endurance athletes (199). Results of intra- and inter-observer measurements (1,45,191,192,197) are summarised in the discussion section (table 38). US is a promising body composition assessment technique, whereby adipose tissue layer thickness can be measured *with an accuracy not reached by any other method* (1,4-6,191,192,194). At the moment, there is a lack in normative data to compare, but preliminary normative data for both athletes and the general population are available (190). According to Blew Sardinha & Milliken (122) US as a laboratory technique has the advantage over other medical techniques, such as DXA or CT. On the one hand, there is no ionising radiation, it's cheaper, the portability, and the speed of measurement are assets. On the other hand, this method still needs to be validated against a four-component model. If this proves to be valid, it would be both a laboratory method and a field method.

Table 12: Features of ultrasound

Advantages	Limitations	Cautions and Assumptions
- High accuracy and reliability - Applicable in the field - No tissue compression - Tissue thickness up to 300 mm measurable - Non-invasive (no radiation exposure) - Minimal subject involvement - Price - Many thickness measurements from a single image - Rapid data acquisition - Minimal subject involvement - Capable of measuring muscle and bone thickness - Standardised protocol available	- Skilled technician is required - Inherent confounders such as fascia and blood vessels can complicate the interpretation of the results - Only samples the subcutaneous fat deposit	- No image distortion - Correct sound speed chosen for the given tissue - Correct tissue layer detection

Cited from Ackland et al. (6), Aragon et al. (48)

Table 13 shows a summary of the most common physique assessment techniques used in medicine and sport science, the information they provide, and their strengths and weaknesses for the use amongst athletes.

Table 13: Summary of the most common physique assessment techniques available, and their features.

Adapted with permission from Slater G, Shaw G, and Kerr A, "Athlete Considerations For Physique Measurement" in *Best Practice Protocols For Physique Assessment in Sport*, edited by T.H. Lohman and L.A. Milliken. (Singapore, Springer, 2017), 55.

Technique; Commercial availability	Accuracy; Reliability	Regional assessment	Level of analysis; Approch; No. of components	Attributes measured	Time commitment; Minimum assessment frequency	Athlete friendly; Health risk	Skilled technician required
4-compartment methodoly; Hard to find	High; High	Not possible	D; Chemical; 4	FM, MM, RM, BM	Very slow ≈6 hr; 8 weeks	Somewhat; Medium	Yes
3-compartment methodology; Hard to find	High; High	Not possible	D; Chemical; 3	FM, NOL, BM	Slow ≈1 hr; 4 weeks	Somewhat; Low	Yes
MRI; Available	High; High	Possible	D; Anatomical; 4	Tissue thickness/ area/volume: Adipose, Bone, Muscle, Other	Medium up to 30 min; 8 weeks	Somewhat; Low	Yes
CT; Available	High; High	Possible	D; Anatomical; 4	= MRI	Quick <10 min; 8 weeks	Very; Medium	Yes
Dual energy X-ray absportiometry; Available	Medium; High	Possible and reliable	D; Chemical; 3	NOL, BM, FM	Quick <10 min; 8 weeks	Very; Medium	Yes
Bod Pod; Available	Medium; High	Not possible	I; Chemical; 2	FFM, FM, TBV	Quick <10 min; 4 weeks	Very; Low	Ideally
Deuterium dilution; Very hard to find	Medium; High	Not possible	D; Chemical; 2 *D; Chemical; 0*	FFM, FM *TBW*	Very slow ≈6 hr; 4 weeks	Somewhat; Low	Yes
3D Scanning; Available	Unknown	Possible	I; Chemical; 2 *D; Anatomical; 0*	FFM, FM, *TBV, SV*	Very quick <5 min; 4 weeks	Very; Low	Yes
Surface Anthropometry; Very available	Medium; High	Possible but not recommend ed	via equation: DI; Anatomical; 2 ∑ SF: I; Anatomical; 1	FM (via equation), ∑ SF	Moderately quick <15 min; 3 weeks	Very; Low	Yes
Bioelectrical impedance analysis/ spectroscopy; Very available	Low; Low	Possible but invalid	I; Chemical; 2	FFM, FM, TBW	Very quick <1 min; 4 weeks	Very; Low	Ideally
Ultrasound; Hard to find	High; Medium	Possible and reliable	D; Anatomical; 3 via equation: DI; Anatomical; 2	mm of fat, skin, muscle FM (via equation)	Quick; 4 weeks	Very; Low	Yes

BM = bone mineral content; D = direct; DI = doubly indirect; FFM = Fat free mass, FM = Fat mass; I = indirect MM = Muscle mass; NOL = non-osseous lean; RM = Residual mass; SV = Segmental volume; ∑SF = sum of skinfolds; TBV = Total body volume; TBW = Total body water.

1.6 Aims

Although the method has already been standardised, and accuracy of this ultrasound thickness measurement technique is only limited by biological reasons (not technically limited), and high inter- and intra- reliability has been found in athletes (45,192) and children (196,197), additional steps are necessary to increase the potential of this method. This doctoral thesis will contribute to the following three topics:

1.6.1 Methodical developments

1. Test of usability of the standardised sites in overweight and obese people

Müller et al. (192) introduced the eight standardised sites and suggested to use an optional site called lateral thigh (LT) in further applications of this novel method. The measurements of this thesis include the new site LT for the first time. High inter-tester-reliability was found in a small group of athletes before, but this has not been shown for the new site and for overweight and obese persons.

2. Comparison of skin thicknesses at the standardised sites between men and women

In other body composition methods (e.g. skinfolds), skin thickness is integrated in the SAT values, therefore, skin thicknesses are to be considered when US SAT measurements are compared to such methods. Additionally, the knowledge of typical skin thickness at the standardised measurement sites is important for detecting the SAT-skin-border correctly in cases when fibrous structures are in the vicinity or attached to the skin.

3. Assessment of mean subcutaneous adipose tissue thickness

Although the eight standardised US sites represent the trunk, the arms, and the legs, it needs further investigation whether these eight sites represent the mean value of SAT thickness.

1.6.2 Intra-observer reliability in overweight and obese persons

See point 1.6.1/1

1.6.3 Fat patterning, fibrous structures, and SAT correlations with anthropometric indices

1. Fat patterning differences between males and females in different groups of normal weight, overweight, and obese persons

Differences between sexes in fat patterning were already found in athletes, but preliminary data (200) indicated that these differences could vary in overweight and obese persons.

2. Quantification of the fibrous structures embedded in the SAT and a comparison between males and females in different groups of normal weight, overweight and obese persons

Previous studies primarily concerned on reliability and accuracy of this novel ultrasound method. Currently, there are only small sets of data of fibrous structures in the SAT available. The amount and the expression of these structures at different fat layer thicknesses are going to be investigated.

3. Comparison of the SAT sums ranging from 5.6 mm to 244.9 mm in this group, to their BMI, and MI_l

4. Comparison of different SAT values (*d*, *D*) to the waist to height-ratio

Waist to height ratio is a good predictor for years of life lost (201). The aim is to compare different SAT values to W/h ratio to investigate a possible surrogate parameter.

2 Material and Methods

As described above, this dissertation consists of three different examination parts embedded in the field of use of this novel ultrasound method:

1) Methodical developments (new site, skin patterning, assessment of total SAT volume and mass)
2) Intra-observer study
3) Assessment of various parameters of the US technique (fat patterning, embedded fibrous structures, SAT tissue and relative body weight)

As different study protocols and numbers of subjects were used to check the established hypotheses of the three parts, subchapters were built to simplify readability. Participants and study protocols were described together for each part in the subchapters 2.3.1 to 2.3.3.
First, the methods used in all parts are described:

2.1 Anthropometry

Anthropometric measurements were carried out according to the International Society for the Advancement of Kinanthropometry (ISAK)(202). Anthropometric parameters were body mass (*m*), body height (*h*), sitting height (*s*) and the circumferences of thigh (*t*), arm girth flexed and tensed (*b*), hip (*g*) and waist (*w*).
Body Mass: According to Sumner & Whitacre body mass exhibits diurnal variation of about one kg in children and two kg in adults (202,203). The most stable values can be obtained in the morning twelve hours after the food intake and after voiding. As it is not always possible to standardise the measurement time, the time of day when measurements were made, were recorded as recommended by Stewart et al (202). For the measurements the Soehnle 7320 and the Seca 700 scale were used.
Body height: It has to be considered that there is diurnal variation in stature (202). Participants are generally taller in the morning. According to the literature a loss of about 1% over the course of a day is common in stature (202,204,205) The stretch stature method can reduce the effect of this diurnal variation and was used as described in the ISAK manual. (202).

Sitting height: The person was sitting on a box or a table - like support such that the thighs are supported by the horizontal surface and the legs are hanging down without touching the floor. The person is to be motivated to stretch the vertebral column and to increase the upper

body length as much as possible. This maximum length between the supporting surface and the highest point of the head (with the head aligned such that the eyes look straight forward) is the correct sitting height value. It is important to always capture the maximum length.

Circumferences: Arm girth flexed and tensed, hip and waist girth were measured according to the ISAK manual (202). The thigh girth was measured perpendicular to the axis of the thigh at the site **front thigh** (ultrasound site marking)(192) with the foot on the support box (enabling 5 cm steps), the thigh in horizontal position, and the leg in vertical position.

Relative body weight: The body mass index (BMI=m/h^2), and the mass index MI_1=0,53m/(hs) were calculated. The MI_1 takes individual sitting height into account (6,19,40,41).

2.2 Standardised US sites for measurement of SAT patterning

All eight standardised sites described by Müller et al.(192) are relative to the size of the individual (no fixed distances). All sites were marked on the right side of the body, in a standing or sitting position, while all US measurements were made with the subjects lying in a supine, prone, or rotated position (192). Figure 1 shows the eight standardised sites for US measurements of SAT patterning. Table 14 summarises the modified site marking (according to the protocol of Müller et al. (192)). In the presented intra-observers study the site lateral thigh (LT) was used for the first time for SAT patterning analysis (1) . Table 14 also includes notes on how to take the US images at the individual sites, and further detailed instructions on the US measurement and evaluation procedure can be found in the appendix of Müller et al. (192).

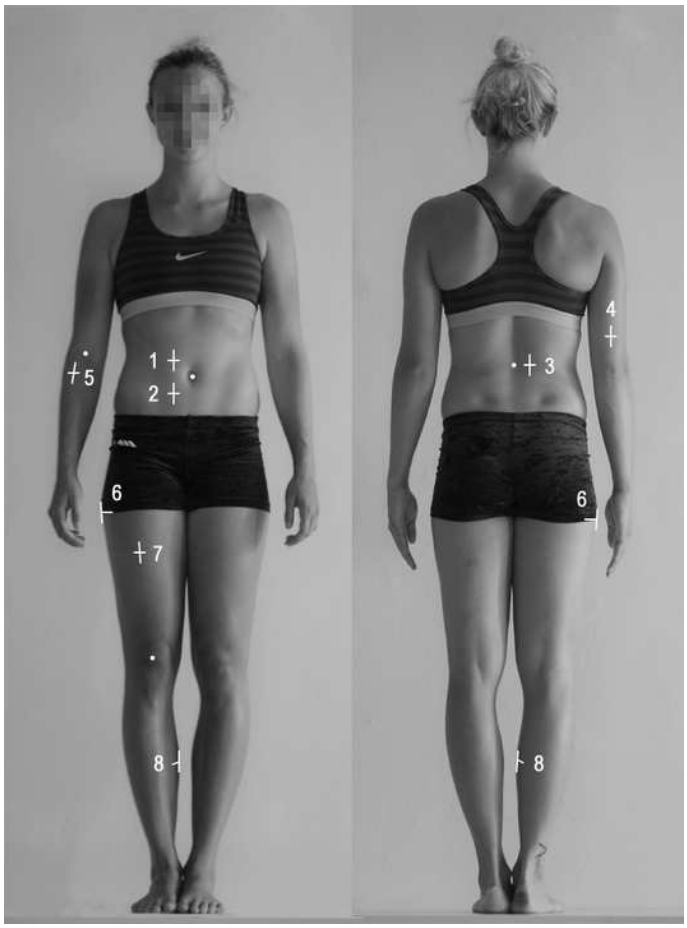

Figure 1: Sites for US measurement of SAT patterning
1: upper abdomen (UA), 2: lower abdomen (LA), 3: erector spinae (ES), 4: distal triceps (DT), 5: brachioradialis (BR), 6: lateral thigh (LT), 7: front thigh (FT), 8: medial calf (MC). Body height was used as the reference length for all distances.
Adapted from (Störchle P, Müller W, Sengeis M, Ahammer H, Fürhapter-Rieger A, Bachl N, et al. Standardized ultrasound measurement of subcutaneous fat patterning: high reliability and accuracy in groups ranging from lean to obese) with permission of publisher (Elsevier).

Table 14: Description of ultrasound sites and measurement procedure of Müller et al., 2016 (192):
Reproduced from [Subcutaneous fat patterning in athletes: selection of appropriate sites and standardisation of a novel ultrasound measurement technique: ad hoc working group on body composition, health and performance, under the auspices of the IOC Medical Commission, Müller W, Lohman TG, Stewart AD, et al., 50, 45-54, 2016] with permission from BMJ Publishing Group Ltd.

SITE NAME	DESCRIPTION OF THE SITES	NOTES ON US IMAGE CAPTURE
1 UA **Upper abdomen**	(1) Mark a vertical line at a distance **d=0.02 h** (ie, 2% of body height h) **lateral** to the centre of the umbilicus (omphalion) (2) Project vertically and mark a horizontal line at **d=0.02 h superior** to the **omphalion**. (In case this site is above a tendinous inscription of the rectus abdominis (where subcutaneous adipose tissue (SAT) is thicker), move the probe some mm to the end of this inscription and measure the thickness there)	Lying in a **supine** position Have the participant **stop breathing** at mid-tidal expiration and then capture the image
2 LA **Lower abdomen**	(1) The same line (1) as for the upper abdomen (2) Project vertically and mark a horizontal line at d=0.02 h **inferior** to the **omphalion**. Measure always exactly at this point	Lying in a **supine** position Have the participant **stop breathing** at mid-tidal expiration and then capture the image
EO **External oblique (optional site)**	(1) Locate and mark the anterior superior iliac spine (ASIS). (2) The participant assists by holding the end of the tape at the apex of the costal arch at the inferior margin of the sternum (where it meets the xiphoid process). The participant looks ahead!	Lying in a supine position Capture the image with the probe held in the direction of the **perpendicular** line
3 ES **Erector spinae**	(1) Mark a **transverse** line at **d=0.14 h** above the solid surface (table) on which the person is sitting in a stretched upper body position with thighs horizontal and legs unsupported (2) Mark the site at **d=0.02 h lateral** to the **spinous process of the vertebra**	Lying in **prone** position
4 DT **Distal triceps**	(1) Put the **lower** arm on a support surface (table) with the hand in the **mid-prone position**; mark a vertical line on the most posterior aspect of the arm. (2) Mark the site on the **vertical** line at a distance from the surface of **d=0.05 h**	Lying in a **prone** position Capture the image with the dorsal surface of the hand on the table. Make sure the **probe orientation** is **perpendicular** to the skin
5 BR **Brachio-radialis**	(1) The participant puts the forearm with the hand in the **mid-prone ('shake-hands') position** on a support table and contracts the brachioradialis (eg, against a resistance provided by the hand of the measurer). (2) Draw a **longitudinal** line on the most **anterior surface** of the **brachioradialis muscle** (3) Mark a **transverse** line at a distance **d=0.02 h** distally from the anterior surface of the **biceps brachii tendon** (press the end of the metre rod onto the stretched tendon). Project this line transversely to intersect with the longitudinal line.	Lying in a **supine** position Take the image with the arm in a mid-prone position and in contact with the thigh (muscles of the arm are relaxed) Avoid imaging the vein in case there is one in the vicinity
6 LT **Lateral Thigh**	(1) Draw a **horizontal** line on the lateral side of the thigh at the height of the **gluteal fold** (at the height of the fold at the **most dorsal** aspect of the thigh); (2) Mark the site on this line at the **midpoint** of the sagittal thigh diameter. Use a caliper for (1) and (2)	Lying in a **rotated** position Participant rolls onto the **left side** with both knees at a **90° angle**, with the right leg over the left leg

7 FT **Front thigh**	(1) Put the foot on the anthropometric box which is placed in front of a wall such that the thigh is horizontal and the big toe and the knee touch the wall. (2) Mark the site at a horizontal distance **d=0.14 h** from the wall.	Lying in **supine** position.
8 MC **Medial calf**	(1) Place the foot on the anthropometric box such that the thigh is horizontal and the leg vertical (2) Mark the site at **d=0.18 h** above the surface at the most medial aspect (use a ruler to determine the most medial aspect when looking vertically down.	Lying in a **rotated** position Participant rolls onto the **right side** with the right knee at a **90° angle** so that the lateral aspect of the right leg is supported

Ultrasound imaging of SAT (B-Mode):
The linear US transducer was placed above a given site without any pressure by using a thick layer of US gel between the probe and the skin to avoid compression of fat (typically, about 3 to 5mm). Conventional US systems can be used; investigations were performed using the ultrasound systems GE logiq-e, GE logiq C5 premium, and Philips CX50. Ultrasound probes with frequencies of 6 to 18 MHz were used (GE 12L-RS, 9 L-RS and Philips L12-3).

Semi-automatic thickness measurement:
US images were evaluated interactively using the FAT-software *NISOS-FAT* v 3.3, Rotosport (Rotosport.at). The software is designed for multiple semi-automatic evaluations of SAT layer thicknesses. A sound speed of 1540 ms^{-1} is used in conventional diagnostic US systems to calculate the distance from the transducer to the boundary between two tissues. According to Herman (206), sound speed was set to 1450 ms^{-1} for distance determinations in SAT (1,192).

Depending on the selected region of interest (ROI), the number of thickness measurements in each individual image was typically 50 to 300. As recommended in the standardised protocol (1,192) tissue segmentation was controlled visually and improved, if necessary, by changing the parameters that influence the automatic contour detection. The FAT-software also enables the operator to distinguish between distance values in which embedded structures (e.g. fibrous tissues or vessels) are included (I) or excluded (E). Excluded values corresponds to the pure fat thickness. Results are given as mean (mm), median (mm), standard deviation (mm), minimum (mm), maximum (mm), lines (numbers), and area (mm^2). Figure 2 shows an example of an evaluation of the site LT. As described by Müller et al.(192) the centre line corresponds to the centre of the transducer, which had to be held exactly above the site marking. The upper black layer corresponds to the thick layer of gel between the transducer and the skin. Below the gel, the skin (epidermis and dermis) form a light band. In this thesis the ROI was usually set symmetrically to the centre line to attain

high accuracy and reliability. The blue ellipses (seeds) were set as starting zones between the skin and the muscle fascia where the algorithm searches for the contours of SAT and measures multiple thicknesses automatically. The red areas represent the subcutaneous fat. It is interrupted by two white bands (fibrous structures). At the end of the evaluation process, a visual control was taken to make sure, that the algorithm detected the SAT layer correctly (1).

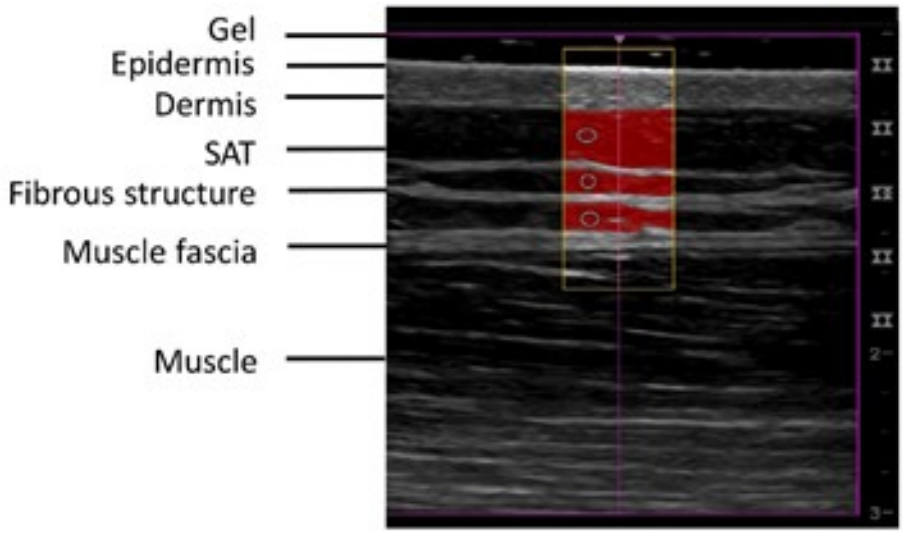

Figure 2: Example of an evaluated US image. (modified from Störchle et al., 2018 (2))
*The red area represents the SAT in the region of interest (ROI). Marked are: the thick layer of US gel (which prevents compression), the epidermis, dermis, SAT, embedded fibrous structure (FS), the fascia of the muscle, and the muscle underneath. In this example, the semi-automatic image evaluation software (USTissue-FAT) measured 92 thicknesses with a mean value of d_I 6.95mm, and d_E= 5.51mm. The d_I value **i**ncludes the thickness of the fibrous structures, d_E represents the pure fat (fibrous structures **e**xcluded).*
Adapted from (Störchle P, Müller W, Sengeis M, Lackner S, Holasek S, Fürhapter-Rieger A. Measurement of mean subcutaneous fat thickness: eight standardised ultrasound sites compared to 216 randomly selected sites) with permission of publisher (Nature Publishing Group).

2.3 Participants and study protocols

All investigations were approved by the ethics committee of the Medical University of Graz (20-295 es08/09). All participants got an information letter and completed a written consent form to use their data anonymously. As described at the beginning of the methods section, the different investigations were performed with different numbers of participants. A total sum of 153 participants were covered (82 men and 71 women). A wide range of SAT thicknesses were examined. BMI values between 17.3 to 40.3 kgm^{-2} were investigated.

2.3.1 Methodical developments

2.3.1.1 Skin patterning

To analyse skin patterning a group of 100 participants were investigated. Anthropometric data are shown in table 15. The age of the group was from 18 to 36 years and the BMI from 17.6 to 32.3 kgm^{-2}.

Table 15: Characteristics and anthropometric data of participants of the skin patterning investigation

Variable	N		*A*	*m*	*h*	*s*	*w*	*g*	*b*	*t*	BMI	MI_1	C	W
Unit			y	kg	m	m	mm	mm	mm	mm	kgm^{-2}	kgm^{-2}	1	1
All	100	Mean	23.8	69.0	1.748	0.921	0.734	0.957	0.311	0.513	22.4	22.5	0.53	0.42
		SD	3.1	12.8	0.101	0.050	0.081	0.053	0.035	0.041	2.6	2.6	0.01	0.04
		Median	23.5	66.4	1.734	0.920	0.728	0.956	0.307	0.511	22.2	22.4	0.53	0.42
		Min	18	47.6	1.538	0.816	0.587	0.859	0.245	0.434	17.6	17.3	0.50	0.35
		Max	36	112.1	2.010	1.060	1.025	1.144	0.393	0.626	32.3	32.5	0.56	0.58
Men	50	Mean	24.5	78.2	1.824	0.956	0.793	0.967	0.338	0.532	23.5	23.7	0.52	0.44
		SD	3.3	10.8	0.076	0.042	0.064	0.056	0.024	0.040	2.7	2.6	0.01	0.04
		Median	24.0	77.5	1.811	0.953	0.789	0.966	0.339	0.526	23.1	23.7	0.52	0.43
		Min	20	61.8	1.674	0.871	0.685	0.877	0.292	0.468	19.1	19.2	0.50	0.38
		Max	36	112.1	2.010	1.060	1.025	1.144	0.393	0.626	32.3	32.5	0.55	0.58
Women	50	Mean	23.1	59.8	1.673	0.886	0.674	0.946	0.285	0.495	21.4	21.4	0.53	0.40
		SD	2.7	6.5	0.058	0.029	0.045	0.048	0.021	0.032	2.0	2.0	0.01	0.03
		Median	22.0	59.1	1.671	0.885	0.673	0.947	0.285	0.494	21.4	21.2	0.52	0.40
		Min	18	47.6	1.538	0.816	0.587	0.859	0.245	0.434	17.6	17.3	0.50	0.35
		Max	29	77.5	1.876	0.979	0.754	1.074	0.342	0.583	27.2	27.2	0.55	0.46

A= age, *m*= Body mass, *h*= Body height, SD = Standard deviation, s= Sitting height, BMI = Body mass index, MI_1 = Mass index, C= Cormic index, W= Waist to height ratio, w = waist girth, g= gluteal girth, b = biceps girth flexed and tensed, t= thigh girth

To get a representative skin patterning at the eight standardised sites, people with different body types were chosen (D_I from 5.6 to 144.6 mm). Because of the age-related changes in skin thickness, young adults (< 40 years) were selected with a mean of 23.8 years. The ultrasound images were taken as usual for the SAT determination. Instead of the fat thickness, skin thickness was evaluated with the Fat software. An example is shown in Figure 3. Epidermis and dermis were measured together. The thin white band on top of the skin is the epidermis and underneath is the dermis. Corresponding results are shown in chapter 3.1.2.

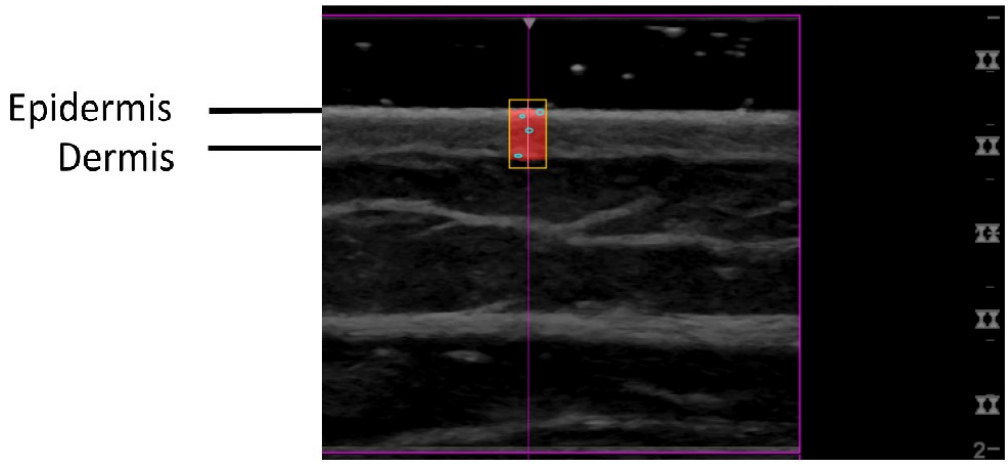

Figure 3: Example of an evaluated US image to determine skin thickness.
The red area represents the skin thickness in the region of interest (ROI).

2.3.1.2 Mean SAT thickness

For this investigation (published in Scientific Reports(2)), 50 young male participants with BMI values below 28.5 kgm^{-2} were investigated at the eight standardised US sites. Ten were selected out of this set, to cover a range of mean SAT thicknesses (from eight sites) from approximately 3 mm to 10mm (d_{IM8}). Ackland and Müller (190) published preliminary normative data for SAT ranges and this group represents the SAT categories "desirable range" (d_{IM8} from 2.5 to 7.5mm) and "noticeable ballast weight" (d_{IM8} from 7.5 to 12.5 mm) for men of the general public. For competitive male athletes, the desirable range is 2.5 to 3.8mm, noticeable ballast weight 3.8 to 6.3mm, and considerable ballast weight is above 6.3mm). For anthropometric data see table 16.

Table 16: Characteristics and anthropometric data of the participants of the mean SAT thickness study

	Unit	P1	P2	P3	P4	P5	P6	P7	P8	P9	P10	**M**	**SD**	**MD**	**MAX**	**MIN**
A	y	21	26	27	23	22	26	20	21	21	31	23.8	3.6	22.5	31	20
m	kg	66.0	64.6	71.6	95.1	72.4	62.5	96.2	85.6	84.1	92.7	79.1	13.2	78.3	96.2	62.5
h	m	1.816	1.749	1.813	1.919	1.674	1.751	1.840	1.941	1.903	1.853	1.826	0.084	1.828	1.941	1.674
s	m	0.940	0.947	0.964	1.060	0.892	0.911	1.065	1.014	0.982	1.017	0.979	0.059	0.973	1.065	0.892
w	m	0.831	0.716	0.745	0.773	0.735	0.776	0.883	0.830	0.728	0.693	0.771	0.060	0.759	0.883	0.693
g	m	0.980	0.898	0.924	0.936	0.910	0.941	1.044	1.055	0.899	0.887	0.947	0.060	0.93	1.055	0.887
b	m	0.337	0.298	0.300	0.345	0.300	0.325	0.367	0.363	0.329	0.334	0.330	0.025	0.332	0.367	0.298
t	m	0.524	0.469	0.464	0.499	0.468	0.510	0.602	0.526	0.494	0.483	0.504	0.041	0.497	0.602	0.464
BMI	kgm^{-2}	20.0	21.1	21.8	25.8	25.8	20.4	28.4	22.7	23.2	27.0	23.6	2.9	23.0	28.4	20.0
MI_1	kgm^{-2}	20.5	20.7	21.7	24.8	25.7	20.8	26.0	23.1	23.9	26.1	23.3	2.3	23.5	26.1	20.5
C	1	0.516	0.526	0.518	0.513	0.523	0.532	0.549	0.522	0.541	0.531	0.527	0.011	0.524	0.549	0.513
W	1	0.44	0.40	0.41	0.45	0.41	0.43	0.48	0.43	0.42	0.38	0.42	0.03	0.42	0.48	0.38

The group included young normal or slightly overweight males (BMI_{min} = 20.0 kgm^{-2}; BMI_{max} = 28.4 kgm^{-2}). The table shows the individual values, mean values (M), standard deviations (SD), median (MD), maximum (MAX), and minimum (MIN) values of the following personal data: A (age), m (body mass), h (body height), s (sitting height), w (waist girth), g (gluteal girth), b (biceps girth flexed and tensed), t (thigh girth). Additionally, the following indices are included: body mass index (BMI), mass index (MI_1), cormic index (C), and the waist to height ratio (W).

Reproduced from (Störchle P, Müller W, Sengeis M, Lackner S, Holasek S, Fürhapter-Rieger A. Measurement of mean subcutaneous fat thickness: eight standardised ultrasound sites compared to 216 randomly selected sites) with permission of publisher (Nature Publishing Group).

SAT was measured twice at eight standardised sites according to the above described protocol. In addition, SAT was also measured with the same US technique at 216 (two series of 108 measurements each) sites that were randomly distributed all over the body, as shown in Fig. 4a-c. The study procedure has been described in the publication of Störchle et al. (2) as follow (adapted to the correct figure numbers, table numbers and citations in this thesis): " *..Eleven body segments (Fig.4c) were covered with a number of sites proportional to their contribution to the total surface area. The body segments were chosen in accordance with the criteria of Lund and Browder(207), but without the segment "genitalia" (which was ignored here). The surface areas of the head, hand, and foot correspond to 7%, 5%, and 7% of the total surface area and should therefore be represented by 16, 12, and 16 measurements, respectively. However, it is extremely difficult to find such a high number of useful sites on hands and feet because of many vessels and complex anatomical structures there. Therefore, only half of the corresponding site numbers were measured, and these values were considered twice. As it is very inconvenient for the participant to measure 16 sites on the head, the same approach was used for the head too."* Corresponding results are presented in chapter 3.1.3.

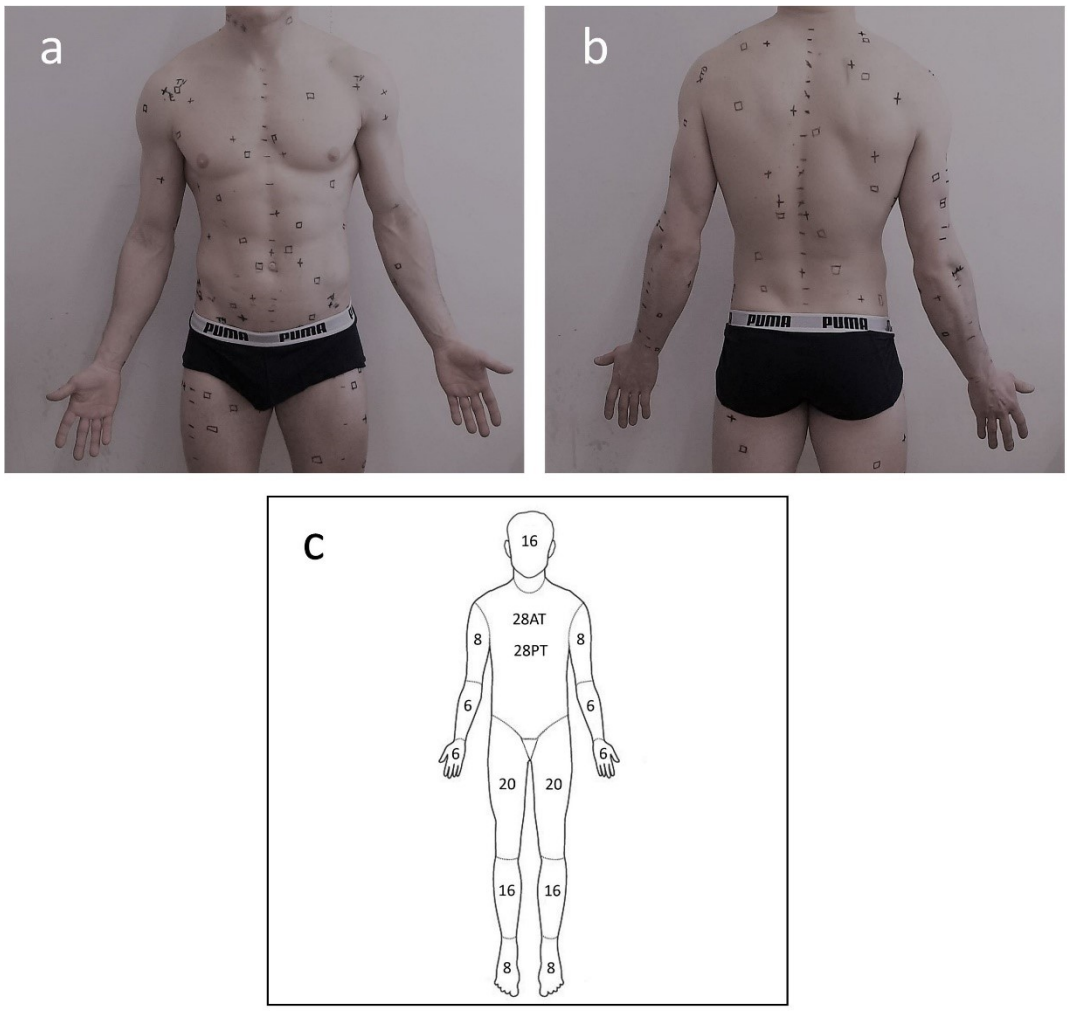

Figure 4: Ultrasound (US) measurement of mean subcutaneous adipose tissue (SAT)
(a) and (b): of exemplarily show randomly distributed measurement sites on the upper body of one of the ten participants. Crosses (+) belong to the first measurement series of 108 sites distributed all over the body, squares (□) to the second series. (c) Schematic drawing according to Lund and Browder (207) indicating the 12 body parts. The segment genitalia was ignored in our study. In order to obtain integer numbers also for subsets of 108 and 54 sites, the following numbers of sites on the individual body parts were used: head HE (7%, 16 sites), neck NE (2%, 4 sites), anterior trunk AT (13%, 28 sites), posterior trunk PT (13%, 28 sites), buttocks BU (5%, 12 sites), upper arms AU (8%, 16 sites), forearms FA (6%, 12 sites), hands HA (5%, 12 sites), thighs TH (19%, 40 sites), legs LE (14%, 32 sites), and feet FE (7%, 16 sites). Adapted from (Störchle P, Müller W, Sengeis M, Lackner S, Holasek S, Fürhapter-Rieger A. Measurement of mean subcutaneous fat thickness: eight standardised ultrasound sites compared to 216 randomly selected sites) with permission of publisher (Nature Publishing Group).

For the intra-observer study, published in Ultrasound in medicine and biology (1), 39 participants (26 men and 12 women) with a BMI from 18.6 to 40.3 kgm^{-2} were investigated. Two groups were observed by two observers. Characteristics of the participants are shown in table 17. During this study a new measurement site was introduced (see Results 3.1.1).

Table 17:Characteristics and anthropometric data of the participants of the intra-observer study

Variable	N		*A*	*m*	*h*	*s*	*w*	*g*	*b*	*t*	BMI	MI_1	C	W
Unit			y	kg	m	m	mm	mm	mm	mm	kgm^{-2}	kgm^{-2}	1	1
G1	19	Mean	32.5	68.7	1.754	0.927	0.738	0.955	0.309	0.567	22.2	22.3	0.53	0.42
		SD	8.3	10.4	0.079	0.037	0.078	0.035	0.036	0.043	1.9	2.1	0.01	0.03
		Median	30.0	69.6	1.775	0.918	0.757	0.964	0.310	0.569	21.8	22.7	0.53	0.42
		Min	23.0	51.2	1.619	0.864	0.615	0.891	0.249	0.511	18.6	18.2	0.50	0.37
		Max	55.0	83.0	1.885	0.981	0.866	1.014	0.362	0.619	24.9	26.3	0.55	0.47
G2	19	Mean	47.4	88.3	1.732	0.913	0.964	1.075	0.339	0.634	29.4	29.5	0.53	0.56
		SD	15.6	14.9	0.082	0.040	0.105	0.099	0.032	0.055	4.2	4.0	0.01	0.05
		Median	50.0	85.5	1.750	0.919	0.950	1.040	0.335	0.622	27.7	27.9	0.52	0.55
		Min	20.0	66.3	1.571	0.813	0.832	0.982	0.283	0.545	23.6	23.1	0.51	0.48
		Max	76.0	128.6	1.900	0.968	1.236	1.328	0.400	0.758	40.3	39.6	0.55	0.69
G1 + G2	38	Mean	39.9	78.5	1.743	0.920	0.851	1.015	0.327	0.618	25.8	25.9	0.53	0.49
		SD	14.5	16.2	0.080	0.039	0.146	0.095	0.036	0.059	4.9	4.8	0.01	0.08
		Median	36.5	77.8	1.755	0.919	0.834	0.992	0.331	0.607	25.1	25.5	0.53	0.48
		Min	20.0	51.2	1.571	0.813	0.615	0.891	0.249	0.511	18.6	18.2	0.50	0.37
		Max	76.0	128.6	1.900	0.981	1.236	1.328	0.400	0.758	40.3	39.6	0.55	0.69

A= age, m= Body mass, h= Body height, SD = Standard deviation, s= Sitting height, BMI = Body mass index, MI_1 = Mass index, C= Cormic index, W= Waist to height ratio, w = waist girth, g= gluteal girth, b = biceps girth flexed and tensed, t= thigh girth Adapted from (Störchle P, Müller W, Sengeis M, Ahammer H, Fürhapter-Rieger A, Bachl N, et al. Standardized ultrasound measurement of subcutaneous fat patterning: high reliability and accuracy in groups ranging from lean to obese) with permission of publisher (Elsevier).

The study protocol was described by Störchle et al. *(1)* as follow *"Group1 (G1, N=19) consisted of participants who were in the normal BMI range (18.5-25) kgm^{-2} (172); they were examined by observerI (OBI). Group2 (G2, N=19; observerII (OBII)) included the categories overweight (pre obese 25-30kgm^{-2}, N=13), obese class I (30-35kgm^{-2}, N=4), obese class II (35-40kgm^{-2}, N=1), and obese class III (>40 kgm^{-2}, N=1). The BMI ranged from 25.4 to 40.3kgm^{-2}. Three measurement series were performed in each participant on two separate days within a week. On day one, the anthropometric and the US SAT thickness measurements were conducted (measurement series M1). On the second measurement day, marking was done again before performing M2, and, after applying a new layer of gel, the third series M3 followed immediately (using the previous marking of M2)".* The corresponding results can be found in chapter 3.2.

2.3.3 Fat patterning, fibrous structures, and SAT correlations with anthropometric indices

The data of the several investigations were merged and resulted in 153 participants. Participants were assessed during a time span of three years from 2015 to 2018. A wide range from elite athletes to obese class III persons are included in the dataset. Characteristics of the participants are shown in table 18. Those were used to analyse fat patterning in different groups (corresponding results 3.3.1.), amount and differences of embedded fibrous

structures (point 3.3.2), the correlations of SAT thickness sums and relative body weight (3.3.3), and to compare SAT tissue thickness sum with the weight to height ratio (3.3.4).

Table 18: Characteristics and anthropometric data of all participants

Variable	N		*A*	*m*	*h*	*s*	*w*	*g*	*b*	*t*	BMI	MI_1	C	W
Unit			y	kg	m	m	mm	mm	mm	mm	kgm^{-2}	kgm^{-2}	1	1
All	153	Mean	27.8	70.9	1.745	0.922	0.829	1.005	0.322	0.497	23.1	23.2	0.53	0.44
		SD	10.4	14.4	0.095	0.048	0.150	0.095	0.039	0.054	3.6	3.6	0.01	0.06
		Median	24.0	68.7	1.739	0.919	0.825	0.987	0.325	0.501	22.5	22.7	0.5	0.4
		Min	18	42.2	1.538	0.813	0.586	0.840	0.241	0.414	17.3	17.2	0.50	0.35
		Max	76	128.6	2.010	1.065	1.236	1.328	0.400	0.626	40.3	39.6	0.58	0.69
Men	82	Mean	28.9	79.6	1.810	0.951	0.882	1.005	0.336	0.539	24.3	24.5	0.53	0.46
		SD	9.9	12.4	0.070	0.039	0.127	0.089	0.031	0.051	3.6	3.5	0.01	0.06
		Median	25.5	78.7	1.800	0.947	0.842	0.988	0.333	0.539	23.7	24.0	0.52	0.44
		Min	19	57.3	1.674	0.871	0.693	0.887	0.283	0.462	18.6	18.6	0.50	0.38
		Max	60	128.6	2.010	1.065	1.236	1.328	0.400	0.626	40.3	39.6	0.58	0.69
Women	71	Mean	26.6	60.9	1.671	0.887	0.735	1.003	0.295	0.487	21.8	21.8	0.53	0.41
		SD	10.8	8.9	0.058	0.032	0.143	0.107	0.039	0.057	3.3	3.2	0.01	0.05
		Median	24.0	59.8	1.671	0.885	0.670	0.987	0.285	0.491	21.3	21.0	0.5	0.4
		Min	18	42.2	1.538	0.813	0.586	0.840	0.241	0.414	17.3	17.2	0.51	0.35
		Max	76	96.7	1.876	0.979	1.057	1.261	0.366	0.551	37.2	36.2	0.56	0.63

A= age, *m*= Body mass, *h*= Body height, SD = Standard deviation, *s*= Sitting height, BMI = Body mass index, MI_1 = Mass index, C= Cormic index, W= Waist to height ratio, *w* = waist girth, *g*= gluteal girth, *b* = biceps girth flexed and tensed, *t*= thigh girth

2.4 Statistical analysis

SPSS Statistics Version 25 software was used. For a group smaller than 50 persons Shapiro-Wilk test was used to determine normal distribution. For groups ≥50 persons, Kolmogorov-Smirnov test was used.

Skin thickness differences were compared using repeated-measures analysis of variance (ANOVA). Mauchly´s test for sphericity was used and the Greenhouse-Geisser correction was applied. Bonferroni's post hoc test was used to assess the differences between each site. Differences between men and women in skin patterning were tested using the T-Test for two independent samples. Levene-Test was used to assess the equality of variances.

Statistical analysis included the standard errors of the estimate (SEE), linear regressions including coefficients of determination R^2, and limit of agreement (LOA)(208).

Differences between not normally distributed data were tested with the Mann-Whitney-U-Test. Spearman´s ρ was used to determine correlations. Boxplots were used to sketch the distributions of measurement differences.

3. Results – Findings

3.1 Methodical developments

3.1.1 Usage of a new measurement site: lateral thigh (LT)

The investigation of a group of male and female participants with SAT thickness sums (D_I) ranging from 12.46 to 244.8mm showed that SAT measurements of the previously measured site external oblique (EO) caused major problems in several cases: in overweight and obese persons, the skin and SAT built a large fold at this site which prohibited reliable and accurate marking. Therefore, the site EO is replaced by LT. It turned out that the site LT which was used for the first time in our research approach showed significant differences between females and males (see section 3.3.1 fat patterning in males and females).

3.1.2 Ultrasound measurements of skin patterning

Cutis and subcutaneous tissue are easily distinguishable when using B-mode ultrasound imaging (see figure 3). ANOVA showed significant differences between all skin thicknesses ($p< 0.05$). Skin thicknesses in this group ranged from a minimum of 0.92 mm at the site BR up to 3.85 mm at the site ES. The mean skin thicknesses obtained from 100 participants are shown in figure 5, and the corresponding values in table 19. Mean skin thicknesses were 1.95 mm for all participants, 2.05 mm for males and 1.86 mm for females. ES was with a mean of 2.72 mm the site with the highest and BR with 1.48 mm the site with the lowest values of skin thickness. Skin thicknesses are normally distributed. Differences between males and females are illustrated in figure 6. At all sites the mean skin thicknesses were higher in male participants (UA 6%, LA 5.4%, ES 5.6%, DT 20.45%, BR 15%, LT 9.7%, FT 15.8%, MC 13.8%). Significant differences between men and women were found for all sites except ES, using the T-Test. Normal distribution was tested using the Kolmogorov-Smirnov test. Figure 7 shows a positive correlation (209) between BMI and the sum of the eight skin thicknesses ($R^2= 0.171$ $p<0.05$).

Table 19: Measurement of mean skin thicknesses at the standardised eight sites

	N	Skin thickness	UA	LA	ES	DT	BR	LT	FT	MC	Mean
All	100	Mean	2.33	2.21	2.72	1.66	1.48	1.92	1.74	1.56	1.95
		SD	0.3	0.31	0.43	0.26	0.22	0.26	0.24	0.21	0.28
		Median	2.34	2.21	2.7	1.59	1.44	1.9	1.72	1.54	
		Min	1.65	1.37	1.93	1.18	0.92	1.37	1.15	1.16	
		Max	3.15	3.12	3.85	2.72	2.09	2.45	2.33	2.31	
Men	50	Mean Male	2.4	2.27	2.8	1.81	1.58	2.	1.87	1.66	2.05
		SD Male	0.31	0.29	0.4	0.25	0.19	0.23	0.22	0.21	0.26
		Median	2.4	2.29	2.81	1.78	1.59	2.02	1.89	1.63	
		Min	1.67	1.37	2.	1.46	1.29	1.39	1.45	1.35	
		Max	3.15	3.	3.85	2.72	2.09	2.45	2.33	2.31	
Women	50	Mean Female	2.27	2.16	2.65	1.51	1.37	1.83	1.61	1.46	1.86
		SD Female	0.28	0.31	0.44	0.16	0.2	0.26	0.18	0.17	0.25
		Median	2.21	2.1	2.64	1.5	1.34	1.78	1.64	1.43	
		Min	1.65	1.55	1.93	1.18	0.92	1.37	1.15	1.16	
		Max	3.01	3.12	3.8	1.83	1.84	2.43	1.93	1.85	

Upper abdomen (UA), lower abdomen (LA), erector spinae (ES), distal triceps (DT), brachioradialis (BR), lateral thigh (LT), front thigh (FT), medial calf (MC).

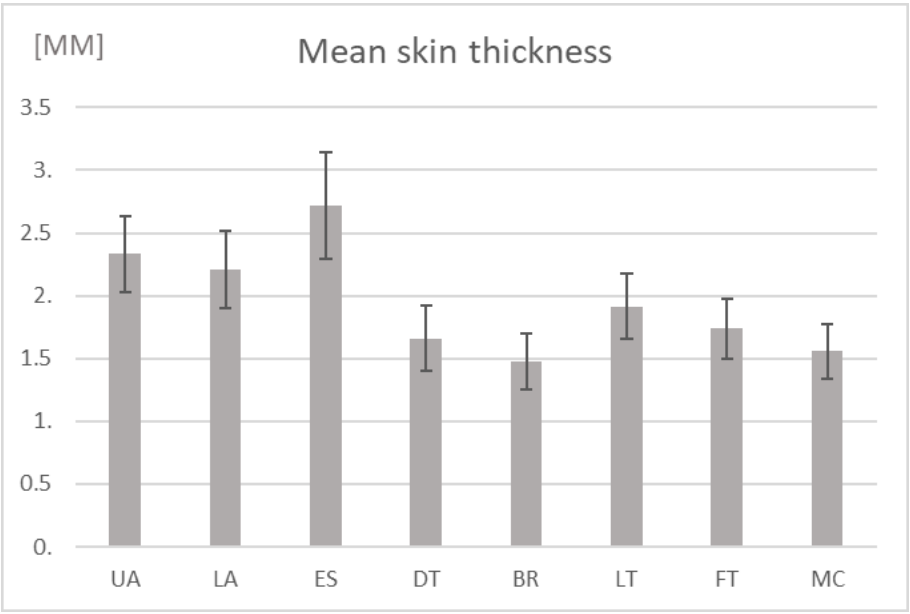

Figure 5: Mean skin thickness at the eight standardised sites:
Upper abdomen (UA), lower abdomen (LA), erector spinae (ES), distal triceps (DT), brachioradialis (BR), lateral thigh (LT), front thigh (FT), medial calf (MC). Mean skin thickness was 1.95 mm with a standard deviation of 0.28 mm. The highest mean value was found at the site ES with 2.72 mm, and the lowest mean value at the site BR with 1.48 mm.

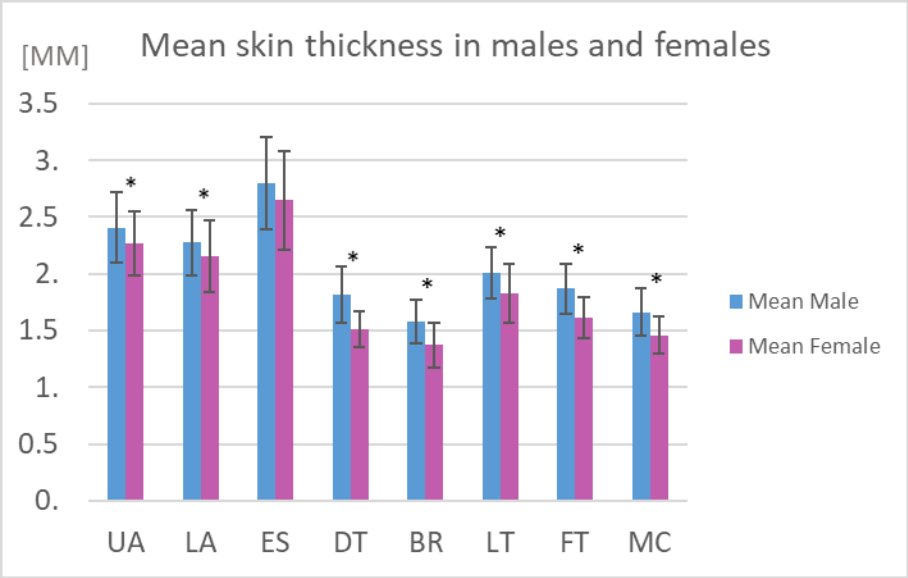

Figure 6: Skin patterning in males (N=50) and females (N=50).
Blue columns correspond to males and pink columns to females. Significant differences ($p<0.05$) between sexes were marked (*) and found for the sites UA, LA, DT, BR, LT, FT and MC.

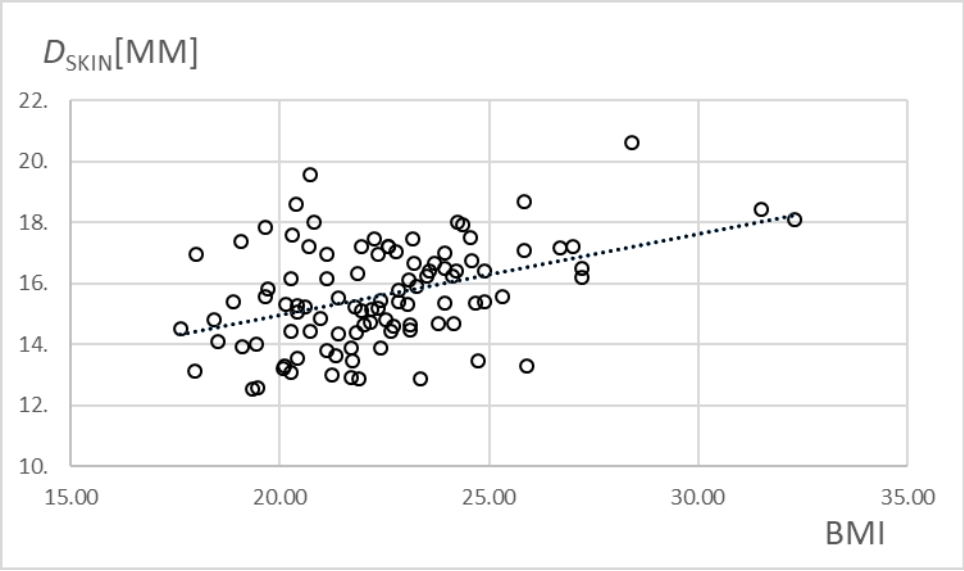

Figure 7: Correlation between the sum of the skin of the eight standardises sites (D_{SKIN}) and the BMI (kgm^{-2})
A moderate positive correlation was found $R^2= 0.171$ ($p<0.05$) (209)

3.1.3 SAT thicknesses measured at 216 sites

The data of this investigation were published in scientific reports (2) and are quoted literally in the following, adapted to the correct figure numbers, table numbers and citations in this thesis. Figures and tables have also been taken over with the permission of publisher (Nature Publishing Group).

"*In a group of ten male participants (table 16), subcutaneous adipose tissue (SAT) was measured twice at eight standardised sites using a recently developed ultrasound (US) method (1,192). As an example, the US image of SAT at one of the eight standardised sites (lateral thigh, LT) is shown in figure 2. In addition, SAT was also measured with the same US technique at 216 sites that were randomly distributed all over the body (figure 4a-c). The sums of the eight SAT thicknesses (D) of all 10 participants are shown in table 20, and mean values of these eight measurements (d_{M8}) are presented in table 21. Thicknesses* ***i****ncluding the fibrous structures embedded in the SAT are indicated by the index "I", measurements where these structures were* ***e****xcluded are indicated by the index "E", and "F" indicates the thicknesses of the fibrous structures. For SAT thicknesses at individual measurement sites, the lower case letter "d" is used, and for the sums obtained from the eight sites at each participant, capital "D" is used. Table 20 also presents the surface areas (S) of the participants according to DuBois (210), Haycock (211), Mosteller (212); and also the means (S_M) of these three.*

Table 20: Sums of subcutaneous adipose tissue from eight sites (Störchle et al., 2018 (2))

	Unit	P1	P2	P3	P4	P5	P6	P7	P8	P9	P10	**M**	**SD**	**MD**	**MAX**	**MIN**
D_I	**mm**	23.5	28.4	31.8	36.	39.7	45.5	51.6	59.6	62.1	81.6	46.0	18.0	42.6	81.6	23.5
D_E	**mm**	18.5	23.2	25.9	30.9	34.9	39.2	44.9	53.5	51.8	74.6	39.8	17.0	37.1	74.6	18.5
D_F	**mm**	5.0	5.2	5.9	5.1	4.8	6.3	6.7	6.1	10.3	7.0	6.2	1.6	6.0	10.3	4.8
D_F/D_I	**1**	0.21	0.18	0.19	0.14	0.12	0.14	0.13	0.10	0.17	0.09	0.14	0.04	0.14	0.21	0.09
S_1	**m²**	1.85	1.79	1.91	2.25	1.82	1.76	2.19	2.17	2.12	2.17	2.0	0.19	2.02	2.25	1.76
S_2	**m²**	1.82	1.77	1.90	2.26	1.85	1.74	2.24	2.14	2.11	2.20	2.0	0.21	2.00	2.26	1.74
S_3	**m²**	1.82	1.77	1.90	2.25	1.83	1.74	2.22	2.15	2.11	2.18	2.0	0.20	2.00	2.25	1.74
S_M	**m²**	1.83	1.78	1.90	2.25	1.83	1.75	2.22	2.15	2.11	2.18	2.0	0.20	2.01	2.25	1.75
$VSAT_I$	**dm³**	3.49	4.05	5.23	6.73	6.16	6.45	10.70	9.45	9.75	13.42	7.54	3.18	6.59	13.42	3.49
$VSAT_E$	**dm³**	2.82	3.26	4.45	5.63	5.05	5.49	9.61	8.31	8.16	12.09	6.49	2.96	5.56	12.09	2.82
$TSAT_I$	**kg**	3.21	3.73	4.81	6.19	5.67	5.94	9.84	8.69	8.97	12.35	6.94	2.92	6.06	12.35	3.21
$TSAT_E$	**kg**	2.59	3.00	4.09	5.18	4.65	5.05	8.84	7.64	7.51	11.12	5.97	2.73	5.12	11.12	2.59
$TSAT_{I\%}$	**%**	4.9	5.8	6.7	6.5	7.8	9.5	10.2	10.2	10.7	13.3	8.56	2.64	8.66	13.32	4.86
$TSAT_{E\%}$	**%**	3.9	4.6	5.7	5.4	6.4	8.1	9.2	8.9	8.9	12.0	7.33	2.51	7.25	12.	3.93

The table presents the sums (D) of subcutaneous adipose tissue (SAT) thicknesses measured at the eight standardised sites: D_I (fibrous structures included), D_E (fibrous structures excluded), D_F (fibrous structures). S_1, S_2, and S_3 represent the surface areas according to DuBois(210), Haycock (211), and Mosteller (212) respectively.
The total SAT volume VSAT [dm³] = d_M[mm] · S_M [m²]. The total SAT mass TSAT=VSAT · ρ, with ρ= 920 [kgm^{-3}] for the density of fat (206). TSAT[%] = 100 · TSAT/m.

Table 21: Measurement of mean SAT (Störchle et al., 2018 (2))

	P1	P2	P3	P4	P5	P6	P7	P8	P9	P10	**M**
d_{IM8}	2.94	3.55	3.98	4.50	4.97	5.69	6.45	7.46	7.76	10.20	5.75
d_{IM216}	1.91	2.28	2.75	2.98	3.36	3.69	4.83	4.39	4.62	6.14	3.69
d_{IM108a}	1.99	2.18	2.72	2.88	3.58	3.91	4.26	4.53	4.44	6.14	3.66
d_{IM108b}	1.82	2.39	2.77	3.09	3.14	3.47	5.40	4.24	4.79	6.15	3.73
d_{EM8}	2.32	2.90	3.24	3.87	4.36	4.90	5.61	6.69	6.48	9.33	4.97
d_{EM216}	1.54	1.84	2.34	2.50	2.76	3.14	4.34	3.86	3.86	5.54	3.17
d_{EM108a}	1.60	1.74	2.32	2.41	2.95	3.34	3.75	4.00	3.69	5.56	3.14
d_{EM108b}	1.48	1.93	2.35	2.58	2.56	2.95	4.93	3.72	4.04	5.51	3.20
d_{FM8}	0.62	0.65	0.74	0.64	0.60	0.79	0.84	0.76	1.28	0.87	0.78
d_{FM216}	0.37	0.44	0.41	0.49	0.60	0.55	0.49	0.53	0.75	0.61	0.52
d_{FM108a}	0.39	0.44	0.40	0.46	0.63	0.57	0.51	0.54	0.75	0.58	0.53
d_{FM108b}	0.34	0.45	0.42	0.51	0.58	0.53	0.47	0.52	0.75	0.64	0.52

Mean SAT thicknesses d_M. The upper part shows mean SAT thicknesses obtained from eight standardised sites (d_{M8}) (192) and from 216 randomised sites on the body of each of the ten participants. The latter measurements were performed in two series of 108 measurements each (d_{M108}). The indices I, E, F stand for

*fibrous structures **i**ncluded in the thickness measurement, E for **e**xcluded, and F for the thickness of the fibrous structures.*

The measurements at the 216 sites resulted in the reference means of SAT thicknesses for each of the participants (table 21). A comparison of the SAT means obtained with the eight standardised sites (1,192) is presented in figure 8. Means of typically 50 to 300 measurements obtained from each US image were used to represent the SAT thickness at a given individual site. The surface areas (S_M) are also displayed in table 20.

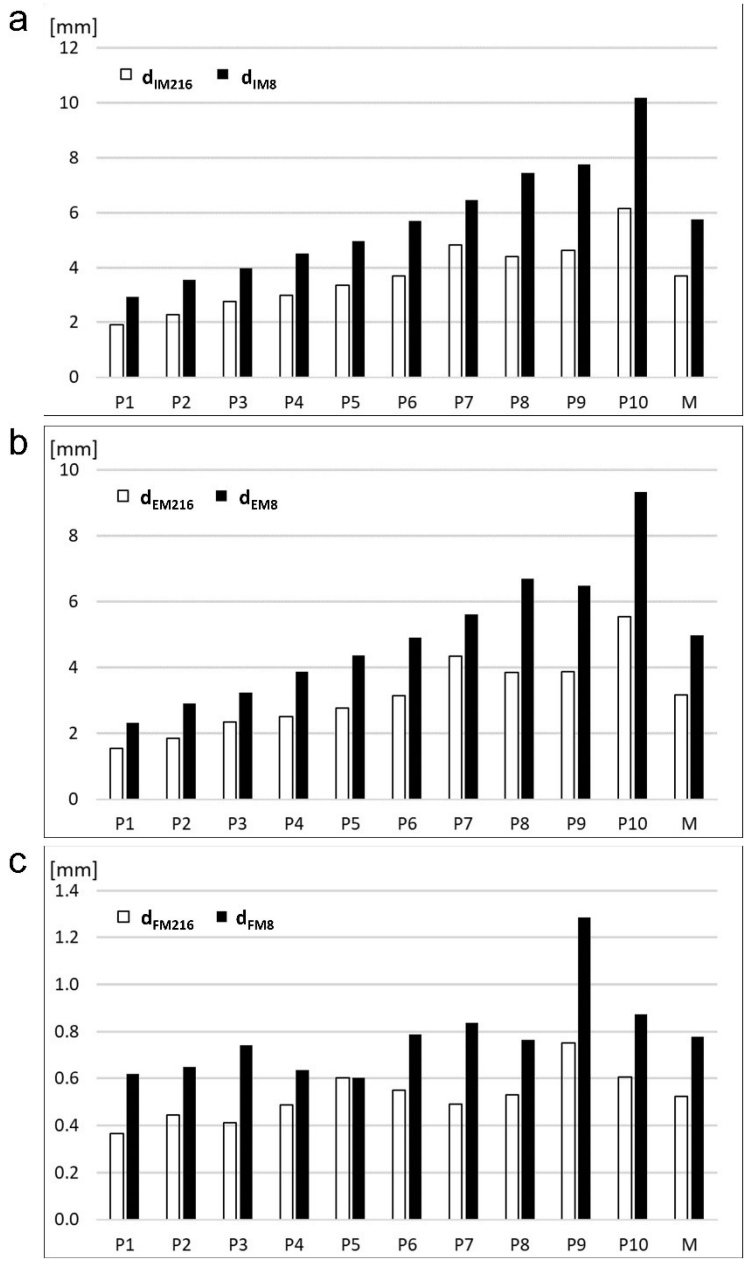

Figure 8: Mean SAT thickness (Störchle et al., 2018 (2))

Black columns are the means (d_{M8}) obtained from the measurements at the eight standardised sites. White columns are the means obtained from 216 sites (d_{M216}) of each of the ten male participants. The participants P1 to P10 are ordered according to increasing means of d_{IM8}. The columns labelled M represent the mean values of the ten participants. (i.e. the mean of all 2160 US measurements, each of them is a mean of typically 50 to 200 thickness measurements in each of the 2160 US images)

(a) Mean thickness values including the embedded fibrous structures (d_{IM}).
(b) Mean thickness values excluding the embedded fibrous structures (d_{EM}).
(c) Mean thicknesses of fibrous structures ($d_{FM}=d_{IM}-d_{EM}$)

The mean thicknesses obtained from the eight standardised sites deviated, as expected from the means obtained from the 216 randomised sites. The factor k represents this for the individual ten participants (table 22), and the mean of them can be used to calibrate results obtained from the eight-site measurements. For measurements that included (index "I") fibrous structures the calibration equation is: $d_{IM216}=d_{IM8} \cdot k_{IM216}$, and for measurements that exclude (index "E") fibrous structures: $d_{EM216}=d_{EM8} \cdot k_{EM216}$. The table also shows the factors when the eight-site measurements were compared to 108-site measurements (the measurement series of 216 sites was taken in two series of 108 sites each).

The k-values corresponding to 216 measurements with fibrous structures included (I), and without (E), are shown in figures 9a and 9c, and for the 108-site measurement series in figures 9b and 9d. Mean k values were 0.65mm in both cases.

Table 22:Mean SAT thickness calibration factor k_M (Störchle et al., 2018 (2))

	P1	P2	P3	P4	P5	P6	P7	P8	P9	P10
k_{IM216}	0.65	0.64	0.69	0.66	0.68	0.65	0.75	0.59	0.59	0.60
k_{IM108a}	0.68	0.61	0.68	0.64	0.72	0.69	0.66	0.61	0.57	0.60
k_{IM108b}	0.62	0.67	0.70	0.69	0.63	0.61	0.84	0.57	0.62	0.60
k_{EM216}	0.66	0.63	0.72	0.65	0.63	0.64	0.77	0.58	0.60	0.59
k_{EM108a}	0.69	0.60	0.72	0.62	0.68	0.68	0.67	0.60	0.57	0.60
k_{EM108b}	0.64	0.67	0.73	0.67	0.59	0.60	0.88	0.56	0.62	0.59
k_{FM216}	0.59	0.69	0.55	0.77	1.00	0.70	0.59	0.69	0.59	0.70
k_{FM108a}	0.63	0.67	0.54	0.73	1.04	0.73	0.61	0.71	0.58	0.66
k_{FM108b}	0.56	0.70	0.57	0.80	0.97	0.67	0.56	0.68	0.59	0.73

The calibration factor k_{M216} is defined as: $k_{M216} = d_{M216}/d_{M8}$, and analogously $k_{M108} = d_{M108}/d_{M8}$. The calibration factor allows assessing the mean SAT thickness of a person based on the measurements at the eight standardised sites.

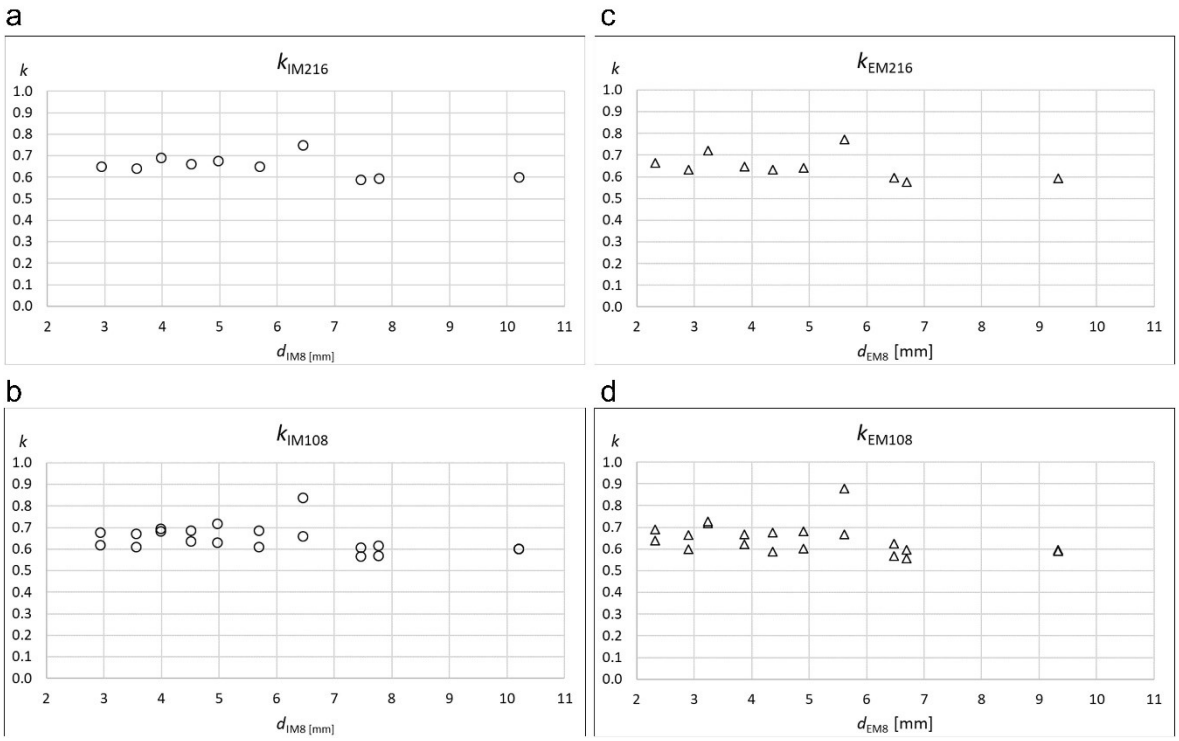

Figure 9: Mean SAT thicknesses at eight standardised sites compared to measurements at 216 and at 108 sites. (Störchle et al., 2018 (2))

*Ten participants were measured at 216 sites (in two series of 108 sites each) distributed randomly all over the body (compare to Figs. 1a-c), and also at the eight standardised sites. The ten participants are ordered according to increasing mean SAT thickness (d_{IM8}). The mean SAT thicknesses (d_M) obtained from measurements at 216 (or at 108) sites deviate by a factor k from the means of the eight standardised sites: $k_{M216} = d_{M216}/d_{M8}$, and analogously $k_{M108} = d_{M108}/d_{M8}$. The factors for SAT thickness **i**ncluding fibrous structures (I) are shown in (a), and the comparison with the two subgroups of 108 sites each are shown in (b). (c) and d) display the factors for thicknesses with fibrous structures **e**xcluded (E).*

Figures 10a and c show the correlations between the mean thicknesses obtained for the 216 randomised sites (d_{M216}) and the calibrated means ($d_{M8,k}$) from the eight standardised sites according to: $d_{M8,k}=k \cdot d_{M8}$. The correlation coefficient R^2 was 0.95 ($p<0.01$), and SEE was 0.34 for data including fibrous structures (figure 10a), and R^2 was 0.94 ($p<0.01$), and SEE 0.36 without fibrous structures (Fig.10c). Fig.10b and d show the respective limits of agreement [-0.63, 0.72]mm and [-0.64, 0.76]mm, respectively.

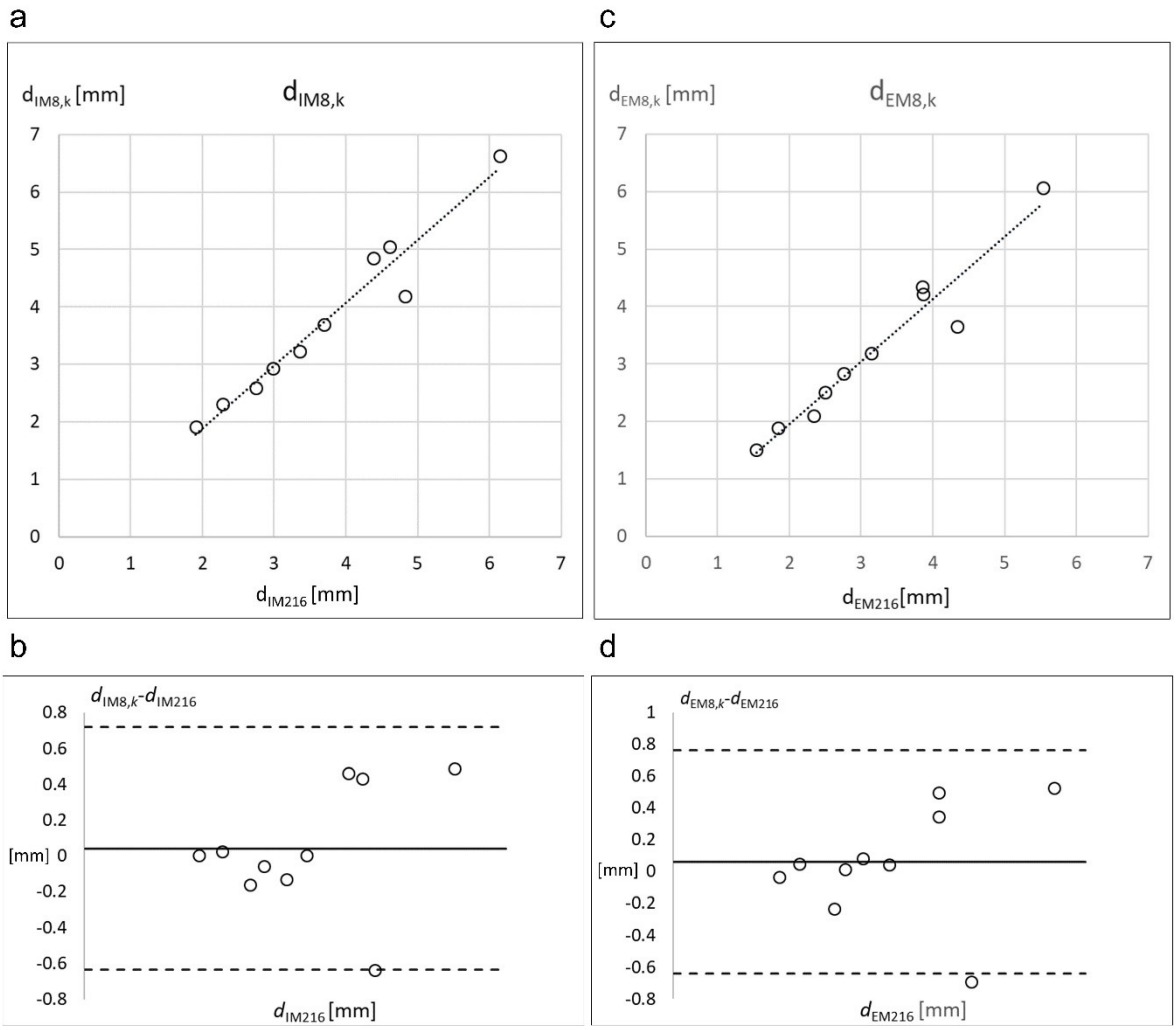

Figure 10:Application of the calibration factor *k* (Störchle et al., 2018 (2))
*The application of the factor k on the eight standardised sites ($d_{M8,k}$) compared with the 216 randomly distributed sites (d_{M216}) all over the body. In figures 10a and 10c, $d_{M8,k}$ is displayed over d_{M216}. Pearson´s correlation coefficient was used. Data was normally distributed. (a) Embedded fibrous structures **i**ncluded (I): R^2=0.951, SEE=0.344. (c) Embedded fibrous structures **e**xcluded (E): R^2=0.938, SEE=0.363. Figures (b) and (d) present Bland-Altmann plots with the data for I: mean M=0.04, standard deviation SD=0.35, limits of agreement were -0.63, and 0.72; for E: 0.06, 0.36, -0.64 and 0.76, respectively.*

Mean SAT thicknesses of the 11 body segments (BS) head, neck, anterior trunk, posterior trunk, upper arms, forearms, hands, buttocks, thighs, legs, an feet ($d_{M,BS}$) are presented in figures 11a and b and table 23. Highest mean value was 12mm at buttocks and lowest was 0.3mm at hands. The SAT percentages ($SAT_{\%,BS}$) for each segment are presented in figures 11c and d and table 23. The columns represent the percentages of the SAT volumes (and thus also of the fat masses) of the 11 body segments.

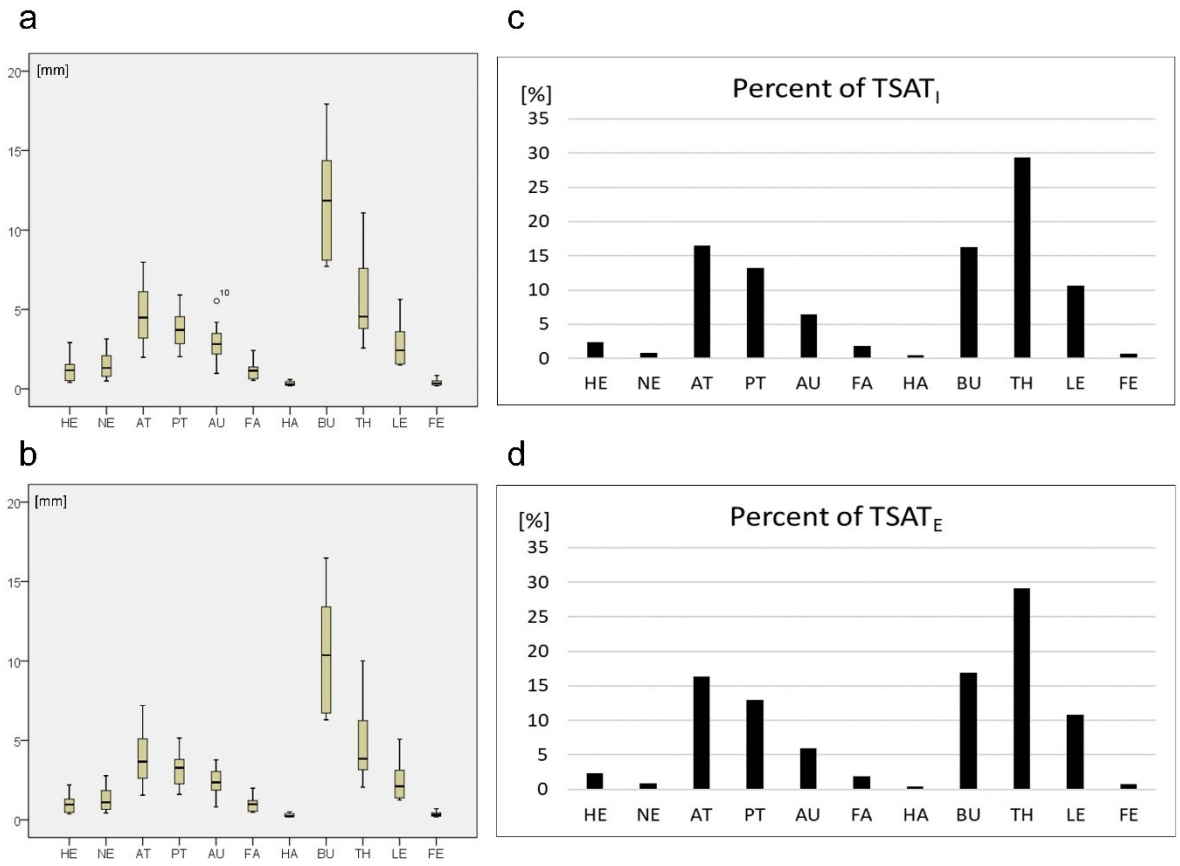

Figure 11:Mean SAT thicknesses *($d_{M,BS}$)* at the 11 body segments (BS) (Störchle et al., 2018 (2))
This data set resulted from 10 · 216 = 2160 US images, captured at 11 body segments (for abbreviations see figure. 4 or table 23*). The individual values of the ten male participants are shown in table 23. (a) Mean SAT thickness of each segment (compare to Fig. 1c) with fibrous structures* ***i****ncluded ($d_{IM,BS}$). (b) Data for thicknesses where fibrous structures were* ***e****xcluded ($d_{EM,BS}$). (c) and (d): the columns show the percentages ($SAT_{\%,BS}$) of the body segment contributions to the total subcutaneous adipose tissue (TSAT). The mean SAT thicknesses $M_{I,2160}$ and $M_{E,2160}$ (mean of 2160 SAT thickness measurements) of all 10 participants measured at 216 sites each were 3.69 and 3.17, respectively (see table 21); therefore, normalisation factors of f_I = 100/3.6947 = 27.07, and f_E = 100/3.1704 = 31.54 result. For SAT thicknesses with fibrous structures included (I) we get $SAT_{I,\%,BS} = d_{IM,BS} \cdot f_I \cdot S_{BS}/S$, and with fibrous structures excluded (E) $SAT_{E,\%,BS} = d_{EM,BS} \cdot f_E \cdot S_{BS}/S$.*

Table 23: Mean SAT thicknesses ($d_{M,BS}$) and SAT percentages of the 11 body segments (BS) (Störchle et al., 2018 (2))

	P1	P2	P3	P4	P5	P6	P7	P8	P9	P10	**MD**	**M**	**$SAT_{\%,BS}$**
$d_{IM,HE}$	0.52	1.08	1.27	0.49	2.20	2.91	1.25	0.40	1.06	1.54	1.17	1.27	2.4
$d_{IM,NE}$	0.50	1.20	1.51	1.19	2.09	2.45	0.67	0.79	3.14	1.43	1.31	1.50	0.8
$d_{IM,AT}$	1.98	3.19	4.13	2.90	4.14	4.84	5.27	6.40	6.12	7.98	4.49	4.69	16.5
$d_{IM,PT}$	2.66	2.03	3.56	3.20	2.84	4.04	3.86	4.54	4.99	5.91	3.71	3.76	13.2
$d_{IM,AU}$	0.97	2.19	2.02	2.74	3.29	2.65	3.49	2.90	4.19	5.53	2.82	3.00	6.5
$d_{IM,FA}$	0.52	0.58	1.37	0.63	0.99	1.30	1.61	0.73	2.41	1.37	1.15	1.15	1.9
$d_{IM,HA}$	0.22	0.26	0.19	0.36	0.45	0.58	0.55	0.20	0.28	0.22	0.27	0.33	0.4
$d_{IM,BU}$	7.71	8.10	7.92	12.62	10.83	12.85	16.99	17.93	11.08	14.36	11.85	12.04	16.3
$d_{IM,TH}$	2.57	3.28	3.80	4.58	4.25	4.52	8.49	7.06	7.59	11.08	4.55	5.72	29.4
$d_{IM,LE}$	1.53	1.48	1.56	2.03	3.23	2.64	4.08	2.22	3.60	5.63	2.43	2.80	10.6
$d_{IM,FE}$	0.19	0.24	0.24	0.37	0.84	0.50	0.56	0.33	0.35	0.31	0.34	0.39	0.7
$d_{EM,HE}$	0.48	0.87	1.14	0.43	1.73	2.19	1.06	0.37	0.76	1.30	0.97	1.03	2.3
$d_{EM,NE}$	0.43	0.99	1.35	1.02	1.84	2.16	0.62	0.67	2.77	1.19	1.10	1.30	0.8
$d_{EM,AT}$	1.55	2.61	3.59	2.35	3.51	3.73	4.53	5.75	5.09	7.20	3.66	3.99	16.4
$d_{EM,PT}$	2.00	1.60	3.12	2.64	2.26	3.60	3.43	3.80	4.10	5.14	3.27	3.17	13.0
$d_{EM,AU}$	0.81	0.96	1.86	2.29	2.42	2.13	3.05	2.98	3.50	3.77	2.35	2.38	6.0
$d_{EM,FA}$	0.50	0.47	1.21	0.55	0.86	1.11	1.43	0.57	1.98	1.19	0.99	0.99	1.9
$d_{EM,HA}$	0.22	0.22	0.19	0.29	0.40	0.47	0.51	0.20	0.24	0.21	0.23	0.29	0.5
$d_{EM,BU}$	6.49	6.72	6.30	11.04	9.42	11.43	16.25	16.47	9.70	13.41	10.37	10.72	16.9
$d_{EM,TH}$	2.05	2.53	3.15	3.73	3.35	3.95	7.50	6.15	6.24	10.01	3.84	4.87	29.2
$d_{EM,LE}$	1.24	1.24	1.37	1.70	2.70	2.33	3.74	1.89	3.12	5.07	2.11	2.44	10.8
$d_{EM,FE}$	0.18	0.23	0.22	0.36	0.70	0.45	0.52	0.26	0.34	0.30	0.32	0.36	0.8

*The indices I and E stand for fibrous structures **i**ncluded in the thickness measurement and E for **e**xcluded. SAT thicknesses of the ten participants were measured at 216 sites each (in two series of 108 each). The numbers of sites on each of the 11 body segments according to Lund and Browder (207) were chosen proportionally to the surface areas of these segments (figure. 4c): 16 on head (HE), 4 on neck (NE), 28 on anterior trunk (AT), 28 on posterior trunk (PT), 16 on upper arms (AU), 12 on forearms (FO), 12 on hands (HA), 12 on buttocks (BU), 40 on thighs (TH), 32 on legs (LE), and 16 on feet (FE). The according box plots are shown in figures 11(a) and (b). The mean percentages (of all ten participants) of the fat mass contributions of the individual body segments are also shown ($SAT_{\%,BS}$); this sums up to 99% because (1%) were ignored.*

3.2 Intra-observer study

This study was used to investigate if this novel ultrasound method is accurate and reliable in all kind of body types. Three measurement series in each person were carried out in 38 untrained, normal weight, overweight and obese participants. The results were published in Ultrasound in Medicine and Biology (1) and are quoted literally in the following. Figures and tables have also been taken over with the permission of publisher (Elsevier). Additionally, a comparison of the SAT data and total body fat in percent (TBF), which was assessed according to the Body roundness model of Thomas et al. (213) was supplemented.

"Figure 12a shows the three sums of D_{INCL} obtained from the eight sites for the three measurements (M1, M2, and M3). Values are plotted over the mean value of the three measurement sums (in a given participant). Figure 12b shows the results for D_{EXCL} (without fibrous structures). Statistical characteristics for D_{INCL} are $\rho=0.999$ ($p<0.01$), SEE=1.1 mm, and for D_{EXCL}: $\rho=0.997$ ($p<0.01$), SEE=1.5mm. Several additional borders have to be determined in order to measure the additional thicknesses of embedded structures for D_{EXCL}, whereas for D_{INCL} deviations were slightly smaller because there is just one upper and one lower border to be determined by the algorithm.

The corresponding correlations between the individual sites of the single measurements are presented in table 24a and 24b. Spearman´s rank correlation coefficient (ρ) was calculated. Including fibrous structures, the highest correlation exists for the site LA. With fibrous structures excluded, UA showed the highest correlation. M2 and M3 showed the strongest correlations (measurements M2 and M3 were done without re-marking the site).

The SAT thickness sums $D_{INCL,MEAN}$ ranged in G1 from 12.46mm to 77.41mm and in G2 from 44.34mm to 244.87mm. In both groups (most participants physically untrained), the thickness sums $D_{INCL,MEAN}$ for women (N=12) ranged from 52.51mm to 244.87mm (mean: 117.3mm), and for men (N=26) from 12.46mm to 167.88mm (mean: 72.8mm).

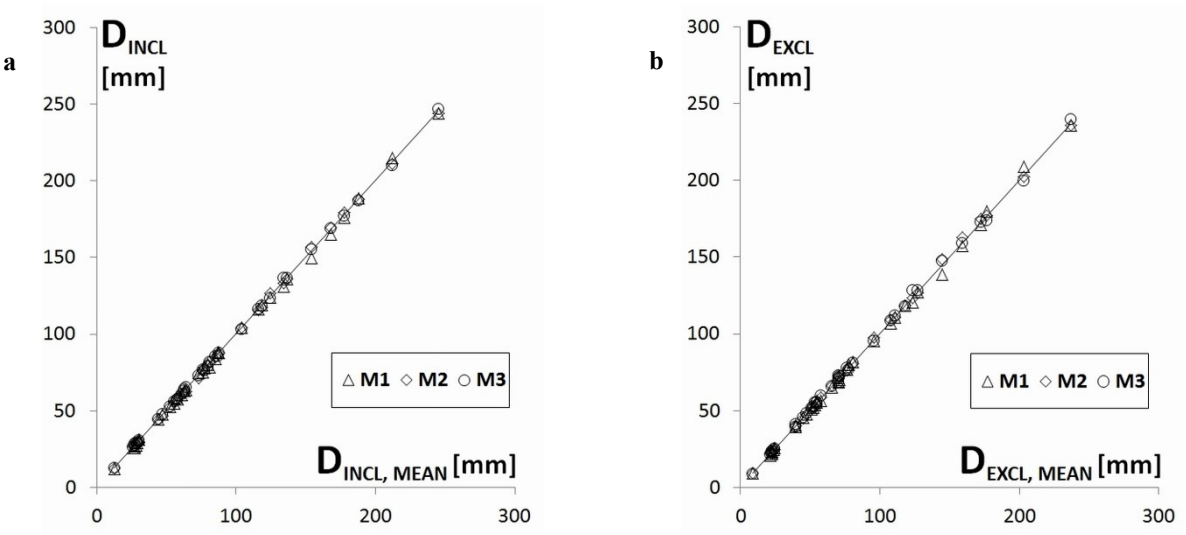

Figure 12: Sums of SAT thicknesses from eight sites measured three times (measurements M1, M2, and M3) in 38 participants (Störchle et al., 2017 (1))

The sums D of each measurement series at the eight sites (in a given participant) are displayed over the mean value of all three measurements.

a: Embedded fibrous structures included (D_{INCL}). *Spearman´s rank correlation coefficient (ρ) was used to determine the correlation. ρ=0.999 (p<0.01), SEE=1.1mm*

b: Embedded fibrous structures excluded (D_{EXCL}). *ρ=0.997 (p<0.01), SEE=1.5mm*

Table 24: Intra-observer correlations (Störchle et al., 2017 (1))
Spearman´s rank correlation coefficients (ρ) were calculated (p<0.01) for each individual site

Correlation of measurements for d_{INCL}			
ρ<0.01 (Spearman's-rho)			
US-Site	$p_{M1,M2}$	$p_{M1,M3}$	$p_{M2,M3}$
UA	*0.995*	*0.994*	*0.996*
LA	*0.997*	*0.996*	*0.999*
ES	*0.968*	*0.971*	*0.994*
DT	*0.940*	*0.930*	*0.956*
BR	*0.975*	*0.975*	*0.993*
LT	*0.991*	*0.988*	*0.995*
FT	*0.994*	*0.989*	*0.998*
MC	*0.982*	*0.982*	*0.989*
Mean	*0.980*	*0.978*	*0.990*

a: *Correlations with fibrous structures included. The highest correlations were found at the site lower abdomen (LA), and the lowest at the site distal triceps (DT). All correlations found for the measurements M2 and M3 were higher than the others.*

Correlation of measurements for d_{EXCL}			
ρ<0.01 (Spearman's-rho)			
US-Site	$p_{M1,M2}$	$p_{M1,M3}$	$p_{M2,M3}$
UA	*0.997*	*0.997*	*0.999*
LA	*0.997*	*0.996*	*0.995*
ES	*0.980*	*0.973*	*0.982*
DT	*0.973*	*0.939*	*0.970*
BR	*0.985*	*0.988*	*0.985*
LT	*0.995*	*0.991*	*0.995*
FT	*0.988*	*0.987*	*0.990*
MC	*0.970*	*0.965*	*0.989*
Mean	*0.986*	*0.980*	*0.988*

b: *Correlations with fibrous structures excluded: The highest correlations were found at the sites upper abdomen (UA), and the lowest at the sites distal triceps (DT) and medial calf (MC). In most cases highest correlations were between the measurements M2 and M3.*

Figures 13a and b show the deviations of the single measurement sums from their mean for each participant. 95% of deviations were within the interval [-2.2mm, 1.9mm] with fibrous structures included, and within [-3.24mm, 3.18mm] when fibrous structures were excluded.

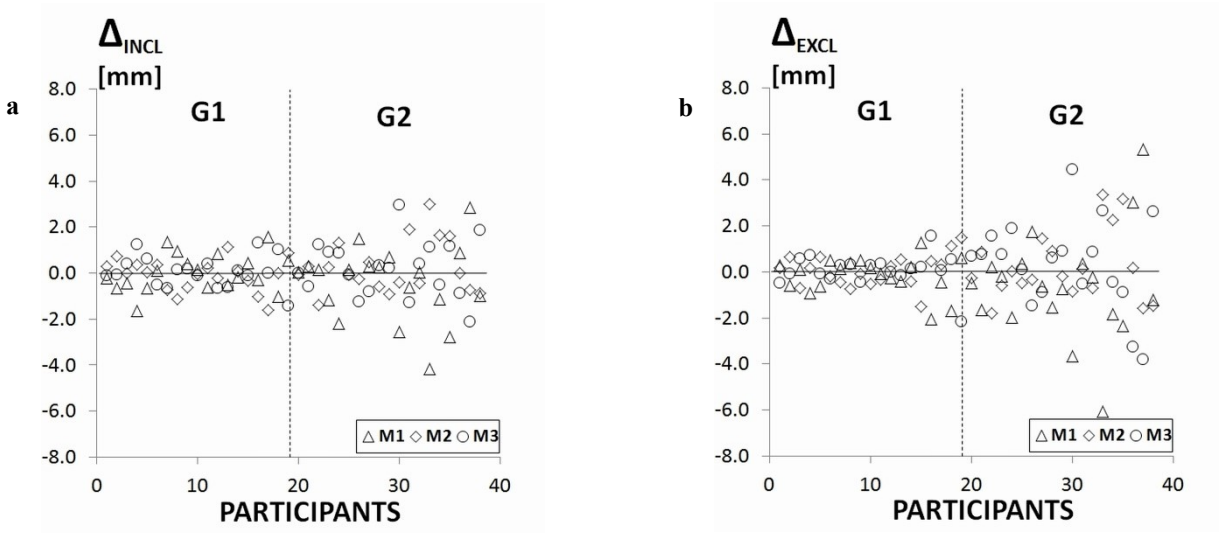

Figure 13: Differences from the mean of the three measurements (M1, M2, and M3) (Störchle et al., 2017 (1))

Three measurement deviations of the sums from the eight sites in each of the 38 participants (both groups combined) are plotted (N=114). ***a: $\Delta_{INCL}=D_{INCL}-D_{INCL,MEAN}$ is shown for all 38 participants.*** *The 19 subjects of each group are ordered according to increasing values of $D_{INCL,MEAN}$. 95% of deviations were within the interval [-2.2, 1.9] mm.* ***b: $\Delta_{EXCL}=D_{EXCL}-D_{EXCL,MEAN}$ is shown for all 38 participants.*** *The 19 subjects of each group are ordered according to increasing values of $D_{INCL,MEAN}$. 95% of deviations were within the interval [-3.24, 3.18] mm.*

Box plots in figures 14a and 14b visualize the absolute values of measurement deviations from their mean. The two observers measured the sums of eight sites three times in their respective groups (G1 and G2, respectively), each with 19 participants (resulting in 2x19x3=114 comparisons of SAT thickness sums). The deviations in the individual groups and in both groups combined are displayed. In G1, the median of the absolute deviations $ABS(\Delta_{INCL})$ was 0.43mm, and the median of $ABS(\Delta_{EXCL})$ was 0.41mm; the interquartile ranges were 0.70mm and 0.45mm, respectively. The highest deviations of the single measurement sums of thicknesses were $ABS(\Delta_{INCL,max})$=1.63mm and $ABS(\Delta_{EXCL,max})$=2.13mm; 95% of data were below 1.44mm (1.57mm). In G2, the medians were in both cases 0.89mm. The highest deviations were $ABS(\Delta_{INCL,max})$=4.16mm and $ABS(\Delta_{EXCL,max})$=6.05 mm; the interquartile ranges were 1.06mm and 1.48mm, respectively; 95% of data were below 2.86mm (3.78mm). $ABS(\Delta_{INCL})$ G1 and G2 together: median 0.61mm, interquartile range 0.91mm, and 95% were below 2.21mm. For $ABS(\Delta_{EXCL})$: median 0.59mm, interquartile range 1.18mm, and 95% were below 3.24mm. Deviations in the normal weight group G1 were lower than in G2.

Figures 14c and 14d represent the distribution of the relative errors $\Delta_{rel}=100\cdot\Delta/D_{MEAN}$ (in percent). For G1, the medians for $\Delta_{INCL,rel}$ and $\Delta_{EXCL,rel}$ were both 1.1%. Maximum values

were 6.4% and 5.8%. 95% were below 3.83% and 3.42%, respectively. For G2: median of $\Delta_{INCL,rel}$ was 0.5%, maximum was 2.8%; 95% of the values were below 2.16%. For $\Delta_{EXCL,rel}$: median was 0.9%, maximum 4.4%; 95% were below 3.03%. In G2, deviations were lower than in the normal weight group G1.

Values for both groups together for $\Delta_{INCL,rel}$ (and $\Delta_{EXCL,rel}$) were: median 0.75% (1.0%), and 95% of the data were below 2.78% (3.42%).

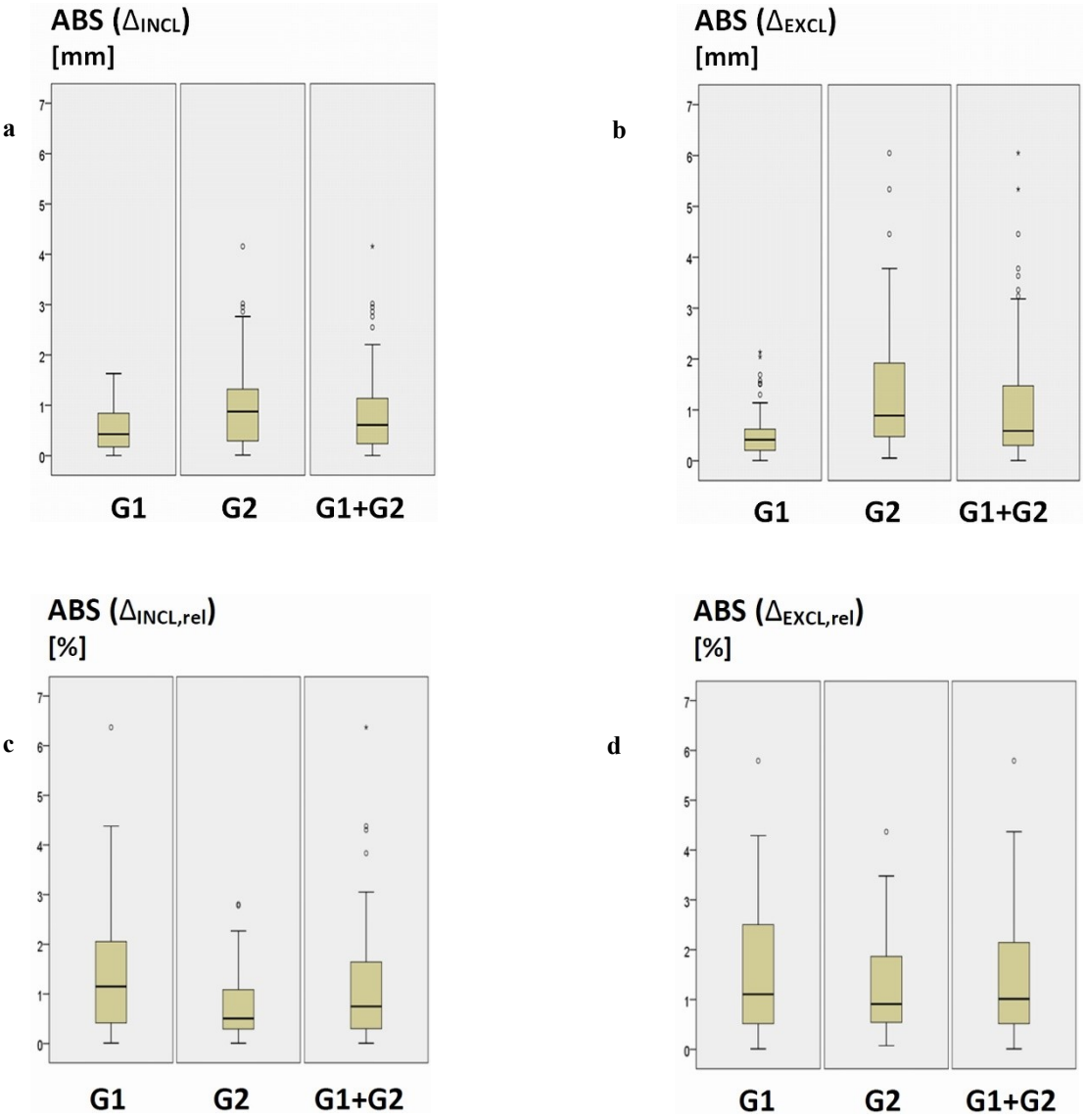

Figure 14: Observer differences of their individual *D*-values from their means (D_{Mean}) (Störchle et al., 2017 (1))

Differences of the three sums from the eight sites in each of the 38 subjects (G1: N=57, G2: N=57 and G1 plus G2: N=114).

a: Absolute differences: $ABS(\Delta_{INCL})=ABS(D_{INCL}-D_{INCL,MEAN})$ *The according relative deviations are presented in figure 14c.*

b: Absolute differences: $ABS(\Delta_{EXCL})=ABS(D_{EXCL}-D_{EXCL,MEAN})$ *The according relative deviations are presented in figure 14d.*

c: Relative deviations in percent of $D_{INCL,MEAN}$: $\Delta_{INCL,rel}=100\cdot ABS(\Delta_{INCL})/D_{INCL,MEAN}$

d: Relative deviations in percent of $D_{EXCL,MEAN}$: $\Delta_{EXCL,rel}=100\cdot ABS(\Delta_{EXCL})/D_{EXCL,MEAN}$

In the figures 15a and 15b the absolute values of deviations of the three measurements at each of the eight sites are shown. The deviation δ is the measurement deviation of each measurement (M1, M2, M3) from the mean of the three measurements at a given site in a given subject. The number of deviations ABS(δ) in the box plots was 114 (38 participants, three measurements). ABS(δ_{INCL}) refers to SAT thickness values with the fibrous structures included, and ABS(δ_{EXCL}) refers to SAT thickness values without fibrous structures. Table 25 presents the statistical characteristics of the box blots in figure 15. For both groups combined, median values of ABS(δ_{INCL}) ranged from 0.13mm to 0.26mm; for G1 from 0.07mm to 0.18mm, and for G2 from 0.18mm to 0.42mm. Interquartile ranges and maximum deviations can also be found in table 25.

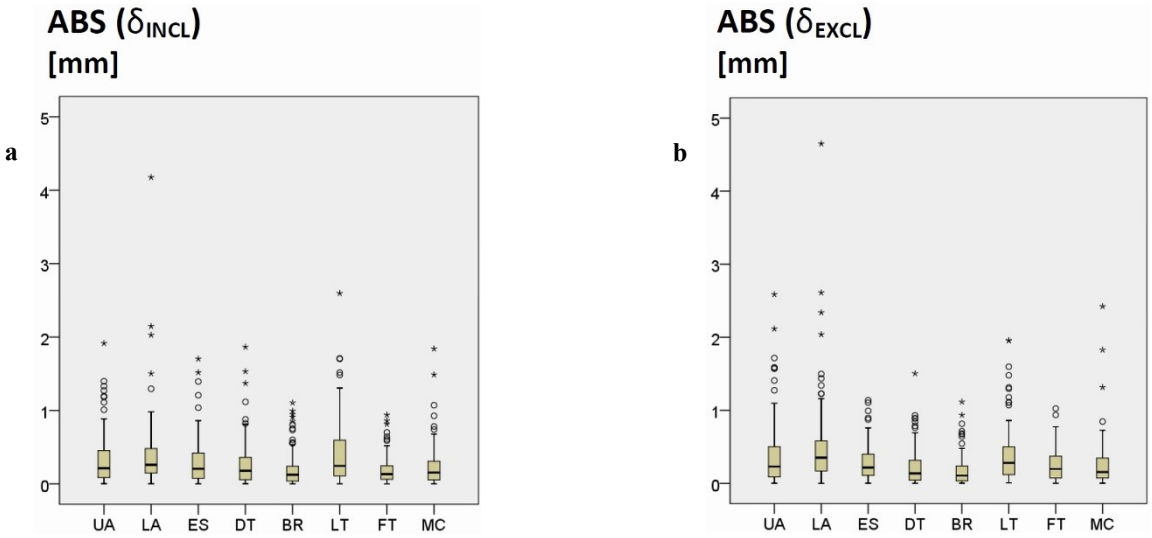

Figure 15: Measurement differences (absolute values) at the individual eight sites (Störchle et al., 2017 (1))
Absolute differences ABS(δ) from both groups together were used. Number of comparisons at each of the eight sites: N=114 (38 participants, three measurements each). Characteristic values are presented in table 25.

a: ABS (δ_{INCL}) for each of the eight sites.

b: ABS (δ_{EXCL}) for each of the eight sites.

Table 25:Absolute thickness value differences from the mean of the three measurements for each of the eight sites (Störchle et al., 2017 (1))

Characteristic values to box plots in figures 15a and b).
Deviations of thickness measurements at individual sites with both, fibrous structures included and excluded

a

ABS(δ_{INCL}); both groups G1+G2								
	UA	**LA**	**ES**	**DT**	**BR**	**LT**	**FT**	**MC**
Median(mm)	0.21	0.26	0.21	0.18	0.13	0.24	0.13	0.15
Interquartile Range (mm)	0.37	0.34	0.35	0.30	0.20	0.49	0.18	0.26
Maximum (mm)	1.9	4.2	1.7	1.9	1.1	2.6	0.9	1.8
ABS(δ_{EXCL}); both groups G1+G2								
	UA	**LA**	**ES**	**DT**	**BR**	**LT**	**FT**	**MC**
Median(mm)	0.23	0.35	0.22	0.14	0.11	0.28	0.20	0.15
Interquartile Range (mm)	0.42	0.41	0.30	0.27	0.20	0.38	0.30	0.27
Maximum (mm)	2.6	4.6	1.1	1.5	1.1	2	1	2.4

b

ABS(δ_{INCL}); group G1								
	UA	**LA**	**ES**	**DT**	**BR**	**LT**	**FT**	**MC**
Median(mm)	0.13	0.18	0.11	0.09	0.07	0.16	0.11	0.08
Interquartile Range (mm)	0.17	0.21	0.20	0.16	0.13	0.29	0.14	0.15
Maximum (mm)	0.6	0.68	1.4	0.6	0.6	0.85	0.6	0.36
ABS(δ_{EXCL}); group G1								
	UA	**LA**	**ES**	**DT**	**BR**	**LT**	**FT**	**MC**
Median(mm)	0.15	0.28	0.14	0.08	0.06	0.26	0.15	0.11
Interquartile Range (mm)	0.17	0.28	0.2	0.2	0.11	0.32	0.24	0.18
Maximum (mm)	0.7	0.9	0.87	0.6	0.4	0.86	1	0.57

c

ABS(δ_{INCL}); group G2								
	UA	**LA**	**ES**	**DT**	**BR**	**LT**	**FT**	**MC**
Median(mm)	0.42	0.42	0.32	0.31	0.18	0.37	0.18	0.24
Interquartile Range (mm)	0.49	0.50	0.50	0.37	0.30	0.72	0.22	0.31
Maximum (mm)	1.9	4.2	1.7	1.9	1.1	2.6	0.9	1.8
ABS(δ_{EXCL}); group G2								
	UA	**LA**	**ES**	**DT**	**BR**	**LT**	**FT**	**MC**
Median(mm)	0.43	0.52	0.30	0.27	0.17	0.35	0.27	0.29
Interquartile Range (mm)	0.53	0.63	0.42	0.41	0.29	0.57	0.30	0.37
Maximum (mm)	2.6	4.6	1.1	1.5	1.1	2	0.9	2.4

a: *For both groups G1 and G2 combined, N=3x38=114 at each site.* ***b:*** *Group G1: N=57* ***c:*** *Group G2: N=57*

Figure 16a shows median SAT thicknesses, and figure 16b shows measurement deviations relative to the median SAT thicknesses. Although the deviation values ABS(δ) increased with increasing d, the relative values were lower at those sites where SAT thickness d was higher. The median SAT thickness at the new site lateral thigh LT (which replaces the previously used external oblique site) was between the values of the UA and LA (Figure 16a; grey column). The relative measurement deviations $\delta_{INCL,rel}$ were below 2%; this is comparable to the values obtained at UA and LA. At all other sites $\delta_{INCL,rel}$ was higher (Figure 16b).

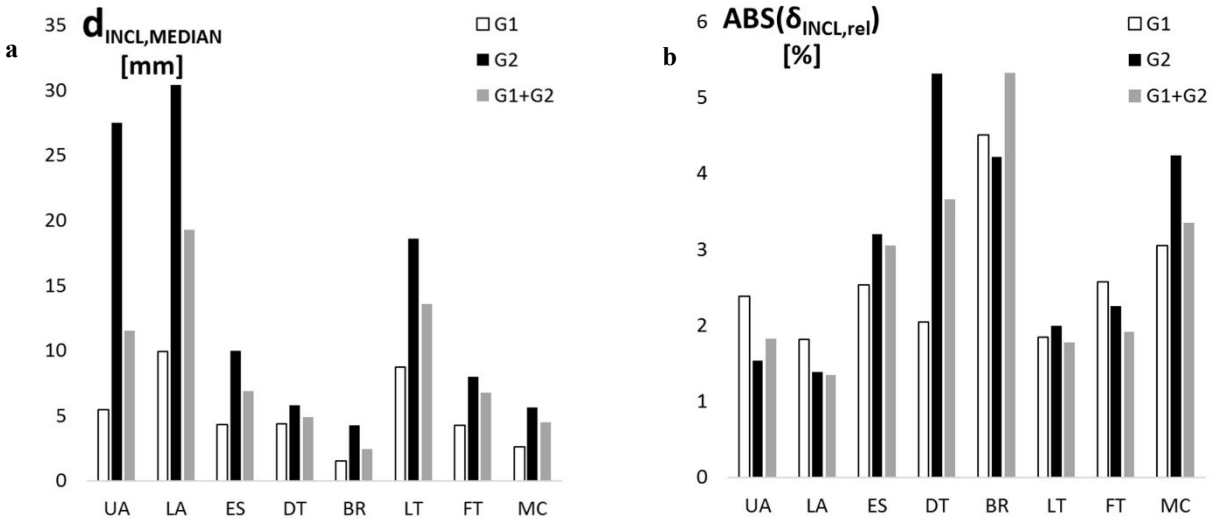

Figure 16: SAT patterning in the groups and relative measurement deviations at the individual sites (Störchle et al., 2017 (1)):
White columns correspond to group G1 (N=57), black to G2 (N=57), and grey to G1 and G2 combined (N=114).
a: Median SAT thicknesses
b: Measurement deviations relative to the median SAT thicknesses d:
$\delta_{INCL,rel}=100 \cdot ABS(\delta_{INCL,MEDIAN})/d_{INCL,MEDIAN}$.
($ABS(\delta_{INCL,MEDIAN})$: absolute values of deviations are used to determine the median)

A comparison of BMI and D_{INCL} is shown in figure 17. There was no correlation in group G1; in G2, there was a moderate correlation of $\rho=0.58$ ($p<0.01$), and for both groups together (N=38) Spearman's rho was $\rho=0.727$ ($p<0.01$). The highest D_{INCL} in this group (245mm, at a BMI of 37.2) was 46% above D_{INCL} of the person with the highest BMI of 40.3 ($D_{INCL}=168mm$).

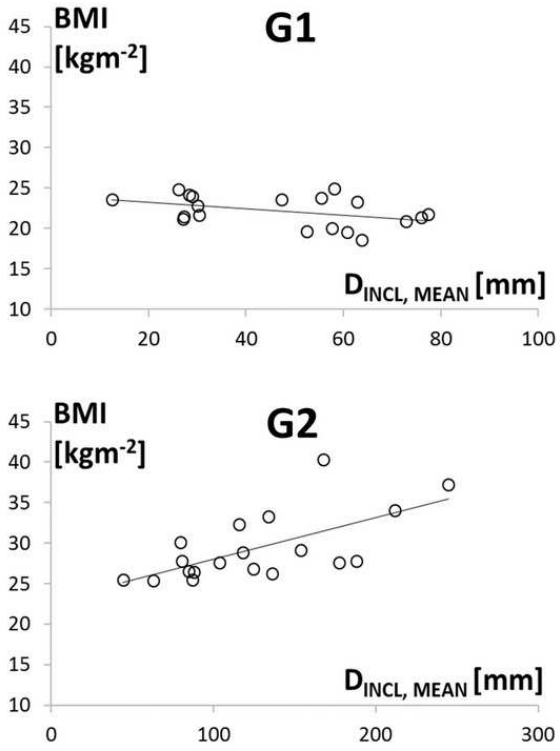

Figure 17: Comparison of body mass index (BMI) and D_{INCL} in groups 1 (G1) and 2 (G2) (Störchle et al., 2017 (1))

Body roundness model (BRM)

Figure 18a shows the correlation between $D_{INCL,Mean}$ and total body fat, which was assessed according to the BRM of Thomas et al. (213). Spearman's rank correlation coefficient ρ was 0.832 ($p<0.05$) for values including the fibrous structures, and 0.842 ($p<0.05$) when fibrous structures were excluded (plot not shown).

a)

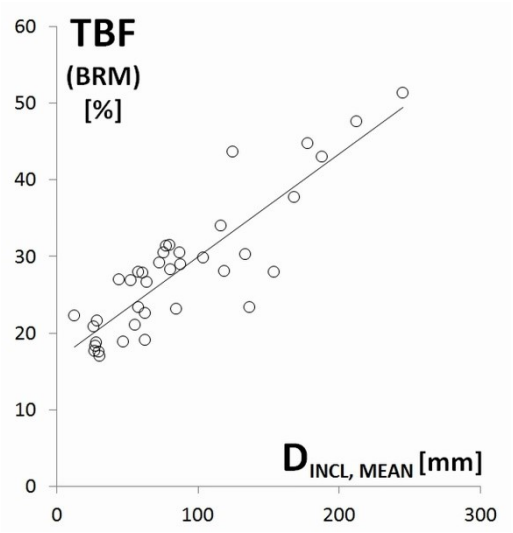

b)

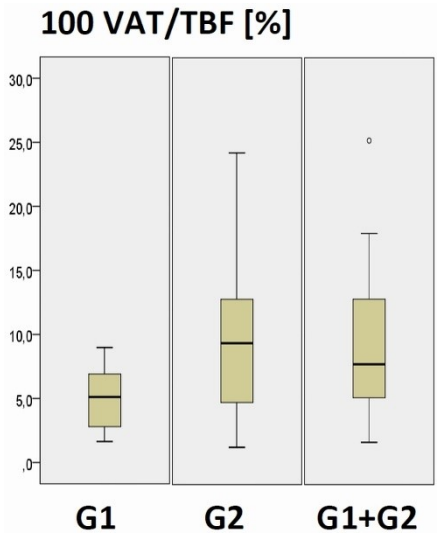

c)

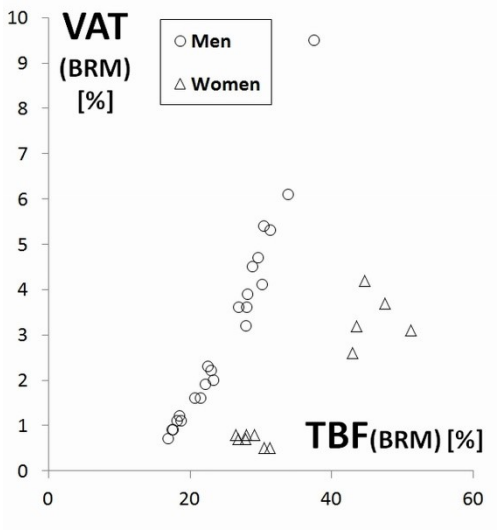

Figure 18: Body roundness model (BRM):
TBF, VAT/TBF-ratios, and Total body fat (TBF) and visceral adipose tissue (VAT) were assessed using the body roundness model BRM (web-based calculator from Thomas et al. (17)). The BRM is a simple method for rough assessment of TBF and VAT obtained by using age, height, sex, waist circumference, hip circumference, race, and products of these parameters.
A: TBF (according to the BRM) is presented over the SAT thickness sums $D_{INCL,MEAN:}$
Spearman´s rank correlation coefficient (ρ): ρ=0.832 (p<0.05)
B: Ratios of VAT to TBF (according to the BRM) for G1, G2, and G1+G2, in percent: 100(VAT/TBF)
For G1: median 5.1%, and maximum 9.0%. G2: median 12.8%, and maximum 25.2%. G1+G2 (both groups combined): median was 7.7%.
C: VAT-dependency on TBF
Spearman´s rank correlation coefficient (ρ) for all 38 participants (G1+G2): ρ=0.554 (p<0.05); for females separated (triangles; N=12): ρ=0.770, and for males (circles; N=36): ρ=0.987.

Figure 18b displays the ratio between visceral adipose tissue (VAT) and total body fat (TBF) according to the BRM. Values for G1: median 5.1%, maximum 9.0%, and for G2: median 12.8% and maximum 25.2%; both groups together: median 7.7%. Spearman´s rank correlation coefficient ρ between VAT and TBF was 0.554 (ρ<0.05, N=38). When separating men and women, ρ was 0.987 in the male group (N=26), and 0.770 in the female group (N=12) (p<0.05 in both cases). This indicates that the dependency of VAT on TBF (as determined by the BRM) differs in a pronounced way between men and women. Within the individual groups G1 and G2 there was, according to the BRM, no significant correlation between VAT and TBF for men and women combined. However, when separating men and women into the individual groups G1 and G2, a significant correlation resulted for men (G1: ρ=0.968, p<0.01; G2: ρ=0.957, p<0.05). There was no significant correlation for women (number of women was only 7 in G1, and 5 in G2). Figure 18c shows the dependency of VAT to TBF according to the BRM for women and men. Men (circles) and women (triangles) are distinctively separated.

3.3 Fat patterning, fibrous structures, and SAT correlations with anthropometric indices

3.3.1 Fat patterning

Fat patterning of 153 participants were analysed. Factors such as sex and body type play an important role in the distribution of fat, therefore results are separated into general fat patterning (point 3.3.1), fat patterning in males and females (point 3.3.1.1) and fat patterning in different groups divided up by BMI and sex (point 3.3.1.2).

The group included a range from young adults, starting with the age of 18 years, to elderly people up to 76 years. A wide range from lean to normal weight and obese people category III were covered (BMI ranged from 17.3-40.3 kgm^{-2} and body mass from 42.2 kg to 128.6 kg). An example of an evaluated image series is shown in figure 19. All eight sites show the same structure. The coloured areas represent the SAT cross-sectional areas within the chosen region of interest. The series of evaluated images in figure 19 corresponds to the survey plot representing the SAT patterning in section 3.3.3 *"*SAT tissue and relative body weight" (figure 33*).*

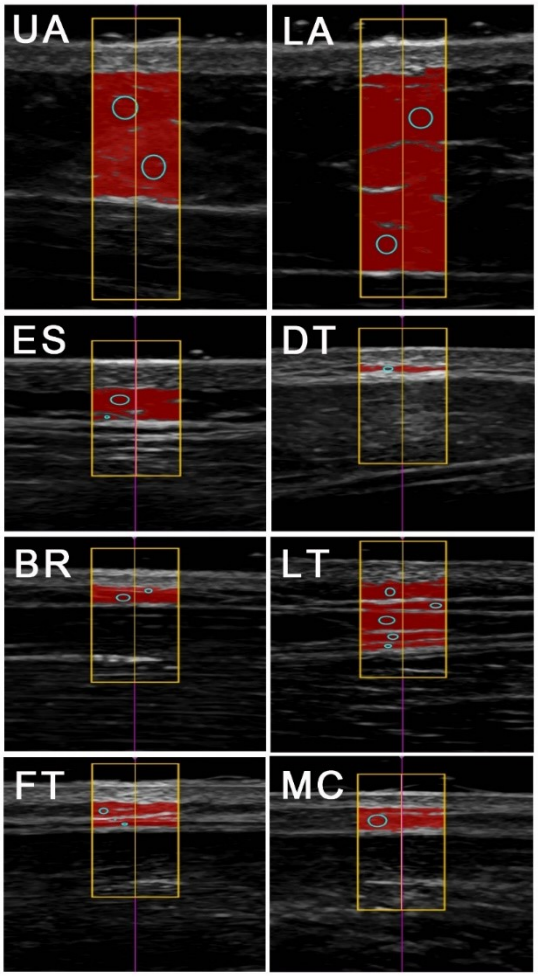

Figure 19: B-mode ultrasound measurement of uncompressed subcutaneous fat
The corresponding analysed patterning is shown in figure 33
US images and evaluations of SAT thicknesses. Participant A: male, BMI=25.5, body mass 80.7kg, stature 1.78m.
Adapted from (Störchle P, Müller W, Sengeis M, Ahammer H, Fürhapter-Rieger A, Bachl N, et al. Standardized ultrasound measurement of subcutaneous fat patterning: high reliability and accuracy in groups ranging from lean to obese) with permission of publisher (Elsevier).

Fat patterning of all participants is visualised in figure 20a and b with the corresponding absolute values in table 26 (a and b). The mean value of the total sum of SAT, including fibrous structures (D_I), was 67.9 mm (ranged from 5.6 mm to 244.9 mm). The relative amount of each site contributing to the total sum (d/D)*100 is shown in the figures 20c and d. Table 26 (c and d) contains the corresponding values.

Table 26: Mean SAT thicknesses at the eight standardised sites

a)

FS included (mm)	UA	LA	ES	DT	BR	LT	FT	MC	D_I
Mean	9.9	15.3	6.0	5.9	2.6	15.9	7.7	4.7	67.9
SD	9.5	10.8	3.7	3.7	1.6	9.4	4.5	3.2	39.4
Median	7.2	12.7	4.9	5.1	2.3	15.8	7.3	4.2	63.8
Min.	0.7	1.4	0.3	0.4	0.1	0.4	0.5	0.2	5.6
Max.	47.2	60.7	22.7	25.0	8.4	51.5	30.7	24.2	244.9

b)

FS excluded (mm)	UA	LA	ES	DT	BR	LT	FT	MC	D_E
Mean	9.1	14.0	5.5	5.0	2.3	14.4	6.7	4.3	61.3
SD	9.3	10.8	3.5	3.5	1.5	9.2	4.3	3.1	38.4
Median	6.1	11.2	4.5	4.2	2.1	14.6	6.1	3.9	57.9
Min.	0.7	1.2	0.2	0.3	0.1	0.2	0.5	0.2	4.1
Max.	44.3	58.8	21.2	23.7	8.1	49.2	29.8	22.7	236.7

c)

FS included (%)	UA	LA	ES	DT	BR	LT	FT	MC
Mean	13.45	22.58	9.29	9.09	3.83	23.05	11.85	6.86
SD	6.03	6.70	3.56	3.64	1.54	7.91	3.76	2.60
Median	12.61	23.14	8.87	9.00	3.66	23.26	12.05	6.71
Min.	2.73	4.74	2.33	1.00	0.99	3.16	1.73	1.05
Max.	28.14	39.91	24.53	23.86	14.16	42.69	22.26	17.75

d)

FS excluded (%)	UA	LA	ES	DT	BR	LT	FT	MC
Mean	13.73	22.72	9.68	8.64	3.86	22.87	11.47	7.03
SD	6.40	7.54	3.76	3.84	1.49	8.56	3.95	2.76
Median	12.87	23.16	9.22	8.36	3.69	23.30	11.54	6.77
Min.	2.59	4.36	2.36	1.03	1.16	2.82	2.02	1.24
Max.	29.15	41.80	23.84	23.27	14.09	44.19	23.05	19.45

a) with fibrous structures included. The highest mean values were at the sites LT and LA with 15.9 mm and 15.3 mm, respectively.
b) for fibrous structures excluded, similar results occurred (highest values LT with 14.4 mm and LA with 14.0 mm)
c) showing the relative values (d_I/D_I)*100 with fibrous structures included. The two sites LT and LA had also the highest values, accounting for more than 45%
d) showing the relative values (d_E/D_E)*100, with fibrous structures excluded.

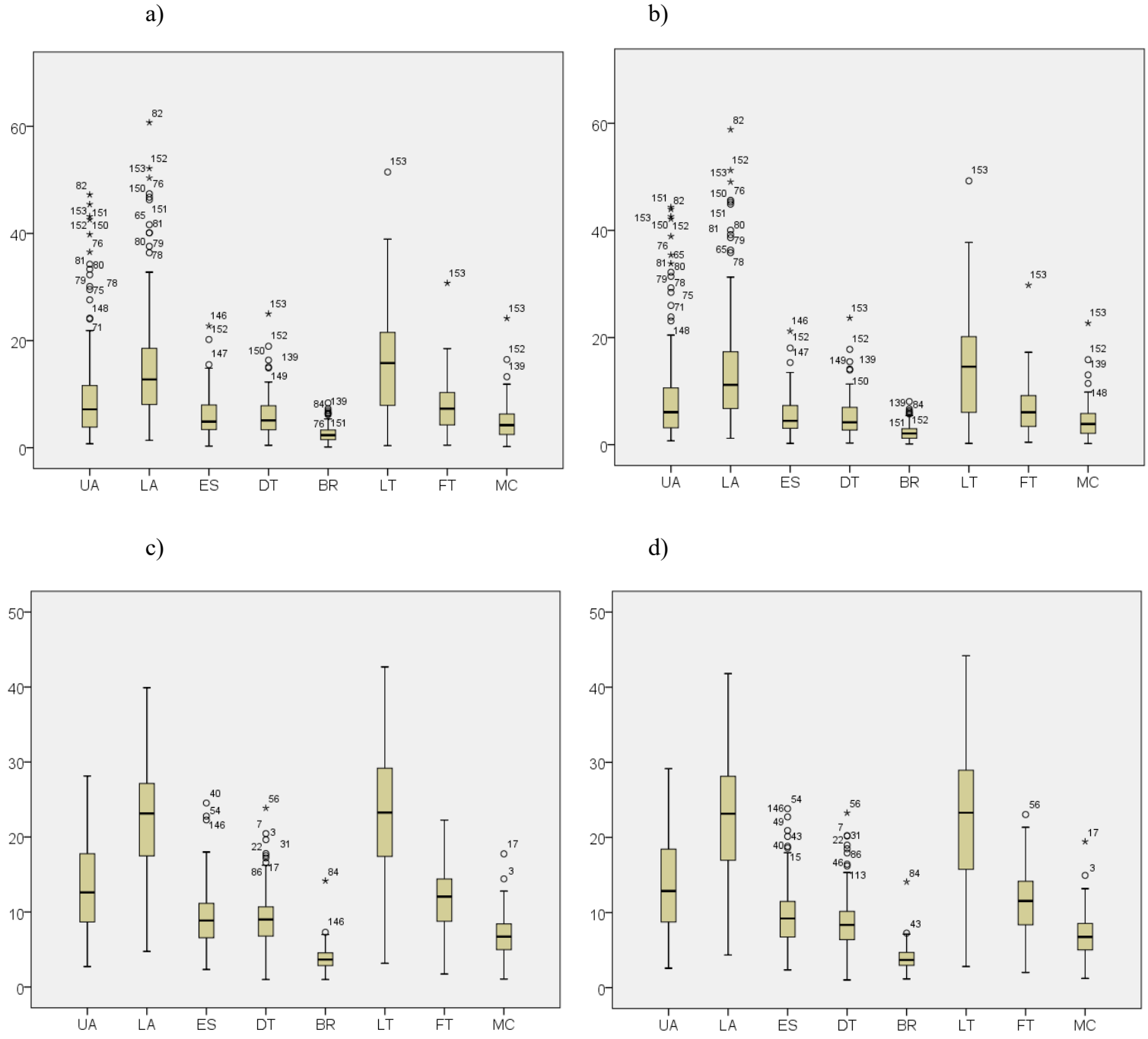

Figure 20: Boxplots showing the mean SAT thicknesses at the eight standardised sites

a) with fibrous structures included

b) with fibrous structures excluded

c) the relative values $(d_I/D_I)*100$, with fibrous structures included

d) the relative values $(d_E/D_E)*100$, with fibrous structures excluded

The corresponding values are shown in table 26

3.3.1.1 Fat patterning in males and females

To show fat patterning differences between males and females, 82 men and 71 women were investigated. Data are shown in table 27.

a) Table 27: Distribution of SAT thickness in males and females

FS included	N	(mm)	UA	LA	ES	DT	BR	LT	FT	MC	Sum
Male	82	Mean	10.0	14.9	5.1	3.9	1.9	9.5	4.9	3.1	53.5
		SD	9.7	11.4	3.3	2.3	1.3	5.9	2.7	2.1	35.7
		Median	6.0	11.2	4.2	3.8	1.7	8.7	4.4	2.7	40.3
		Min.	0.7	1.4	0.3	0.4	0.1	0.4	0.5	0.2	5.6
		Max.	47.2	60.7	14.8	12.2	6.1	25.5	14.7	9.7	167.9
Female	71	Mean	9.9	15.8	7.0	8.1	3.3	23.2	10.9	6.4	84.6
		SD	9.3	10.1	4.0	3.7	1.5	7.0	3.9	3.3	37.0
		Median	7.7	14.0	6.2	7.5	2.9	21.7	10.2	6.1	76.0
		Min.	0.9	2.1	1.9	2.5	0.7	10.1	5.3	1.8	33.5
		Max.	45.4	52.1	22.7	25.0	8.4	51.5	30.7	24.2	244.9

b)

FS excluded	N	(mm)	UA	LA	ES	DT	BR	LT	FT	MC	Sum
Male	82	Mean	9.2	13.6	4.5	3.1	1.7	8.1	4.0	2.8	47.1
		SD	9.4	11.4	2.9	2.0	1.2	5.8	2.4	2.0	34.2
		Median	5.2	9.8	3.7	3.1	1.4	6.9	3.7	2.2	35.0
		Min.	0.7	1.2	0.2	0.3	0.1	0.2	0.5	0.2	4.1
		Max.	44.0	58.8	13.5	11.0	5.5	24.4	14.1	9.3	159.2
Female	71	Mean	9.1	14.3	6.6	7.2	3.0	21.6	9.9	6.0	77.8
		SD	9.2	10.1	3.7	3.6	1.5	6.9	3.8	3.2	36.6
		Median	6.8	12.5	5.9	6.9	2.7	20.2	9.2	5.6	69.8
		Min.	0.9	1.8	1.8	2.4	0.6	7.9	4.0	1.7	27.7
		Max.	44.3	51.2	21.2	23.7	8.1	49.2	29.8	22.7	236.7

c)

FS included	N	%	UA	LA	ES	DT	BR	LT	FT	MC
Male	82	Mean	16.1	26.8	10.2	8.5	3.7	18.1	10.5	6.2
		SD	5.6	5.1	3.6	4.3	1.4	6.0	4.0	2.8
		Median	15.0	26.7	9.4	8.0	3.6	17.7	9.3	5.7
		Min.	6.6	13.0	4.1	1.0	1.0	3.2	1.7	1.1
		Max.	28.1	39.9	24.5	23.9	7.0	30.7	22.3	17.8
Female	71	Mean	10.4	17.7	8.3	9.7	4.0	28.8	13.4	7.7
		SD	5.0	4.7	3.2	2.6	1.6	5.6	2.7	2.1
		Median	9.9	17.4	7.6	9.3	3.7	29.2	13.5	7.4
		Min.	2.7	4.7	2.3	4.0	2.0	17.9	7.9	3.6
		Max.	24.3	27.3	22.8	16.6	14.2	42.7	18.7	12.4

d)

FS excluded	N	%	UA	LA	ES	DT	BR	LT	FT	MC
Male	82	Mean	16.7	27.4	10.7	7.9	3.8	17.3	9.9	6.3
		SD	5.8	6.0	3.9	4.5	1.4	6.1	4.1	3.1
		Median	15.8	27.7	9.8	7.1	3.6	16.8	8.7	6.0
		Min.	6.4	10.4	5.1	1.0	1.2	2.8	2.0	1.2
		Max.	29.2	41.8	23.8	23.3	7.3	29.3	23.1	19.5
Female	71	Mean	10.3	17.3	8.5	9.5	4.0	29.3	13.3	7.8
		SD	5.3	5.1	3.2	2.6	1.6	6.0	2.9	2.2
		Median	9.8	17.1	8.2	9.2	3.8	29.2	13.0	7.6
		Min.	2.6	4.4	2.4	4.0	1.9	17.9	8.1	3.6
		Max.	25.2	27.7	22.7	16.4	14.1	44.2	20.0	13.2

a) absolute values including fibrous structures. b) absolute values excluding fibrous structures. c) relative values including fibrous structures. d) relative values excluding fibrous structures. The corresponding results and significant differences are plotted in figure 21.

In absolute values, both results included and excluded showed the same significant differences between men and women (ES, DT, BR, LT, FT, MC and the sum of the eight sites). Using the median (data were not normally distributed) each site had higher values in women. When looking at the relative values, seven sites (UA, LA, ES, DT, LT, FT and MC) showed significant differences between men and women in this group, whereas BR did not. In men, the two sites at the abdomen UA und LA contributed 41.7% (median) to the sum of the eight thicknesses, whereas in women it was only 27.3%. In women, all sites at the extremities showed higher values. Except for BR, four of the five sites showed significant differences (Mann-Whitney U Test was used). To demonstrate distribution and outliers, boxplots are shown in figure 22.

a)

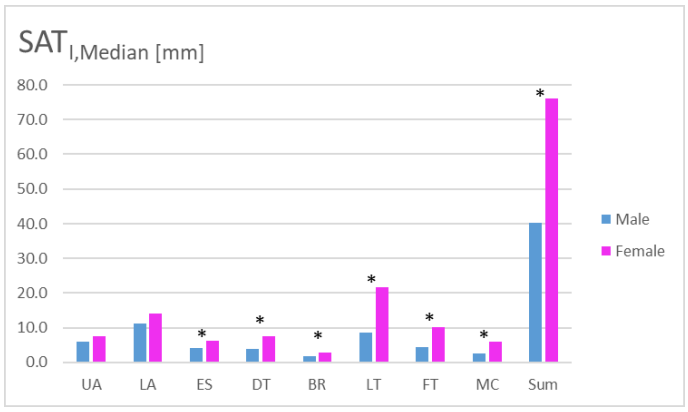

b)

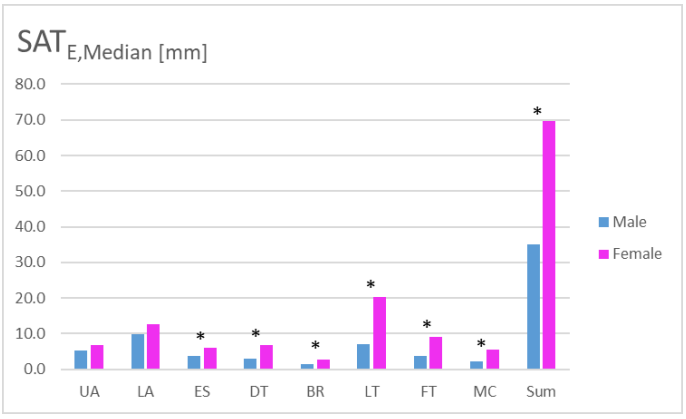

c)

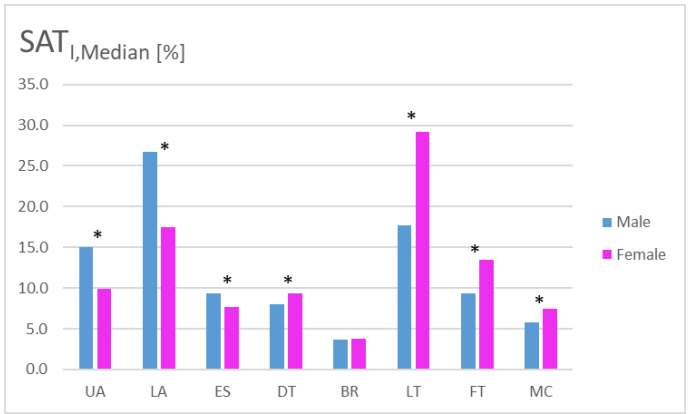

d)

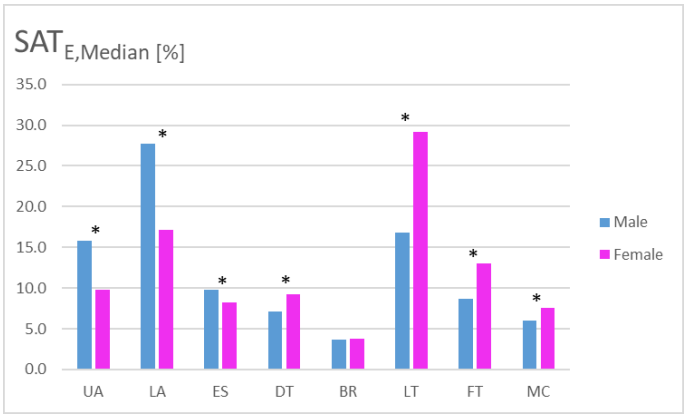

Figure 21: Sat patterning differences in men and women of 153 participants (82 men and 71 women)
a) absolute values including fibrous structures. Significant differences were found (*) for ES, DT, BR, LT, FT, MC, and the sum of the eight sites.
b) absolute values excluding fibrous structures. Significant differences were found (*) for ES, DT, BR, LT, FT, MC, and the sum of the eight sites.
c) including fibrous structures. Significant differences were found (*) for the sites: UA, LA, ES, DT, LT, FT, and MC.
d) excluding fibrous structures. Significant differences were found (*) for the sites: UA, LA, ES, DT, LT, FT, and MC.

a)

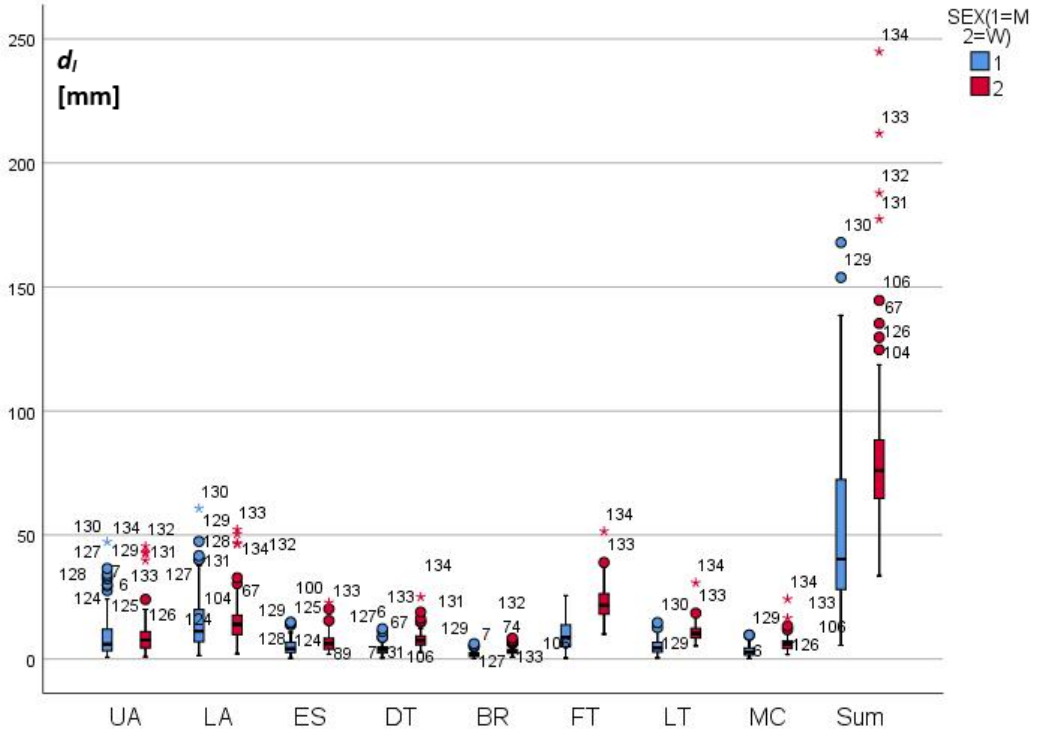
d_I
[mm]
SEX(1=M
2=W)
1
2
250
200
150
100
50
0
UA
LA
ES
DT
BR
FT
LT
MC
Sum

b)

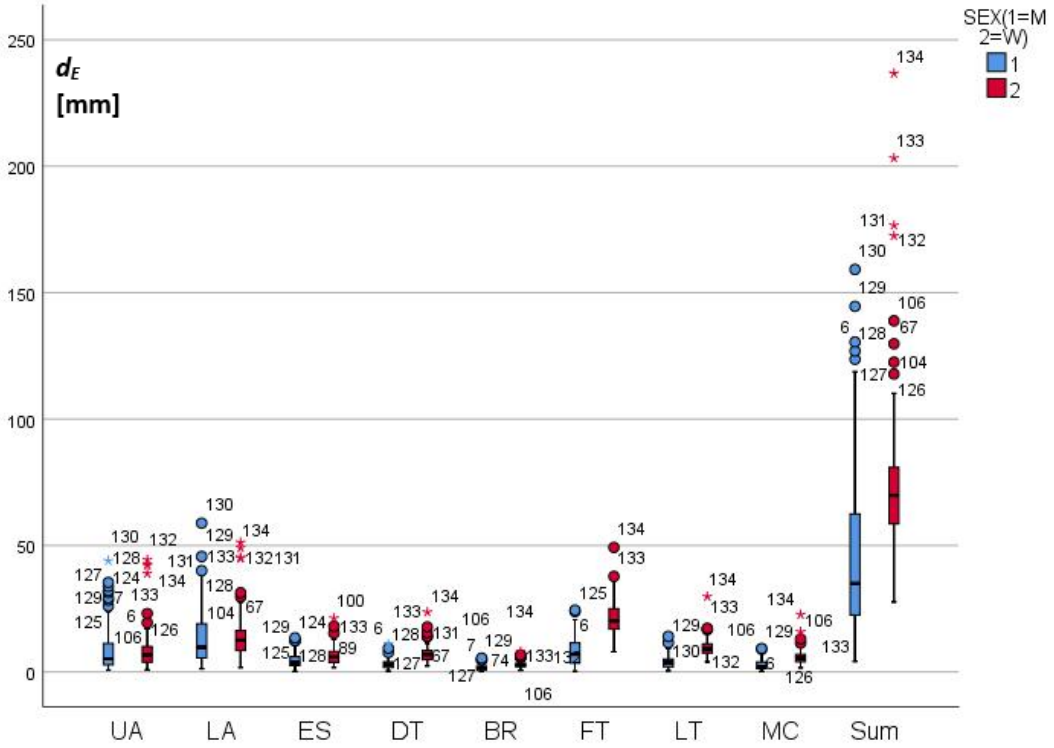
d_E
[mm]
SEX(1=M
2=W)
1
2
250
200
150
100
50
0
UA
LA
ES
DT
BR
FT
LT
MC
Sum

c)

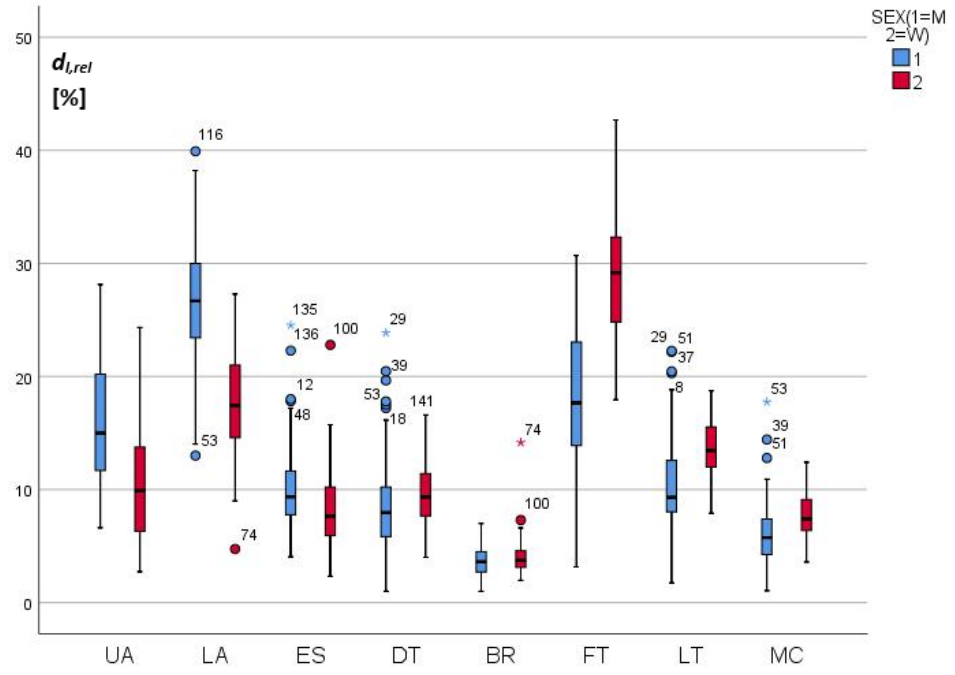

d)

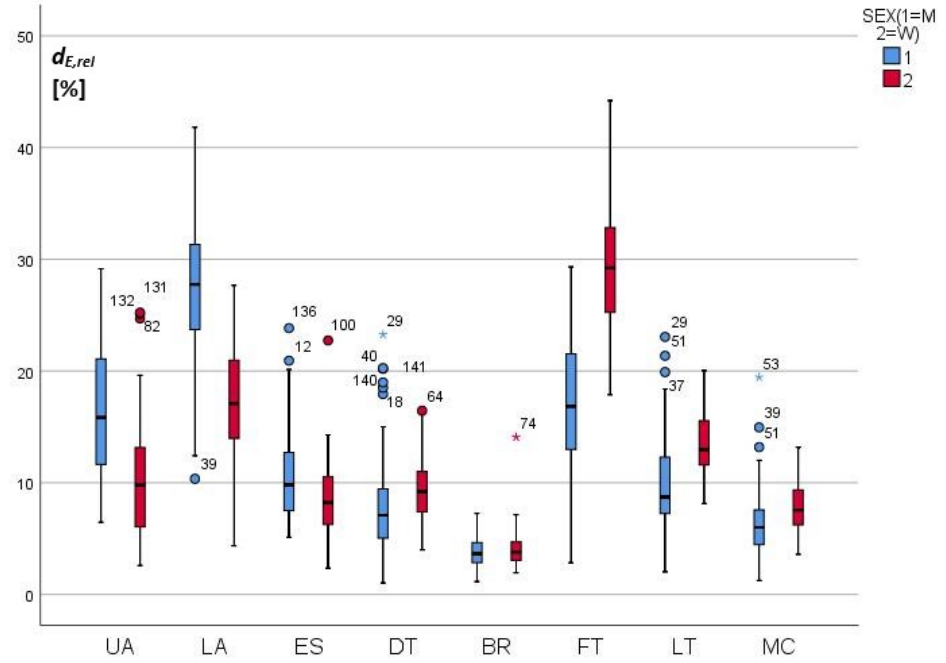

Figure 22: Boxplots of SAT patterning differences in men and women of 153 participants (82 men and 71 women)
a) absolute values including fibrous structures. Significant differences were found for ES, DT, BR, LT, FT, MC, and the sum of the eight sites
b) absolute values excluding fibrous structures. Significant differences were found for ES, DT, BR, LT, FT, MC, and the sum of the eight sites
c) including fibrous structures. Significant differences were found for the sites: UA, LA, ES, DT, LT, FT, and MC
d) excluding fibrous structures. Significant differences were found for the sites: UA, LA, ES, DT, LT, FT, and MC

3.3.1.2 Fat patterning differences between normal weight and overweight persons

The 153 participants were divided into groups according to the BMI classification of the WHO (172) . 57 normal weight men built the lean/normal weight group for men with a BMI ≤24.9 (group 3). The remaining 25 men built the overweight/obese men group with a BMI ≥25 (group 4). Women were separated into 65 lean/normal weight (BMI ≤24.9; group 5) and six overweight/obese participants (BMI ≥25; group 6). Absolute values are shown in table 28 for measurements including fibrous structures and in table 30 for excluding them. Relative values including fibrous structures are shown in figure 23 and the corresponding values can be found in table 29. Figure 24 and table 31 show the equivalent excluding fibrous structures. In the next paragraph, results for relative values with fibrous structures included are described.

Between men, significant differences were found for the sites UA, LA, DT, and FT ($p<0.05$). Sum of SAT ranged from 5.6 mm to 82.5 mm with a median of 30.3 mm in the normal weight group for men (group 3), and 36 mm to 167.9 mm and a median of 84.9 mm in group 4 (overweight/obese men according to BMI). In the groups of women, the sites UA, LA, LT and FT showed significant differences. Data are shown in figure 23 and the corresponding values in table 29. The sum *D* ranged in group 5 from 33.5 to 144.6 mm (median: 73.3mm) and in group 6 from 124.7mm to 244.9mm (median: 182.7mm). In both sexes, the proportions changed only to a higher amount in the abdominal region. In men the sites UA and LA changed from 40.1% to 51.3% of the total amount of SAT, and in women from 29.8% to 43.4%. In the female group, the total amount of the site LT dropped from 29.7% to 19.3% from normal weight to overweight persons. Comparing men and women, the same results for the normal weight group (BMI ≤24.9) occurred as in chapter 3.3.1.1, with the exception that there was no significant difference at the site DT (UA, LA, ES, LT, FT, and MC showed significant differences). In the overweight group, significant differences between men and women were found only at three sites (LA, ES, DT).

Table 28: Fat patterning in different groups with fibrous structures included

FS included	N	(mm)	UA	LA	ES	DT	BR	LT	FT	MC	Sum
Male BMI <25	57	Mean	5.8	10.1	3.9	3.3	1.4	7.4	3.9	2.4	38.2
		SD	4.3	5.9	2.2	1.7	0.8	4.7	1.8	1.7	19.7
		Median	4.6	8.1	3.7	3.2	1.4	6.3	3.7	2.1	30.3
		Min.	0.7	1.4	0.3	0.5	0.1	0.4	0.5	0.2	5.6
		Max.	21.9	27.3	10.6	8.7	3.5	18.6	9.8	8.2	82.5
Male BMI >25	25	Mean	19.6	26.0	8.0	5.4	3.2	14.4	7.2	4.9	88.6
		SD	11.8	13.3	3.7	2.7	1.3	5.7	3.1	2.1	39.2
		Median	18.6	24.9	7.9	4.8	3.2	13.0	7.3	4.6	84.9
		Min.	3.8	7.5	2.3	0.4	1.0	6.7	1.7	1.3	36.0
		Max.	47.2	60.7	14.8	12.2	6.1	25.5	14.7	9.7	167.9
Female BMI <25	65	Mean	7.6	13.3	6.6	7.3	3.0	21.9	10.2	5.8	75.7
		SD	4.2	5.4	3.5	2.4	1.3	5.3	2.8	2.1	19.9
		Median	7.2	13.0	6.0	7.4	2.8	21.3	10.0	5.9	73.3
		Min.	0.9	2.1	1.9	2.5	0.7	10.1	5.3	1.8	33.5
		Max.	20.0	30.4	22.7	14.9	7.3	35.3	17.9	13.3	144.6
Female BMI >25	6	Mean	34.6	42.7	12.0	16.6	6.1	36.6	18.4	13.5	180.3
		SD	13.3	10.0	5.6	4.9	1.4	8.8	6.6	5.9	45.5
		Median	41.2	46.5	12.4	15.7	5.9	36.2	17.0	11.1	182.7
		Min.	12.5	27.9	2.9	11.9	4.5	24.8	11.4	8.8	124.7
		Max.	45.4	52.1	20.2	25.0	8.4	51.5	30.7	24.2	244.9

57 normal weight men built the normal weight group with a BMI ≤24.9 (group 3). 25 men built the overweight/obese group with a BMI ≥25 (group 4). Women were separated into 65 lean and normal weight (BMI ≤24.9; group 5), and 6 overweight and obese participants (BMI ≥25; group 6)

Table 29: Relative values of fat patterning in different groups with fibrous structures included

FS included	N	%	UA	LA	ES	DT	BR	LT	FT	MC
Male BMI <25	57	Mean	14.1	25.9	10.6	9.5	3.6	18.5	11.4	6.3
		SD	4.6	5.2	4.1	4.6	1.6	6.5	4.3	3.1
		Median	14.1	26.0	9.8	9.1	3.3	18.6	10.6	6.0
		Min.	6.6	13.0	4.1	1.8	1.0	3.2	1.7	1.1
		Max.	27.2	38.2	24.5	23.9	7.0	30.7	22.3	17.8
Male BMI >25	25	Mean	20.5	28.8	9.1	6.4	3.8	17.2	8.4	5.8
		SD	5.3	4.6	1.9	2.4	1.1	4.7	2.4	2.0
		Median	21.9	29.3	8.8	6.0	3.7	16.2	8.3	5.2
		Min.	10.6	20.7	6.1	1.0	2.1	9.0	3.9	2.9
		Max.	28.1	39.9	12.6	11.8	6.3	30.3	14.6	10.9
Female BMI <25	65	Mean	9.6	17.2	8.4	9.8	4.0	29.5	13.7	7.7
		SD	4.2	4.5	3.2	2.7	1.7	5.2	2.5	2.1
		Median	9.7	17.1	8.0	9.3	3.9	29.7	13.7	7.4
		Min.	2.7	4.7	3.5	4.0	2.0	19.6	7.9	3.6
		Max.	24.3	27.3	22.8	16.6	14.2	42.7	18.7	12.4
Female BMI >25	6	Mean	18.9	23.8	6.6	9.3	3.4	20.6	10.1	7.4
		SD	5.5	2.0	2.8	1.6	0.5	3.6	2.0	2.0
		Median	19.0	24.4	6.6	9.4	3.4	19.3	9.2	7.3
		Min.	9.2	20.6	2.3	6.5	2.8	17.9	8.4	4.9
		Max.	24.3	26.4	9.5	11.1	4.3	27.5	12.8	9.9

The corresponding results and significant differences are plotted in figure 23.

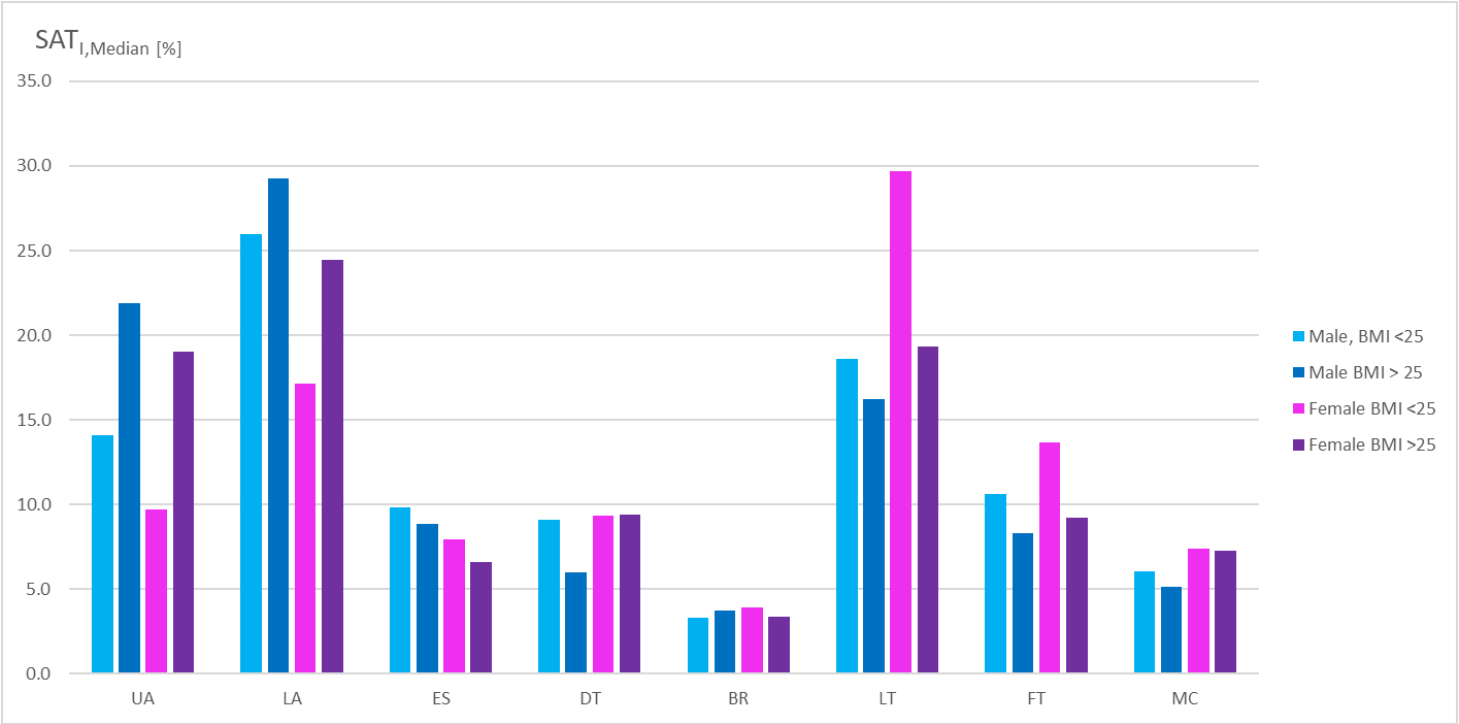

Figure 23: Fat patterning in different groups with fibrous structures included
Between men, significant differences were found for the sites UA, LA, DT, and FT ($p<0.05$). Between women, the sites UA, LA, LT and FT showed significant differences. Between men and women, the sites UA, LA, ES, LT, FT, and MC showed significant differences.

When fibrous structures were excluded in men, significant differences were found at four sites (UA, LA, DT and FT). Compared to the included values, ES showed no significant differences.

Table 30: Fat patterning in different groups with fibrous structures excluded

FS excluded	N	(mm)	UA	LA	ES	DT	BR	LT	FT	MC	Sum
Male BMI <25	57	Mean	5.1	8.8	3.5	2.6	1.2	6.0	3.1	2.1	32.4
		SD	3.9	5.9	1.9	1.5	0.7	4.3	1.6	1.5	18.4
		Median	3.7	6.5	3.4	2.5	1.1	5.0	3.1	1.9	24.7
		Min.	0.7	1.2	0.2	0.3	0.1	0.2	0.5	0.2	4.1
		Max.	19.7	26.0	9.3	7.1	3.1	17.1	9.3	7.5	74.8
Male BMI >25	25	Mean	18.5	24.7	6.9	4.5	2.8	12.9	6.0	4.4	80.8
		SD	11.6	13.2	3.4	2.5	1.3	5.9	2.9	2.0	38.4
		Median	17.4	22.9	6.5	3.8	2.9	11.5	6.0	4.3	76.6
		Min.	3.0	6.7	2.0	0.4	0.9	5.2	1.3	1.2	28.8
		Max.	44.0	58.8	13.5	11.0	5.5	24.4	14.1	9.3	159.2
Female BMI <25	65	Mean	6.8	11.9	6.2	6.5	2.8	20.4	9.2	5.4	69.0
		SD	4.0	5.3	3.4	2.2	1.2	5.3	2.7	2.0	19.6
		Median	6.5	11.5	5.6	6.7	2.5	19.4	9.0	5.4	66.3
		Min.	0.9	1.8	1.8	2.4	0.6	7.9	4.0	1.7	27.7
		Max.	19.5	29.6	21.2	13.9	6.7	32.0	16.7	13.0	138.9
Female BMI >25	6	Mean	33.9	41.4	11.1	15.6	5.7	34.8	17.5	12.8	172.8
		SD	13.2	10.1	4.9	4.7	1.4	8.9	6.5	5.6	44.5
		Median	40.5	45.1	11.9	14.8	5.4	34.1	16.1	10.6	174.5
		Min.	12.0	26.6	2.8	11.3	4.3	22.4	10.7	8.2	117.8
		Max.	44.3	51.2	18.1	23.7	8.1	49.2	29.8	22.7	236.7

57 normal weight men built the normal weight group with a BMI ≤24.9 (group 3). 25 men built the overweight/obese group with a BMI ≥25 (group 4). Women were separated into 65 lean and normal weight (BMI ≤24.9; group 5), and 6 overweight and obese participants (BMI ≥25; group 6)

Comparing the groups 5 and 6 and the groups 3 and 5, the same results were found as when fibrous structures were included: significant differences at UA, LA, LT, FT and UA, LA, ES, LT, FT, MC, respectively. Comparing overweight men and women, additional to the sites LA, ES and DT the site FT showed significant differences excluding fibrous structures.

Table 31: Relative values of fat patterning in different groups with fibrous structures excluded

FS excluded	N	%	UA	LA	ES	DT	BR	LT	FT	MC
Male BMI <25	57	Mean	14.7	26.3	11.5	8.9	3.8	17.4	10.8	6.5
		SD	4.7	6.2	4.2	4.9	1.5	6.6	4.3	3.3
		Median	14.5	26.3	10.4	8.2	3.5	17.4	9.6	6.0
		Min.	6.4	10.4	5.2	1.8	1.2	2.8	2.0	1.2
		Max.	27.2	41.2	23.8	23.3	7.3	29.2	23.1	19.5
Male BMI >25	25	Mean	21.2	30.0	8.7	5.8	3.7	16.9	7.8	5.9
		SD	5.6	4.9	2.0	2.4	1.1	4.8	2.4	2.4
		Median	23.3	30.6	8.6	5.4	3.8	15.3	7.4	5.4
		Min.	10.3	20.1	5.1	1.0	1.9	8.5	3.2	2.7
		Max.	29.2	41.8	13.8	11.2	6.6	29.3	13.5	12.0
Female BMI <25	65	Mean	9.4	16.7	8.7	9.5	4.0	30.2	13.6	7.8
		SD	4.4	4.8	3.2	2.7	1.7	5.5	2.8	2.2
		Median	8.7	16.9	8.3	9.2	3.9	30.2	13.4	7.6
		Min.	2.6	4.4	3.5	4.0	1.9	18.7	8.1	3.6
		Max.	25.2	27.7	22.7	16.4	14.1	44.2	20.0	13.2
Female BMI >25	6	Mean	19.3	24.0	6.4	9.1	3.4	20.4	10.1	7.3
		SD	5.8	2.1	2.6	1.5	0.5	3.9	2.1	2.1
		Median	19.4	24.7	6.3	9.3	3.3	18.8	9.1	7.3
		Min.	9.3	20.7	2.4	6.4	2.8	17.9	8.3	4.7
		Max.	25.1	26.3	9.2	10.9	4.2	28.2	13.0	9.7

The corresponding results and significant differences are plotted in figure 24.

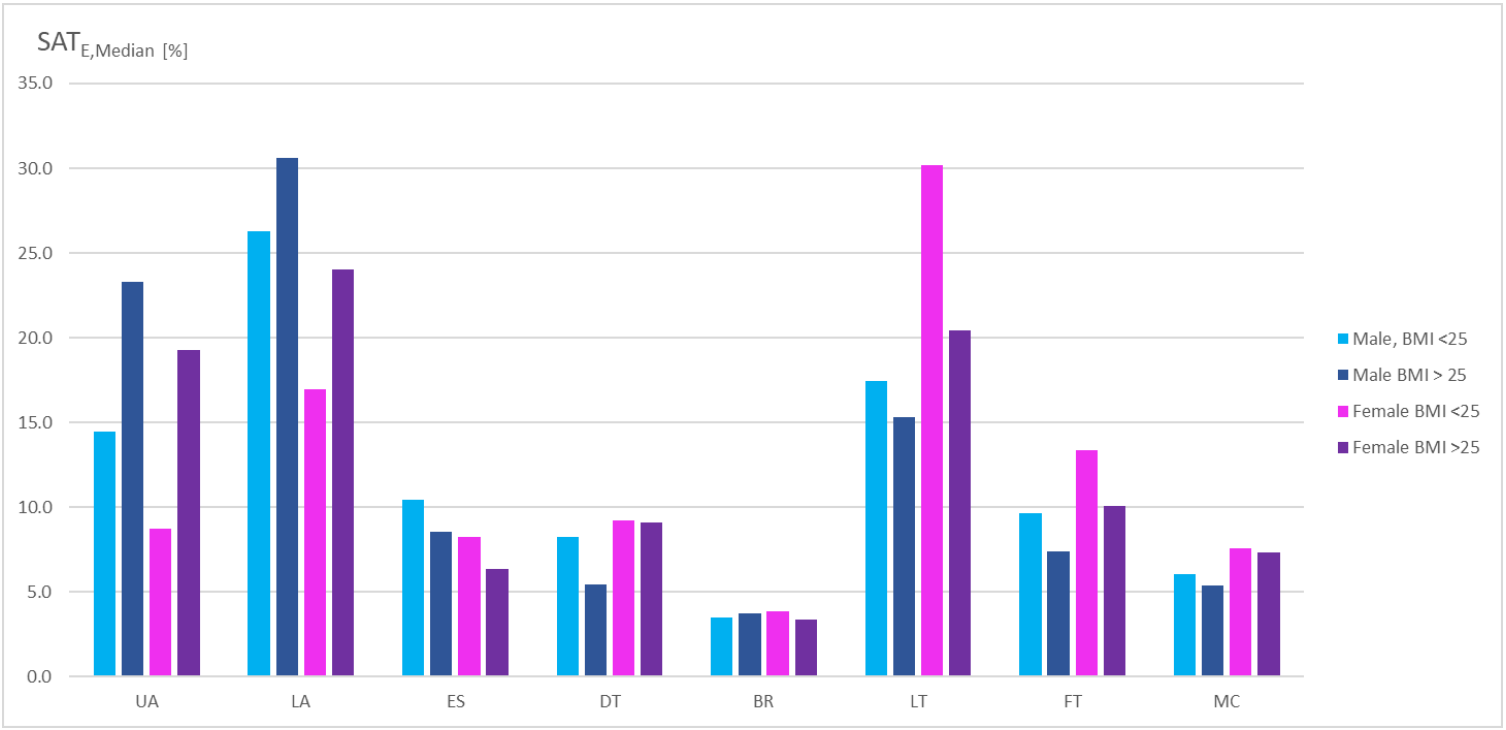

Figure 24:Fat patterning in different groups with fibrous structures excluded
Significant differences ($p<0.05$) were found in men for the sites UA, LA, DT, and FT; in women for UA, LA, LT and FT; and between men and women for UA, LA, ES, LT, FT, and MC

3.3.2 Fibrous structures

As described in the methods section, fibrous structures (FS) embedded in the SAT can also be quantified (see figure 2). The amount of fibrous structures (sum) ranged from 2.8% to approximately one third of the total measured SAT thickness. Median was 6.5 mm. Looking at each site individually, DT showed the highest amount of all sites with a median of 15.34%. Table 32 shows the absolute and relative amount of FS embedded in the SAT. Figure 25 shows the distribution a) for absolute values given in mm and b) for relative values given in percent.

Table 32: Amount of fibrous structures embedded in the SAT

FS	(mm)	UA	LA	ES	DT	BR	LT	FT	MC	Sum
N=153	Mean	0.8	1.4	0.5	0.8	0.3	1.5	1.0	0.4	6.6
	SD	0.5	0.6	0.6	0.4	0.2	0.7	0.5	0.2	1.9
	Median	0.7	1.3	0.3	0.8	0.2	1.4	0.9	0.4	6.5
	Min.	0.0	0.1	0.0	0.0	0.0	0.0	0.0	0.0	1.0
	Max.	3.3	3.8	2.3	1.7	0.9	3.7	2.6	1.5	11.4
	%	UA	LA	ES	DT	BR	LT	FT	MC	Sum
	Mean	11.3	12.7	8.6	17.5	10.6	13.6	15.4	10.2	12.2
	SD	6.6	8.1	8.0	10.2	8.1	10.2	8.8	7.8	5.7
	Median	10.72	10.49	6.11	15.34	8.61	9.75	13.96	8.23	10.87
	Min.	0.5	0.2	0.2	0.2	0.0	1.0	2.2	0.6	2.8
	Max.	33.8	45.0	42.0	59.0	44.6	51.5	47.4	59.2	29.3

The upper half of the table shows the absolute values in mm and the lower half the relative values ($d_{FS,rel}=100\cdot((d_I-d_E)/d_I)$) in percent.

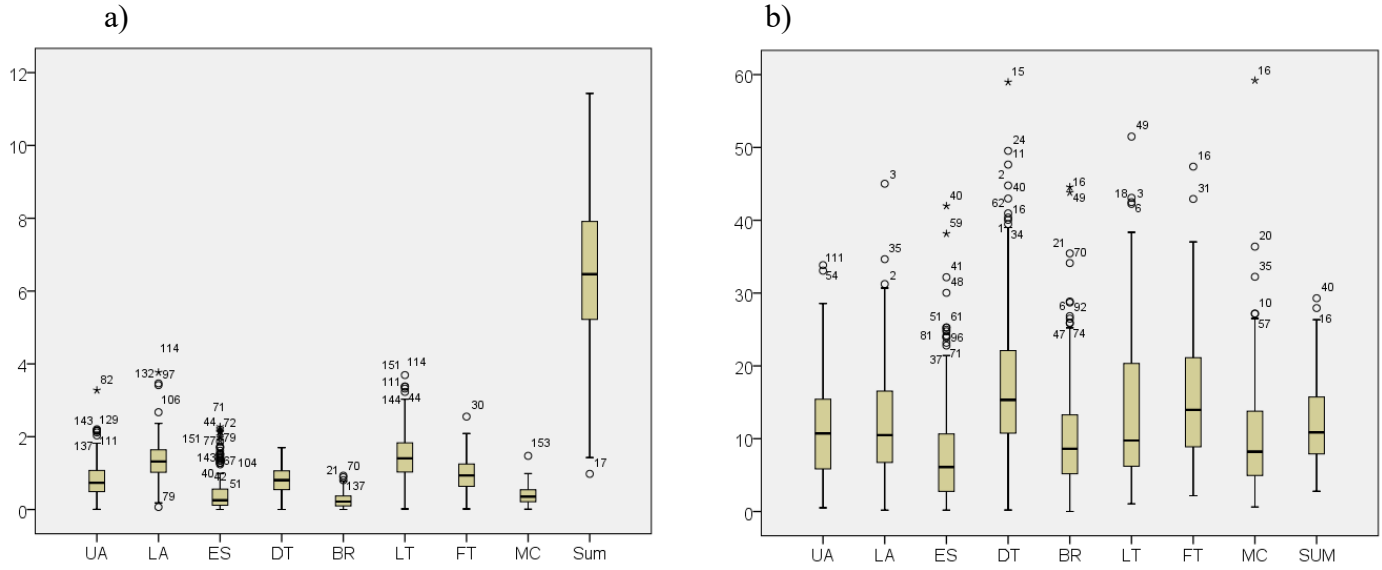

Figure 25: Distribution of the amount of fibrous structures embedded in the SAT

Comparing the absolute values of fibrous structures included in the SAT between men and women (see table 33), significant differences were only found for the site MC ($p<0.05$). Median of the sum of embedded FS was 6.3 mm for men and 6.7 mm for women. Using the

relative values ($d_{FS,rel}=100\cdot((d_I-d_E)/d_I)$) differences ($p<0.05$) were found for the following sites ES, DT, LT, FT, MC and the total amount (sum) of fibrous structures in the SAT. Median for the sum was 15.3% in men and 9.2% in women (see table 34).

Table 33:Differences in the amount of fibrous structures in SAT between men and women

FS	N	(mm)	UA	LA	ES	DT	BR	LT	FT	MC	Sum
Male	82	Mean	0.8	1.3	0.6	0.8	0.2	1.4	0.9	0.3	6.4
		SD	0.5	0.5	0.7	0.4	0.2	0.7	0.5	0.2	2.1
		Median	0.8	1.3	0.3	0.7	0.2	1.4	0.8	0.3	6.3
		Min.	0.0	0.1	0.0	0.0	0.0	0.0	0.0	0.0	1.0
		Max.	3.3	2.4	2.3	1.7	0.9	3.4	2.6	0.9	11.2
Female	71	Mean	0.8	1.4	0.4	0.9	0.3	1.6	1.0	0.4	6.8
		SD	0.5	0.6	0.5	0.4	0.2	0.7	0.4	0.2	1.7
		Median	0.7	1.3	0.2	0.9	0.2	1.6	1.0	0.4	6.7
		Min.	0.0	0.4	0.0	0.0	0.0	0.3	0.2	0.0	3.6
		Max.	2.2	3.8	2.2	1.7	0.9	3.7	1.9	1.5	11.4

Table 34: Relative differences in the amount of fibrous structures in SAT between men and women

FS %	N	%	UA	LA	ES	DT	BR	LT	FT	MC	Sum
Male	82	Mean	11.5	13.5	10.8	22.7	11.9	19.1	20.1	12.7	15.1
		SD	6.8	9.2	9.2	10.9	9.6	10.9	8.9	9.3	5.8
		Median	10.8	10.9	8.7	21.0	9.2	18.0	19.8	11.4	15.3
		Min.	0.5	0.2	0.4	0.2	0.0	1.8	2.4	0.6	5.2
		Max.	33.8	45.0	42.0	59.0	44.6	51.5	47.4	59.2	29.3
Female	71	Mean	11.0	11.7	5.9	11.5	9.1	7.3	10.0	7.4	8.9
		SD	6.4	6.7	5.4	4.8	5.6	3.7	4.4	4.1	3.0
		Median	10.4	10.3	4.3	11.3	8.1	7.1	10.1	6.6	9.2
		Min.	3.6	1.0	1.7	0.2	0.3	0.2	1.0	2.2	1.0
		Max.	33.1	29.7	23.9	23.9	26.5	21.3	23.8	19.0	17.5

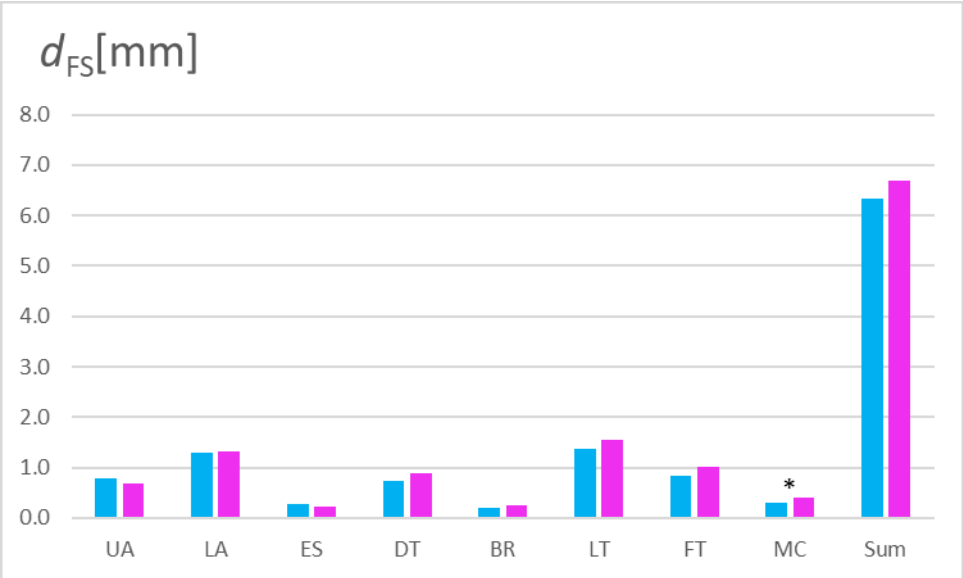

Figure 26: Differences in the amount of fibrous structures in SAT between men and women
Significant differences (*) were found for the site MC

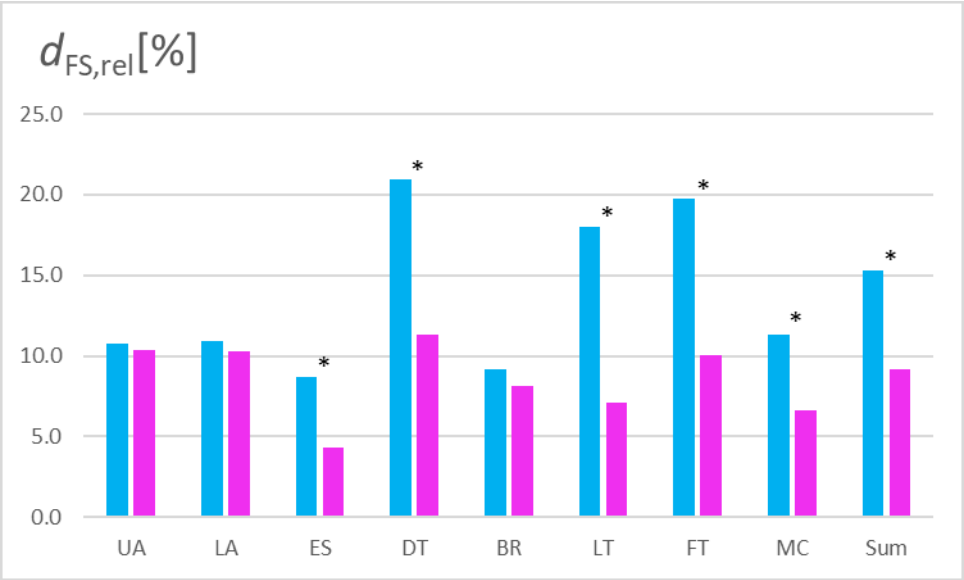

Figure 27: Relative differences in the amount of fibrous structures in SAT between men and women
Significant differences (*) were found for the sites ES, DT, LT, FT, MC, and the sum of the eight sites

Between the individual groups (group 3: men BMI ≤24.9, group 4: men BMI ≥25, group 5: women BMI ≤24.9, and group 6: women BMI ≥25), the following site differences were detected for absolute values: 1) group 3 – group 4: UA, ES, DT, BR, FT, MC and the sum of all sites; group 3 – group 5: DT, BR, FT, MC, and the sum of all sites; group 3 – group 6: DT, BR, and MC; 2) group 4 – group 5: UA, ES, and the sum of all sites; group 4 – group 6: no sites showed significant differences; 3) group 5 – group 6: MC. The data are presented in table 35 and figure 28

Table 35: Absolute differences in the amount of fibrous structures in SAT in normal weight and overweight men and normal weight and overweight women

FS	N	(mm)	UA	LA	ES	DT	BR	LT	FT	MC	SUM
Male BMI <25	57	Mean	0.7	1.3	0.4	0.7	0.2	1.4	0.8	0.3	5.8
		SD	0.5	0.5	0.5	0.4	0.2	0.7	0.4	0.2	2.0
		Median	0.7	1.2	0.2	0.6	0.2	1.4	0.7	0.3	5.6
		Min.	0.0	0.2	0.0	0.0	0.0	0.0	0.0	0.0	1.0
		Max.	2.2	2.4	2.2	1.7	0.8	3.4	2.6	0.9	11.2
Male BMI >25	25	Mean	1.0	1.3	1.1	1.0	0.3	1.5	1.2	0.4	7.9
		SD	0.6	0.5	0.8	0.4	0.2	0.6	0.5	0.2	1.5
		Median	0.9	1.3	1.3	1.0	0.3	1.4	1.1	0.4	8.0
		Min.	0.3	0.1	0.1	0.0	0.0	0.7	0.4	0.1	4.6
		Max.	3.3	2.2	2.3	1.7	0.9	3.0	2.1	0.8	10.5
Female BMI <25	65	Mean	0.8	1.4	0.4	0.8	0.3	1.6	1.0	0.4	6.7
		SD	0.5	0.7	0.4	0.4	0.2	0.7	0.4	0.2	1.7
		Median	0.7	1.3	0.2	0.9	0.2	1.6	1.0	0.4	6.6
		Min.	0.0	0.4	0.0	0.0	0.0	0.3	0.2	0.0	3.6
		Max.	2.2	3.8	1.7	1.7	0.9	3.4	1.9	1.0	11.4
Female BMI >25	6	Mean	0.7	1.3	0.9	1.0	0.3	1.8	0.9	0.7	7.6
		SD	0.3	0.2	1.0	0.2	0.2	1.2	0.3	0.4	2.3
		Median	0.7	1.3	0.4	1.0	0.4	1.7	0.8	0.6	7.5
		Min.	0.4	0.9	0.1	0.6	0.1	0.7	0.6	0.4	4.9
		Max.	1.1	1.5	2.2	1.3	0.6	3.7	1.2	1.5	11.3

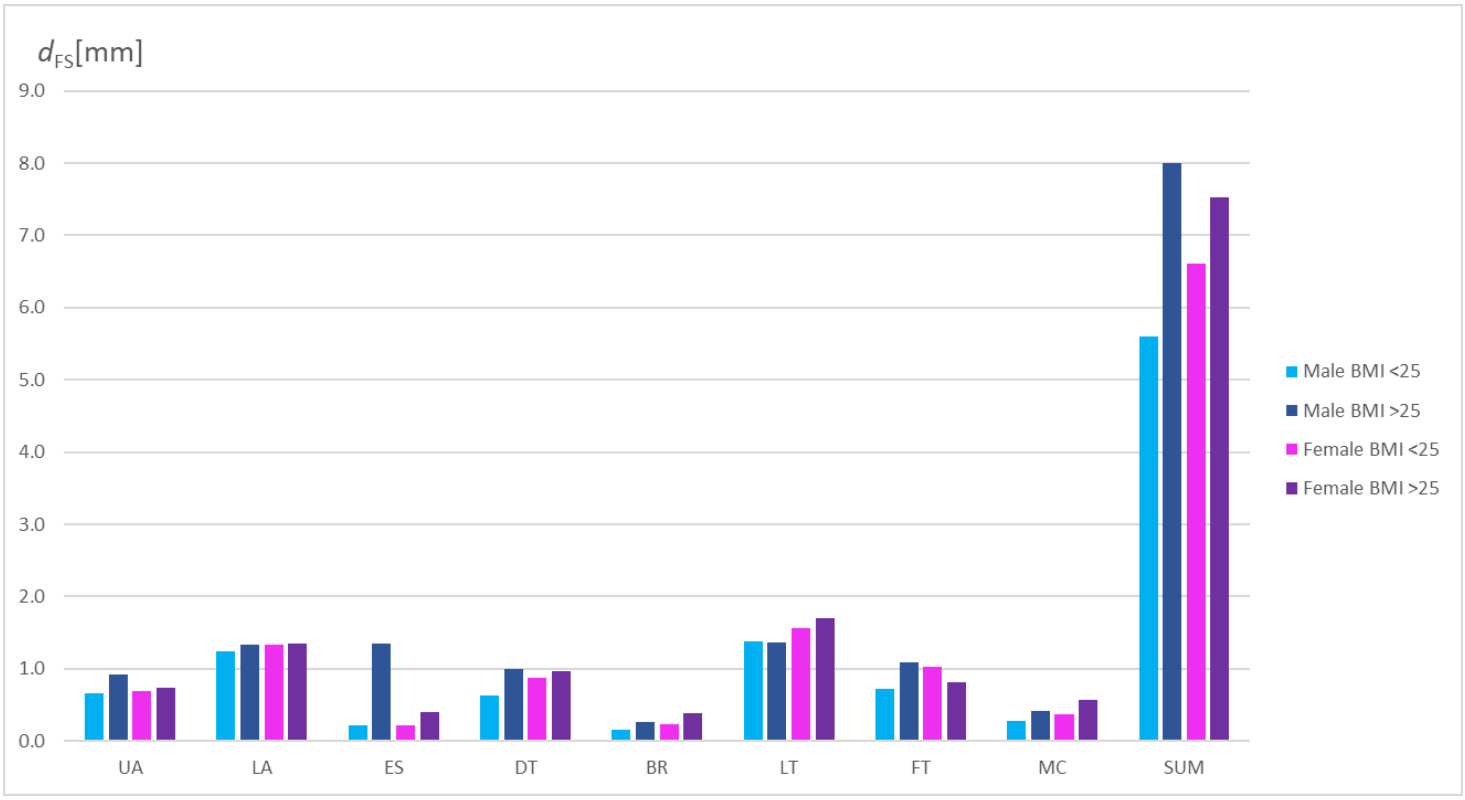

Figure 28: Absolut differences in the amount of fibrous structures in SAT in normal weight and overweight men and normal weight and overweight women
Group 3 = men BMI ≤24.9, group 4 = men BMI ≥25, group 5 = women BMI ≤24.9, and group 6 = women BMI ≥25. Significant differences were found: group 3 – group 4: UA, ES, DT, BR, FT, MC and the sum of all sites; group 3 – group 5: DT, BR, FT, MC, and the sum of all sites; group 3 – group 6: DT, BR, and MC; group 4 – group 5: UA, ES, and the sum of all sites; group 5 – group 6: MC.

The following site differences were measured for relative values: 1) group 3 – group 4: UA, LA, ES, LT, and the sum of all sites; group 3 – group 5: LA, ES, DT, LT, FT, MC, and the sum of all sites; group 3 – group 6: UA, LA, DT, LT, FT, MC, and the sum of all sites; 2) group 4 – group 5: UA, LA, ES, DT, LT, FT, MC; group 4 – group 6: all sites showed significant differences; 3) group 5 – group 6: UA, LA, DT, FT, and the sum of all sites. No significant differences in the sum of eight sites could be found between overweight/obese men (group 4) compared to normal weight women (group 5). Data are presented in table 36 and figure 29.

Table 36: Relative differences in the amount of fibrous structures in SAT in normal weight and overweight men and normal weight and overweight women

FS %	N	%	UA	LA	ES	DT	BR	LT	FT	MC	SUM
Male BMI <25	57	Mean	13.2	16.5	9.5	24.0	11.9	22.0	21.0	14.0	17.1
		SD	6.7	9.1	9.0	11.6	10.2	10.9	9.8	10.4	5.3
		Median	11.9	15.2	6.6	22.4	9.3	20.7	21.4	13.0	16.2
		Min.	0.5	2.8	0.4	0.2	0.0	1.8	2.4	0.6	5.5
		Max.	33.8	45.0	42.0	59.0	44.6	51.5	47.4	59.2	29.3
Male BMI >25	25	Mean	7.5	6.5	13.9	19.6	11.8	12.4	17.8	9.8	10.4
		SD	5.5	3.9	9.0	8.5	8.3	7.6	6.2	4.9	4.2
		Median	5.9	5.8	11.1	18.1	9.1	9.9	18.8	9.5	9.7
		Min.	0.9	0.2	1.6	7.2	2.4	4.2	8.5	3.5	5.8
		Max.	22.1	16.5	38.2	41.0	34.1	30.1	27.3	24.0	20.2
Female BMI <25	65	Mean	11.8	12.5	5.9	12.0	9.5	7.5	10.5	7.6	9.3
		SD	6.0	6.4	5.4	4.7	5.6	3.6	4.3	4.2	2.8
		Median	11.1	11.1	4.1	12.2	8.1	7.2	10.6	6.8	9.3
		Min.	1.5	2.5	0.2	0.3	0.2	1.0	2.2	1.0	3.7
		Max.	33.1	29.7	23.9	23.9	26.5	21.3	23.8	19.0	17.5
Female BMI >25	6	Mean	2.4	3.3	6.0	6.0	5.6	5.2	5.0	5.0	4.3
		SD	1.1	1.2	5.4	1.0	3.0	3.8	1.5	1.3	1.2
		Median	2.4	3.1	4.8	5.7	5.6	3.7	4.9	4.9	4.1
		Min.	1.0	1.7	0.7	5.2	1.5	1.8	3.1	3.7	2.8
		Max.	3.9	4.7	14.2	7.9	8.8	10.5	6.7	6.8	6.0

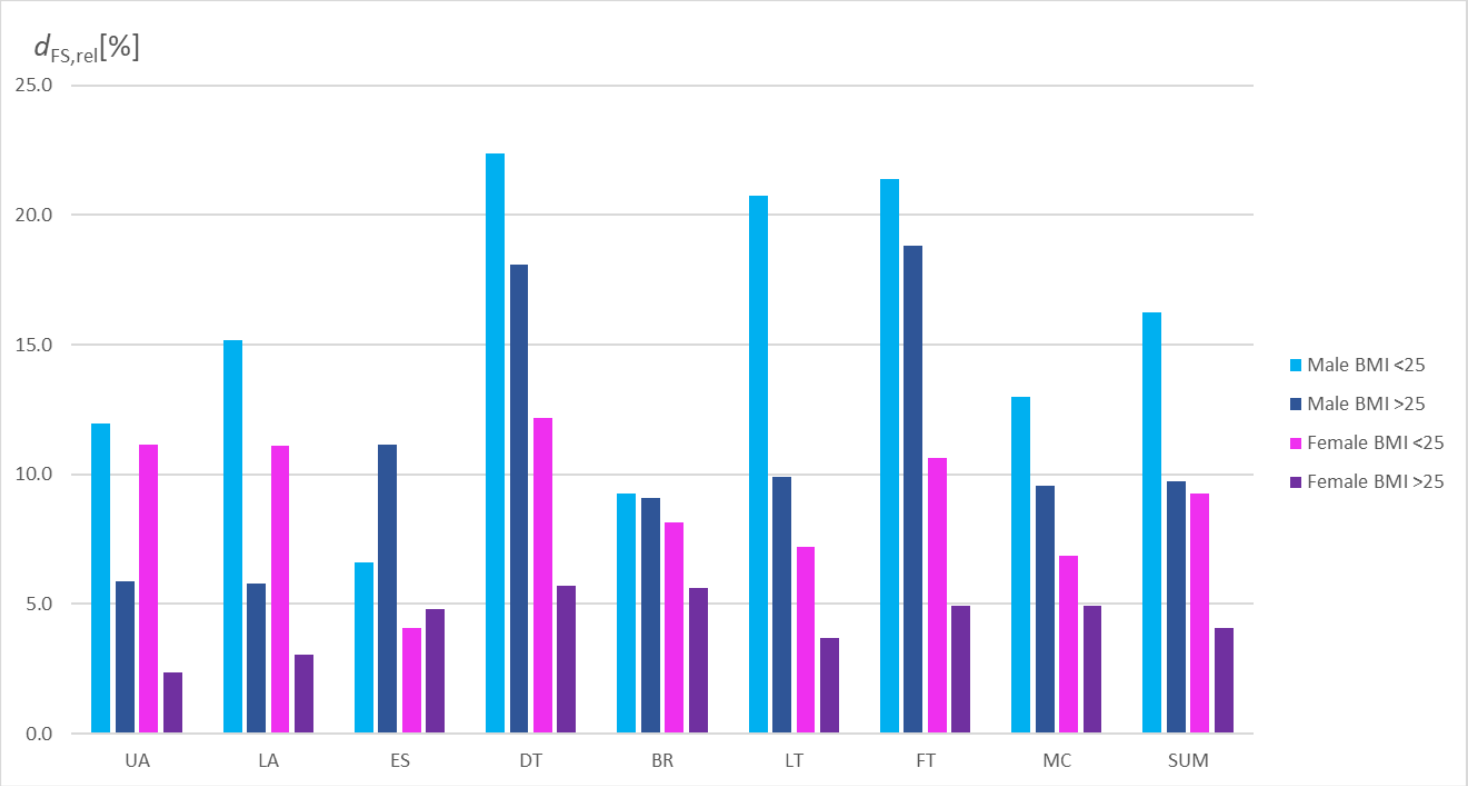

Figure 29:Relative differences in the amount of fibrous structures in SAT in normal weight and overweight men, and normal weight and overweight women
Group 3 = men BMI ≤24.9, group 4 = men BMI ≥25, group 5 = women BMI ≤24.9, and group 6 = women BMI ≥25. Significant differences were found: group 3 – group 4: UA, LA, ES, LT, and the sum of all sites; group 3 – group 5: LA, ES, DT, LT, FT, MC, and the sum of all sites; group 3 – group 6: UA, LA, DT, LT, FT, MC, and the sum of all sites; 2) group 4 – group 5: UA, LA, ES, DT, LT, FT, MC; group 4 – group 6: all sites showed significant differences; 3) group 5 – group 6: UA, LA, DT, FT, and the sum of all sites.

3.3.3 SAT tissue and relative body weight

Figures 30a and b show the correlations between the sum of the eight standardised sites (*D*) and the BMI of all 153 participants. Spearman´s correlation coefficient was ρ = 0.346 ($p<0.05$) including fibrous structures and ρ = 0.335 ($p<0.05$) excluding fibrous structures. When using the mass index (MI_1) instead of the BMI ρ was 0.322 ($p<0.05$) and 0.310 ($p<0.05$) respectively (see figures 30c and d).

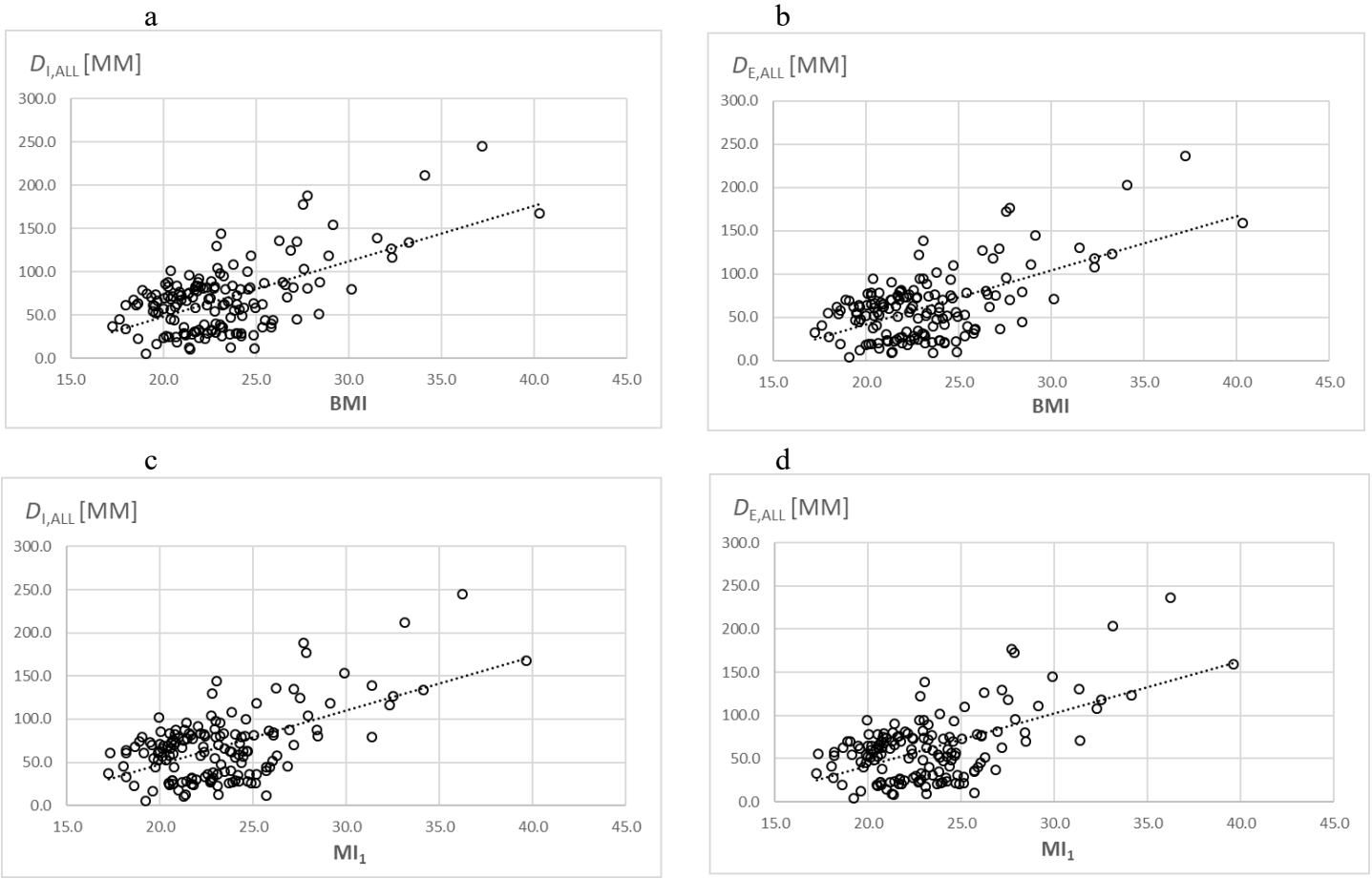

Figure 30: Correlations between the sum of the eight standardises sites (*D*): the BMI (a,b), and the MI (c,d)
a) Including fibrous structures, spearman´s correlation coefficient was ρ = 0.346 ($p<0.05$) and ρ = 0.335 excluding fibrous structures (b). Using the mass index (MI_1) ρ was 0.322 (c) and 0.310 (d) respectively.

Distinguishing between sexes, for males (N = 82) the following correlation coefficient between the sum *D* and the BMI resulted: ρ = 0.720 including, and ρ = 0.716 ($p<0.05$) excluding fibrous structures. For the mass index ρ = 0.729 and 0.727 ($p<0.05$) resulted. Data are shown in figure 31.

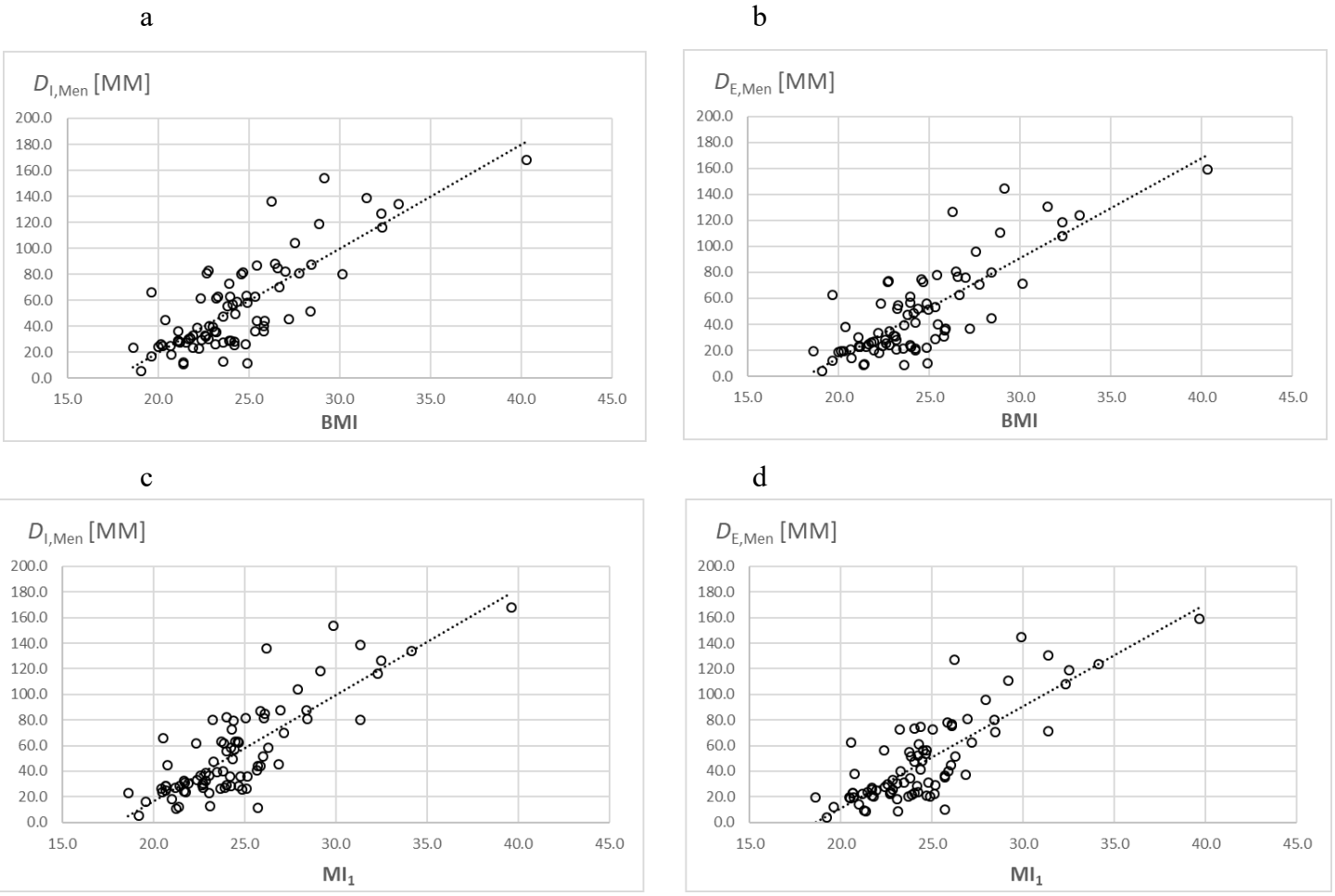

Figure 31: Correlations between the sum of the eight standardised sites (D): the BMI (a,b), and the MI_1 (c,d) in men
$\rho = 0.720$ ($p<0.05$) including (a) and $\rho = 0.716$ (b) excluding fibrous structures. For the MI_1 $\rho = 0.729$ (c) and 0.727 (d) resulted.

In 71 women the correlation coefficient for the sum D_I and the BMI was $\rho = 0.710$ and for D_E 0.714 ($p<0.05$). Spearman´s rho was 0.708 comparing D_I with the MI_1 and 0.710 excluding fibrous structures.

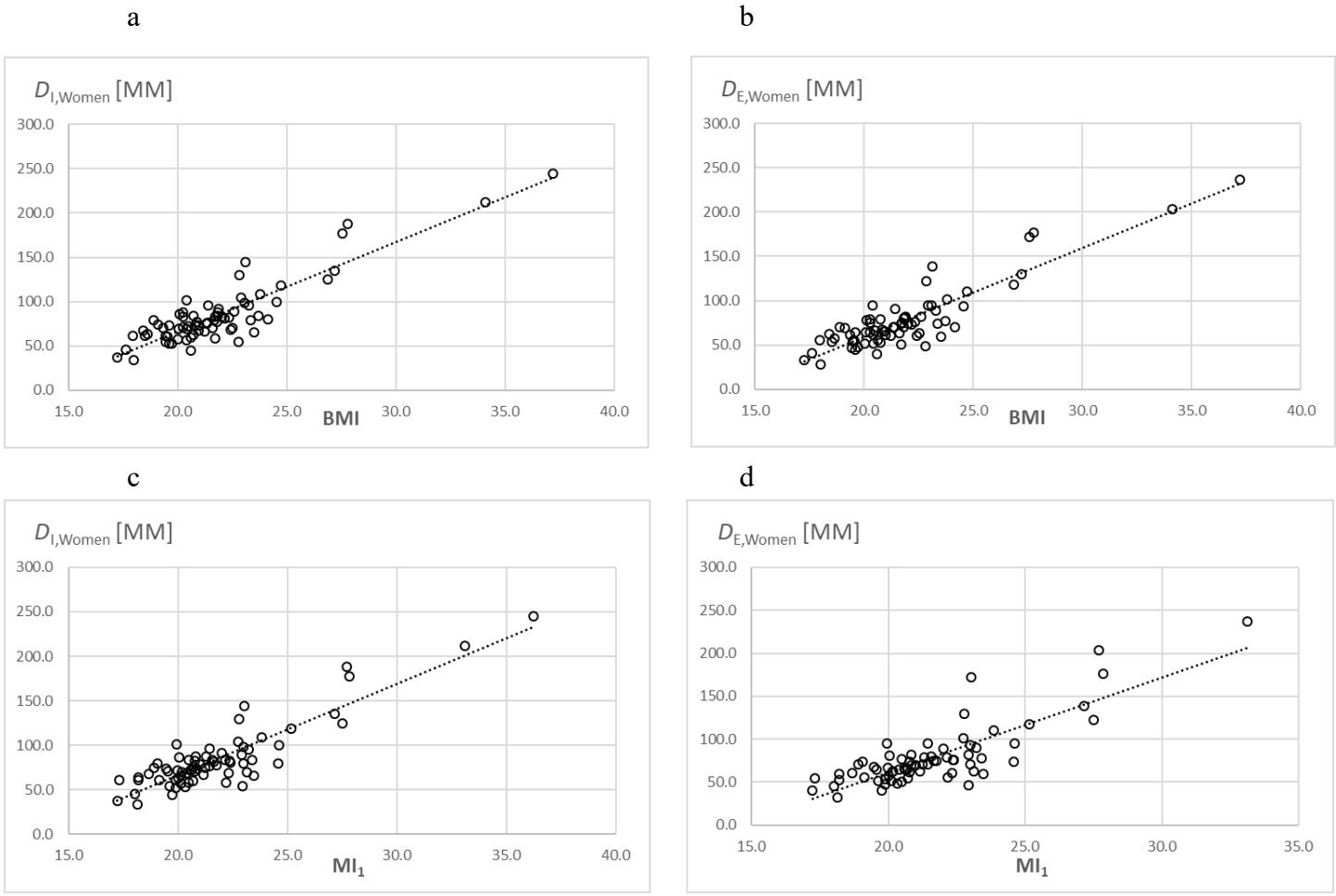

Figure 32: Correlations between the sum of the eight standardises sites (*D*): the BMI (a,b) and the MI (c,d) in women
Spearman's rank correlation coefficient for the sum D_I and the BMI was $\rho = 0.710$ (a) and for D_E 0.714 (b), and 0.708 (c) and 0.710 (d) for the MI_1.

An example, for the problems that can occur using the BMI as a measure of body fat, is shown in the figures 33 and 34 (published (1)). The grey columns represent values of thickness sums from the eight standardised sites with fibrous structures included (D_I) and the black columns show the sums without embedded structures. In figure 33, participant A had a SAT thickness sum of D_I 44.3mm and a BMI of 25.5 kgm^{-2}. Figure 34 show a pattern from another participant with almost the same BMI (25.4kgm^{-2}), but the SAT sum (D_I) was 86.9mm. The sums differ by almost a factor of two (96% difference). This example shows that the BMI should not be used as a measure of body fat.

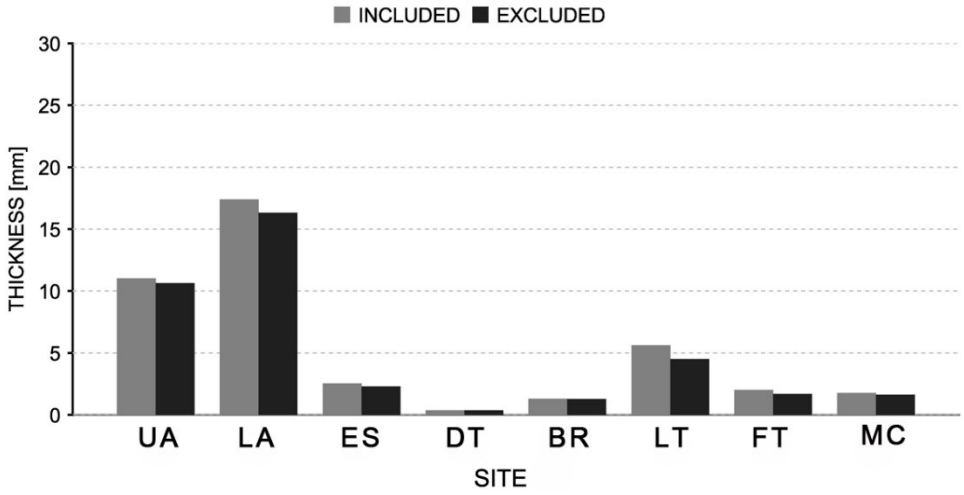

Figure 33: Survey plot of SAT patterning according to figure 19

The columns show the mean values of the semi-automatic multiple thickness measurements for the eight US sites. The mean thickness value of the SAT thickness in a given ultrasound image (within the region of interest) is termed D_{INCL} (grey) when fibrous structures are included, and it is termed D_{EXCL} (black) when fibrous structures are subtracted. Sum of the eight thicknesses D_I=44.3mm (D_E=39.8mm). BMI=25.5 kgm^{-2}; body mass of 80.7 kg, stature of 1.78 m.

Adapted from (Störchle P, Müller W, Sengeis M, Ahammer H, Fürhapter-Rieger A, Bachl N, et al. Standardized ultrasound measurement of subcutaneous fat patterning: high reliability and accuracy in groups ranging from lean to obese) with permission of publisher (Elsevier).

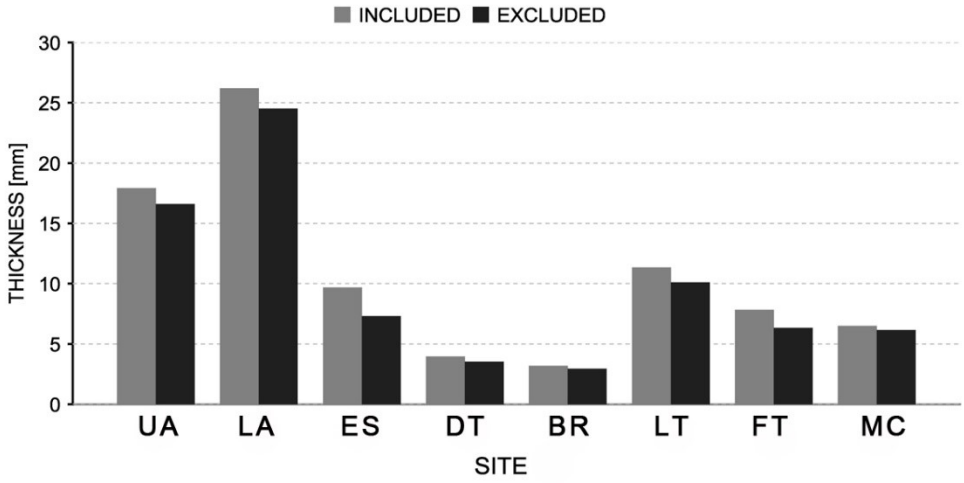

Figure 34: Survey plot of a participant B with similar BMI (Störchle et al., 2017 (1))

BMI=25.4 kgm^{-2}; body mass of 75.5 kg, stature of 1.72 m. The SAT thickness sum was 86.9 mm (77.9 mm), i.e. 96% higher than in participant A.

Adapted from (Störchle P, Müller W, Sengeis M, Ahammer H, Fürhapter-Rieger A, Bachl N, et al. Standardized ultrasound measurement of subcutaneous fat patterning: high reliability and accuracy in groups ranging from lean to obese) with permission of publisher (Elsevier).

3.3.4 SAT thicknesses compared to waist to height ratio

Table 37 shows the correlations between waist to height ratio (W/h) and different SAT thicknesses. Spearman's rank correlation coefficient was used. The highest correlation was a moderate correlation of $\rho = 0.534$ for the site UA including fibrous structures ($p<0.05$).

Table 37: Correlations between waist to height ratio and ultrasound measurements

	UA	LA	ES	UA+LA	UA+LA+ES	*D*
W/h	p < 0.05 Spearman´s rho					
incl. FS	0.534	0.505	0.298	0.521	0.502	0.263
excl. FS	0.532	0.509	0.251	0.523	0.500	0.256

Spearman´s rank correlation coefficient was used, and the highest correlation was found for the site UA including fibrous structures ($\rho = 0.534$ ($p<0.05$)).

4. Discussion

4.1 Methodical developments

1) Test of usability of the standardised sites in overweight and obese people

Due to skin and fat folds at the site EO in some persons with very thick fat layers in the abdominal region, the site was very difficult to mark and measure, because of the large folds that skin and SAT formed. The investigation of these persons underlined that the site EO should be replaced. Therefore, the new site LT suggested by Müller et al.(192) was used instead of EO.

A significant difference was found between men and women ($p<0.05$). The average contribution of the thickness at LT (with fibrous structures included; d_I) to the sum of the eight sites (D_I) was 18.1% (min. 3.2%, max. 30.7%) in men, and 28.8% (min. 17.9%, max. 42.7%) in women.

The results of this thesis with 82 men and 71 women are consistent with those of preliminary published data (1,214), which already indicated that LT provides interesting information on fat patterning, especially related to sex differences. The difference between men and women was about 70% in both preliminary studies, and about 60% in this larger study group. However, the results confirm that LT represents an interesting fat depot area for comparative studies of SAT patterning in men and women and should be used in future investigations instead of EO.

2) Skin thickness

The highest skin thicknesses measured with B-mode US were found at the trunk (mean 2.4 mm) followed by the lower (mean 1.7 mm) and the upper (mean 1.6 mm) extremities. The

results quantified the statement of Marfell-Jones et al. (215) , that skin thickness differ from site to site.

Results of skin thicknesses found in this thesis are similar compared to those found in the literature. E.g. Van Mulder et al. (216) investigated skin thicknesses with high frequency US (40 MHz) at the dorsal side of the proximal forearm (PDF) which is at a similar place to the site BR and similar mean values were found in healthy adults (PDF: 1.43 mm and BR 1.48 mm). Gibney et al. (217) investigated skin thickness in adults with diabetes, at sites used for insulin injections and the results are in accordance with the findings in this thesis (abdomen 2.2 mm, thigh 1.9 mm; UA 2.3 mm, LA 2.2 mm, LT 1.9 mm, and FT 1.7 mm). Some studies (216,218) used the base of the deltoid muscle until the level of the acromion to measure the skin thickness and found values of about 2.1 mm. The only site at the upper arm of the standardised US protocol is the DT (1.7 mm), which is at the distal end of the upper arm. This may explain the differences found compared to deltoid site and again shows that the skin thickness varies at different sites of the body. The differences in skin thickness contribute to the inaccuracy of skin fold measurements for determining SAT.

The results clearly demonstrated an important sex effect. The data showed significant higher values (mean of about 10%) at all sites in males compared to females, except for the site ES: the mean value at the ES site for men (2.8 mm) was 5.6% higher than in women (2.65 mm) but this was not significant. The lack of significance may be due to the high standard deviation (SD = 0.4 mm in men and 0.44 in women) at this site. The sex effect is in accordance with the findings of Escoffier et al. (219) who investigated skin thicknesses at the forearm in adults using ultrasound. They concluded that the skin of men was 16% thicker than that of women, which is similar to the values of the forearm site BR (15%) in the results of this thesis. Van Mulden et al. (216) found also a significant difference, but only of about 8% at the site PDF. Further studies (217,218,220) also found significant differences in skin thickness related to sex. This sex effect should be considered in future investigations where skin thickness matters.

A weak positive correlation between BMI and the sum of the eight skin thicknesses (R^2= 0.171 $p<0.05$) was found in this thesis. Similar results were found in the literature (216,218,220); however, such weak correlations cannot be used for estimating skin thickness of individuals based on BMI.

3) Assessment of mean subcutaneous adipose tissue thickness

As described in the results section, this investigation was published in scientific reports (2) and is quoted literally in the following, adapted to the correct figure numbers, table numbers and citations in this thesis, with the permission of the journal.

"A representative mean SAT value is important for correct calculation of the total subcutaneous adipose tissue (SAT) mass. For this purpose, the mean obtained from the eight sites needs to be calibrated by a representative mean obtained from a large number of sites distributed randomly all over the body. The classification of body segments according to Lund and Browder (figure 4c) (207) implies to use: 4 sites on the head, 1 on neck, 7 on anterior trunk, 7 on posterior trunk, 3 on buttocks, 4 on upper arms, 3 on forearms, 3 on hands, 10 on thighs, 8 on legs, and 4 on feet. This would amount to 54 (the genital area was neglected). Several series of 54 sites in the same individual (pilot study, not shown) indicated that scattering of the means of the 54 sites was too high for the purpose of this calibration study. When using 108 sites, scattering is still noticeable as can be seen in figures 9b and d. Therefore, we used 216 sites corresponding to about one site per dm^2 in adults.

The mean values of the individual calibration factors (table 22) were 0.65 for both k_{IM216} and k_{EM216} (derived from comparisons of 2160 measurements at randomly chosen sites – 216 measurements in ten participants - and additional two times eight measurements at the standardised sites; this amounts to 2320 US measurements and 4640 US image evaluations for d_I and for d_E).

Each thickness measurement at an individual site was represented by the mean of typically 100 thickness values (depending on the breath of ROI setting) measured by the evaluation software (amounting to more than 200,000 thickness values). Although there is still a rest of scattering when using 216 sites due to the randomisation, the standard deviation of the mean calibration factor is low because it is obtained from all ten persons which reduces the "randomisation"-scattering. The means obtained from the eight sites for each individual participant in this group of male participants ranged from 2.9 to 10.2 mm, and the corresponding means obtained from the 216 randomised sites ranged from 1.9 to 6.1 mm.

The mean of eight sites used in the standardised ultrasound method for studying SAT patterning (1,192) overestimated the mean obtained from 216 randomly distributed sites in all individual cases (figures. 8a and b, table 21). This overestimation is not surprising as the standardised eight sites were developed to investigate the fat patterning of the body and

therefore includes some of the main fat depot areas for subcutaneous fat deposition (femero-gluteal region, back, and anterior abdominal wall). These fat depot areas are represented by five of the eight sites (FT, LT, ES, UA, and LA). The calibration factors (derived from values in table 22) correct this overestimation for both thickness measurements with fibrous structures included ($d_{IM8,k} = 0.65 \cdot d_{IM8}$, SD=0.05) and excluded ($d_{EM8,k} = 0.65 \cdot d_{EM8}$, SD=0.06). For the measurement series at eight sites ($d_{IM8,k}$) compared to 216 sites (d_{IM216}) R^2 was 0.95 ($p<0.01$), the SEE was 0.36 mm, and LOA were [-0.63, 0.72]. This scattering transforms linearly when the calibrated mean SAT thickness $d_{IM8,k}$ (or $d_{EM8,k}$ for the assessment of pure fat) is used for calculating total SAT volume according to: volume is mean thickness times surface area S (S can be measure accurately by calibrated scanning systems, or determined approximately according to surface area formulas (210-212)). For SAT mass determination, we used the density of $\rho=0.92$ for fat (206)".

In addition to this discussion, I want to point out that this calibration factor was derived from persons with SAT thickness means ranging from about 3 mm to 10 mm; in lean or obese persons the calibration factor may be different.

4.2 Intra-observer study

This part of the thesis was published in Ultrasound in Medicine & Biology (1); parts of the discussion are quoted literally in the following, with the permission of the journal.

"All SAT images at the eight sites (figure 19) show the same structure: skin, SAT, muscle fascia, and muscle. Standardised marking, US images capturing, and image analysis are necessary for obtaining the high accuracy and reliability possible. Fibrous structures embedded in the SAT could also be quantified because these structures were clearly visible in the US image and could therefore be detected by the contour detection and evaluation algorithm. Embedded structures were found in many images. The SAT contour detection has to be "semi-automatic" (a visual control and interactive evaluation parameter setting cannot be replaced by a fully automatic algorithm), otherwise border detection errors would occur because of intermediate structures: e.g. Camper's fascia in the abdomen region, Müller et al. (191,192,194), or embedded fibrous structures as shown in figure 19 at LT and FT."

*"**Measurement accuracy of brightness-mode (B-mode) US in thick SAT layers***

In conventional US systems, the speed of sound used to calculate distances is 1540 ms^{-1} ("mean value for soft tissue"). Here, a sound speed of 1450 ms^{-1} was set for analysis of SAT

in the evaluation software to avoid a sound speed error of about 6% (192,206). The axial resolution in an US image depends on pulse length, and the lateral resolution is determined by diffraction. Technically obtainable accuracy of thickness measurements equals approximately the wavelength (wavelength determines diffraction of US waves and thus the limits of image resolution). A probe frequency of 18 MHz results in an image resolution of about 0.1 mm, and 6 MHz result in approximately 0.3 mm. SAT borders are furrowed and therefore biologically given limitations determine the obtainable accuracy. The influence of these biological limitations is minimised because the image evaluation algorithm used takes mean values of many thickness measurements in a given image.

In the overweight and obesity groups, low frequencies were necessary to penetrate the thick layers. In these groups, SAT thicknesses can be many centimetres, and in such cases the relative errors δ_{rel} (=δ/d, in %) are of relevance rather than the absolute errors δ (in mm). For instance, at a 60mm thick SAT layer, the relative error (at 6 MHz) due to border detection in-accuracy is approximately 0.3/60, i.e. 0.5%. Such small border detection errors can be neglected when compared to deviations because of wrong sound speed setting. A deviation of only 15 ms^{-1} (1%) would already affect a thickness measurement error of 1%. The absolute accuracy for in-vivo measurements of thin fat layers using 12-18 MHz cannot be overcome by any other measurement technique. In thick layers, the correct choice of sound speed (1450 ms^{-1}) predominantly determines the accuracy. SAT is very sensitive to compression (194) and errors due to that were minimised by using a thick layer of gel between the probe and the skin (192,194)

Reliability of US SAT thickness measurements

Even breathing influences the SAT thickness. US images were therefore captured when the participant stopped breathing at mid-tidal expiration. Because of visco-elasticity, it is of paramount importance to mark the sites and capture the images in the standardised positions (192)…" In this thesis, the reliability analyses were extended to participants with BMI values up to 40.3 kgm^{-2} (D_I ranged from 12.5 to 244.9 mm). The data were also published in Ultrasound Medicine & Biology (1).

"Intra-observer reliability of the measurements of two observers who investigated a sub-group of lean participants (G1, OBI), and a sub-group of people with overweight or obesity (G2, OBII) was analysed. Absolute deviations (in mm) between sums of thicknesses at the

eight sites increased with thicker SAT layers (Figures 13 and 14a-b); however, relative deviations were smaller in the overweight/obese group (median of ABS($\Delta_{INCL,rel}$) =0.5%) when compared to the lean group (median ABS($\Delta_{INCL,rel}$) =1.1%), Figures 14c-d. This is not surprising when relative deviations are determined ($\Delta_{rel}=100\cdot(\Delta/D_{MEAN})$) because tissue border detection errors play a larger role in lean persons where the sum of fat thicknesses D is small".

A comparison of the measurement deviations (ABS(δ)) at the individual eight sites (Figures 15a and b, Table 25a-c) shows that highest absolute deviations occurred at the sites UA, LA, and LT, where average SAT thicknesses were highest (Figure 16a). This is to be expected: the plasticity, visco-elasticity, and compressibility of subcutaneous adipose tissue cause the largest deviations from measurement to measurement at sites where SAT layers are thick. In the abdomen region, additional compression artefacts can occur due to breathing (the pressure status of the lungs when breathing is stopped at "mid-tidal" expiration can be slightly different from measurement to measurement). Fat thickness differences in the abdomen due to the pressure change associated with the heartbeat can sometimes also be observed, but these effects are usually of minor importance.

The thickness of the SAT layer at LT may change when the leg is not positioned in the same way. At FT, measurement deviations were small (Figure 15a). The SAT compressibility is lowest at FT when compared to the other US sites (194). In the US image, quite often thick intermediate fasciae can be seen at FT which may be the reason why skinfold measurement is difficult at this site.

The deviations when measurements were repeated (mainly caused by marking deviations, body position differences, and by intra-abdominal pressure changes) increased at all eight sites with increasing SAT thickness (Table 25b and c). To obtain high reproducibility, it is very important to position the person before the US measurement takes place precisely in accordance with the standardised US measurement technique (192).

Figure 16a shows the median values of the SAT thicknesses at the individual sites. The ratio of the median deviation at a given site in relation to the median thickness at this site is shown in Figure 16b. The relative errors (in %) were smallest at the three sites UA, LA, and LT where the average SAT thicknesses were largest (Table 25a). Lowest absolute v values (in

mm) of measurement deviations occurred at the sites ES, DT, BR, FT, and MC where SAT depth was low.

Table 38 summarises all (1,45,191,192,197) reliability studies which were carried out using the US approach developed by Müller et al. (192). Measurement deviations found in the lean group G1 (where D_I ranged from 12.5 to 77.4mm) in this thesis are similar to the results received in an intra-observer study (45) with experienced observers in a group of lean athletes (D_I range 6 to 70 mm): LOA ±1.4, Median of ABS(ΔD_I):0.43, LOA ±1.4 mm, Median of ABS(ΔD_I):0.39, respectively. Another study (192) was applied the standardised approach to analyse inter-observer reliability (a group of lean athletes with BMIs from 18.6 to 26.6 kgm^{-2}, and D_I from 10.2 to 51.2 mm). The median measurement deviation was 0.24 mm, and the relative deviation was 1.0%; this is also close to the value of 1.1% found here in the intra-observer study for G1. Since the results obtained in this thesis for G2 are the first for overweight and obese, there are no comparative values available yet.

Table 38: Obtainable intra and intertester reliability results

Intra-observer studies					
Study reference	Sample	Observers	D_I range [mm]	95% LOA D_I [mm]	Median of ABS(ΔD_I) [mm]
Müller et al. (45)	Adults	Experienced	6 – 70	± 1.4	0.4
Störchle et al. (1)			12 - 77	± 1.4	0.4
			12 - 245	± 2.2	0.6
			44 - 245	± 2.9	0.9
Müller et al. (45)		Novice	6 - 70	± 3.1	0.6
Kelso et al. (196)	Children	Experienced	35 - 112	± 2.0	0.9
Inter-observer studies					
Study reference	Sample	Observers	D_I range [mm]	95% LOA D_I [mm]	Median of ABS(ΔD_I) [mm]
Müller et al. (192)	Adults	Experienced	10 - 51	± 1.1	0.2
Müller et al. (45)			6 - 70	± 1.2	0.3
		Novice	6 - 70	± 3.1	1.0
Kelso et al. (197)	Children	Experienced	26-86	± 2.1	0.8

Intra- and inter-observer reliability of novice measurers who had no preceding experience with US imaging, only a two-day training course, were investigated in five independent

research centers (45). Deviations were found to be twice as high for intra- and three times larger for inter-tester reliability compared to the results obtained by the experienced measurers. These results show the necessity of sufficient experience and training to obtain highest accuracy and reliability when using this ultrasound approach (45).

The results obtained by Störchle et al. (1) show that the US method can also be applied in overweight and obese groups: *"In addition to investigating medical problems using this standardised US method in underweight persons and in athletes (20,25,221), results obtained here, encourage choosing this technique also for studies in groups of overweight and obese persons when highly accurate and reliable measurement results are desired."* (1).

Body roundness model

Anthropometrists have developed a simple approach for estimating TBF based on the body height, the waist and hip circumferences. Although this simple approach can only result in rough estimates, we compared these results obtained with the BRM for our persons to the sums D_I of our US SAT measurements.

There was a correlation between D_I and TBF according to the TBF determined by the means of BRM. However, several of the individuals deviate substantially from the regression line indicating that the anthropometric data used for the BRM can only partly capture the amount of body fat. For this comparison, it should be noted that the values obtained by the US measurement capture the amount of SAT, not TBF. However, SAT amounts for about 80% (222) of TBF and can therefore be seen as a good representative of TBF.

The comparisons of the results obtained here with the TBF values determined according to the BRM (213), which is based on a few easily determinable anthropometric parameters, cannot replace the validation study against a 4-component model or against high resolution MRI measurements, because the BRM only gives a rough estimate of TBF and of VAT and is far from the accuracy demands for a study capable to validate this highly accurate and reliable US thickness measurement method in terms of TBF estimation. Particularly in persons with low sums of SAT thicknesses, the BRM predicts too high TBF values: the linear regression line in Figure 18a intercepts the TBF axis at a too high value.

4.3 Fat patterning, fibrous structures, and SAT correlations with anthropometric indices

In this thesis, SAT thickness sums differed by approximately a factor of two between men (median 40.3 mm) and women (median 76.0 mm), although the group of women (21.8 kgm^{-2}) had lower BMI values compared to men (24.3 kgm^{-2}). Previous studies in athletes found even higher differences. In elite judokas, the median D_I in men was 22 mm, and the BMI 26.5 kgm^{-2}, compared to 66 mm and 22.9 kgm^{-2} in women (175). Müller et al. (45) investigated weight sensitive and non-weight sensitive athletes and found three times higher D_I medians in women (17 vs 51 mm). In rowing (198), also substantially higher thickness values were found (27.6 mm, 23.8 kgm^{-2} in the male group compared to 65.5 mm in the female group). The highest differences were found in elite long-distance runners (223), where women had more than six times higher thickness sums (9 mm, BMI 19.1 kgm^{-2} vs 58 mm, BMI 18.6 kgm^{-2}). It is known that women have a higher amount of body fat due to biological reasons, but the above mentioned results found with the standardised US method until today indicate that this effect is even more pronounced in elite sports.

1. Fat patterning

The fat patterning of 153 participants (82 males, 71 females) was investigated. The results obtained in this group showed the pronounced SAT thickness differences at the eight standardised sites. The two biggest fat depot sites were LA with 22.6% and LT with 23.1%.

A pronounced dimorphism between sexes was detected for SAT thicknesses. All individual sites had higher median values in female participants. Both the thickness values at the individual sites (d) and the sums of them (D) differed significantly between sexes, except for the two abdominal sites UA, LA (for both values including and excluding fibrous structures). In a study of highly trained junior athletes by Kelso et al.(198), all sites and the sums showed significant differences between men and women. This may be due to the different study populations of young trained athletes (homogeneous group) and the wide range from lean to obesity class III participants in this group. The SAT thickness heterogeneity of the population in this thesis requires the use of relative values rather than absolute values. For relative values ($d_{I\%}$), significant differences were found for all sites except for BR. The largest differences between men and women of all BMI categories together were found at the sites UA (men:15%, women 9.9%), LA (men:26.7%, women 17.4%) and LT (men 17.7%, women 29.2%). This changes when comparing normal weight

and overweight people separately. As can be seen in figure 23, the female fat patterning comes closer to the male patterning in overweight and obese people. Significant differences between men and women with a BMI higher than 25 kgm^{-2} where only found for the three sites ($d_{I\%}$) LA, ES and DT.

When the sexes are considered individually, changes from normal weight persons to overweight and obese ones were found at the site UA: in men from a median of 14.1% in the normal weight group to 21.9% in the overweight and obese group, and in women the value nearly doubled from 9.7% to 19%, respectively. In overweight and obese men, this results in a contribution of 51% total amount of SAT from only the two abdominal sites (UA and LA). This confirms the findings of Vague (224) related to android obesity which is associated with premature atherosclerosis and diabetes. In obese women, SAT was predominantly shifted from the site LT to the abdominal sites. At LT, the amount dropped from 29% in normal weight to 19% in the overweight and obese group. Our findings point out that the "gynoid" type of obesity (224) is not so pronounced in overweight and obese women when compared to normal weight women. In overweight and obese women, 41.7% of the total amount of SAT was contributed by the two abdominal sites and there was no significant difference at the legs when women were compared to overweight and obese men. According to the results found in this thesis, overweight and obese women show a "masculinisation" related to fat patterning. However, a limitation of these findings is that the group of overweight and obese women consisted of only six participants.

Another conspicuousness was that the sums of SAT thicknesses were higher in females (N=71, median D_I: 76.0 mm) compared to males (N=82, 40.3 mm), although relative body weight was lower in females (BMI 21.8 kgm^{-2}) than in males (24.3 kgm^{-2}). This corroborates the data of Sengeis et al.(175) and Kelso et al. (198) which found similar results in elite judokas and rowers. All these findings are in accordance with existing research on sexual dimorphism of adipose tissue, highlighting that female adults have a higher amount of SAT (225).

2. Fibrous structures (fasciae) embedded in the SAT

US has the advantage that it is the only body composition method which can quantify the amount of connective tissues embedded in the SAT. For the group of all participants

(N=153), the fibrous structures amounted to a median of 10.9% (6.5 mm) of the SAT thickness values (D_I).

The relative amount of embedded connective tissues was significantly higher in male (15.3%) compared to female participants (9.2%). Müller et al. (45) found similar results (18% in men, 11% in women), although the groups studied there consisted of elite athletes with low amounts of fat. This effect also persists when the groups were divided into a normal weight (BMI < 25 kgm^{-2}, men 16.2%, women 9.7%) and an overweight and obese (>25 kgm^{-2}, men 9.3%, women 4.1%) group. The absolute values of fibrous structures were higher in the normal weight compared to the overweight and obese group; but due to the SAT thickness increase, the percentages of fibrous structures decreased.

Higher percentages of fibrous structures in men compared to women were also reported previously: Kelso et al. (198) found 11.4% in men and 7.9% in women (but these results were not significant, probably because of the low number of participants). In judokas (175) the median percentage of embedded fibrous structures was about 2.5 times higher in men (21.7% men and 8.8% women.

The results of this thesis show that men had about 10% higher skin thickness and about 6% higher amounts of fibrous structures embedded in the SAT compared to women, who had a higher amount of SAT. This indicates that skinfold measurements can be severely misleading because skin thicknesses and embedded fibrous structures (fasciae) are not considered; additionally, skinfolds measure the fat in a compressed state. Sengeis et al. (175) showed an example where two competing athletes who had almost the same skinfold sums at the eight ISAK sites, differed by a factor of four when their SAT thicknesses were measured with the standardised US method (175).

3. SAT tissue and relative body weight

The BMI or Quetelet's index is just a measure of relative body weight and not of body fatness (6). Figures 30 (a,b) show that there was only a weak correlation between BMI and the SAT sums (D_I): ρ = 0.34 when all 153 participants were studied together. When distinguishing between sexes, the correlation was higher in men: ρ was 0.72 and in women, ρ was 0.71. But, in the lean group G1 of the intra-observer part (D_I ranged from 12-77 mm) there was no correlation between BMI and the SAT thickness sum *D* at all (Figure 17). Similar results were previously found for athletes in the literature (45,175,198). An example for the problems, which can occur when using the BMI as a measure of body fat, is presented in the figures 33 and 34. Participant A had almost the same BMI as participant B, but the sums of SAT thicknesses differed by almost 100%. This shows that individual assessments of body fat cannot be derived from BMI (1).

According to the WHO, the BMI, also when used as a measure for relative body weight, has severe shortcomings because it does not consider the individual leg length of a person (172). The BMI can be replaced by an improved measure, the mass index (MI_1) that considers the individual's sitting height s: MI_1=0.53m/(hs). Although the MI_1 measures relative body weight on a finer scale than the BMI does, it still is just a measure for 'ponderosity', but not a useful measure for the body fat content of an individual (5,6). Sitting height or leg length is easy to measure and should be included in all basic data sets of athletes (172). It can be expected that the application of the M_{I1} in young persons and youth athletes will be helpful for studies of their growth in connection with changes of their body dimensions (6).

4. SAT thicknesses compared to waist to height ratio

Only moderate correlations were found between W/h ratio and different thickness sums or thicknesses at individual sites. The highest correlation was found at UA where ρ was 0.53. Therefore, the aim to find a possible surrogate parameter from the standardised protocol has failed. But, for future investigations, the W/h ratio should be included in all basic data sets of athletes: Ashwell et al. (226) showed that W/h ratio is more predictive of years of life lost than the BMI.

4.4 Limitations and further developments

1. For the skin thickness measurements, only persons under 40 years were included due to the age-related changes in skin thickness. A future focus should also be on older adults, who are not included here. This hold also true for children and youth athletes.
2. As this standardised method has been developed recently, some time will be necessary to get comprehensive sets of reference data. This thesis contributes to this data collection, however, the amount of overweight and obese women (N=6) was low: this should be considered when interpreting the fat patterning comparisons.
3. As described in Scientific Reports (2), a fat density value of 0.92 kgm^{-3} found in the literature (206) was used for SAT mass calculations. A detailed study of the density of human body fat, which may depend on the site, the temperature, the age, and hydration status, is missing. Such a study is being prepared in the lab of W. Müller at the Medical University of Graz. These expected results will increase the accuracy of body fat mass determinations of all methods that are based on volumetry, e.g., US, MRI, and CT.
4. SAT mass calculation is based on the mean SAT thickness, on the density of the adipose tissue, and on the determination of the body surface. In this thesis, body surface was determined using DuBois' formula and two related formulas. This body surface calculation contributes to the error of fat mass estimation. 3D scanning could improve the assessment error that resulted from the simple surface calculation used here (2).
5. This thesis and the underlying scientific publications focus on determining the amount of SAT, but do not determine the amount of visceral fat. This has been pointed out in our recent publication: "*Determination of SAT (or pure subcutaneous fat) mass by US as used here does not capture visceral fat. Attempts to assess visceral fat by US have been made by other groups (227,228) however, US only detects surrogate parameters like intra-abdominal distances. MRI is capable of measuring visceral fat, although fat layer thickness measurements do not reach the accuracy of US thickness measurements because the pixel size is typically 1.3 to 2 mm in total body scans, and MRI measurement sequence and image segmentation protocols are not standardised for this purpose. Development of improved MRI methods towards higher standards for fat studies is in progress in our laboratories at the Medical University of Graz. Comparisons of SAT (measured by US) with VAT (measured by MRI) will show the possibilities and limitations of total body fat (TBF) assessment (on the anatomical level) based on US SAT measurements solely. We assume that there is a good chance to find useful correlations for acceptable assessment accuracy because SAT, which can be determined with high*

accuracy by US, accounts for typically about 80% of TBF (222,227,229) and therefore scattering of the VAT percentage can be expected to have minor effect on the TBF assessment error. However, there may be outliers, particularly in groups with obesity or extreme underweight. Meanwhile, we use the waist to height ratio (W = w/h), which is the most important anthropometric predictor of health and premature death caused by obesity (201), as a surrogate measure for VAT. The studies in progress will also show whether a combined approach (US SAT measurements and anthropometric indices like W) will improve the assessment accuracy." (2)

6. The ratio of the SAT mean thickness obtained from the eight standardised sites to the mean thickness found at 216 sites is only representative for persons whose body fat content is not as low as in highly trained athletes or in skinny persons, and not as high as in obese persons. The investigated range only covers d_{M8} -values (means of the eight sites) from 3 to 10 mm. Preliminary studies indicate that in underweight groups, the SAT thickness of fat depots can get closer to the SAT thickness of other sites, which would result in a higher calibration factor (2). Similar studies with women, other ethnic groups, children, and older adults which were not included here, will be of interest and should be focused in future investigations. As described in the work of 2018 (2) :"…*it would be surprising when results deviated substantially in such cases because the eight sites cover a representative set of fat depot sites, and differences from site to site in different groups can be expected to equal out to a large extend when means of all eight sites are taken."*
7. Currently, scientific results obtained with the standardised US method have not been compared to body fat mass determination on the molecular level: *"..Validation studies against a four-component model* (6) *will reveal which US sites will enable the best prediction of total body fat in particular groups of persons. Ethnicity, anthropometric parameters, sex and age are assumed to play a role in obtaining equations that fit optimally to the four-component model reference data"* (1). Such a validation study is in progress in our lab in cooperation with the laboratories of LB. Sardinha (Lisbon, Portugal) and T. Lohman (Tucson, USA).

4.5 Conclusion

1. Introduction of a new measurement site

   The usage of the site external oblique (EO) caused major problems in the overweight and obese persons studied within the framework of this thesis. This experience makes

clear that the site EO should be replaced by another one. Lateral thigh (LT) had been suggested by Müller et al. (192), and the results obtained using this new site support this replacement because no measurement problems are associated with LT, and, additionally, this site is of high relevance for studying sexual differences of fat pattering.

2. Sexual dimorphism and site dependency of skin thicknesses

   Significant differences between the skin thicknesses at all sites were found, and mean skin thickness was 10% higher in males compared to females. This result explains a part of the errors associated with skinfold measurements. Additionally, the large data set obtained from the eight sites adds to the knowledge on human skin thicknesses. Detecting the SAT-skin-border correctly (based on the knowledge of typical skin thickness at a given site) in cases when fibrous structures are in the vicinity or attached to the skin will help to avoid US measurement errors.

3. Mean thickness of subcutaneous adipose tissue (SAT)

   Mean SAT thickness measured in men at 216 sites showed that the standardised eight sites overestimates the mean SAT thickness due to their predisposed location at some of the main fat depot areas (femero-gluteal region, back, and anterior abdominal wall). This has to be considered when determining SAT mass. A calibration factor $k = 0.65$ would correct this overestimation, but this correction cannot be applied to skinny persons and athletes or to overweight and obese persons because the measurements presented here do not cover the SAT thicknesses of these groups.

4. Reliability of the standardised ultrasound method in a large range of body fatness

   The intra-observer study showed, that high reliability can be obtained for all groups of persons, from extreme leanness to obesity class III. The relative errors of US measurements were even lower in the overweight and obese group compared to the normal weight group. Site marking with the new site LT instead of EO turned out to be just as easy as in the normal weight group, as distances are percentages of body height, and only two anatomic landmarks are necessary. Therefore, the replacement of EO by LT increases reliability. (1).

5. SAT thickness sums in men and women

   In this thesis, women showed about two times higher SAT thickness sums compared to men, although their relative body weight was much lower.

6. Fat patterning in men and women

   Fat patterning differed significantly between men and women, and the median SAT thicknesses were higher at all sites in women. The highest ratio of thicknesses between

females and males was found at the site LT, which is the predominant fat depot site in women. In overweight and obese people, the female fat patterning comes closer to the male patterning (ratios of LT thicknesses decrease, ratios of UA and LA thicknesses increase).

7. Amount of fibrous structures (fasciae) embedded in the SAT tissue

   The results found within the framework of this thesis, supports the findings of previous studies that showed that the percentage of fibrous structures was larger in male groups compared to female groups. In the 82 males and 71 females studied here, the percentages were 15% and 9%, respectively. This further increases the difference in subcutaneous fat between men and women. The relative amount of fibrous structures decreases significantly with increasing fat layer thickness.

Bibliography

(1) Störchle P, Müller W, Sengeis M, Ahammer H, Fürhapter-Rieger A, Bachl N, et al. Standardized ultrasound measurement of subcutaneous fat patterning: high reliability and accuracy in groups ranging from lean to obese. Ultrasound Med Biol 2017;43(2):427-438.

(2) Störchle P, Müller W, Sengeis M, Lackner S, Holasek S, Fürhapter-Rieger A. Measurement of mean subcutaneous fat thickness: eight standardised ultrasound sites compared to 216 randomly selected sites. Scientific reports 2018;8(1):16268.

(3) Slater G, O´Connor H, Kerr A. Optimising Physique For Sports Performance. In: Hume P, Kerr D, Ackland T, editors. Best Practice Protocols for Physique Assessment in Sport. 1st ed.: Springer Singapore; 2017. p. 42-47.

(4) Meyer NL, Sundgot-Borgen J, Lohman TG, Ackland TR, Stewart AD, Maughan RJ, et al. Body composition for health and performance: a survey of body composition assessment practice carried out by the Ad Hoc Research Working Group on Body Composition, Health and Performance under the auspices of the IOC Medical Commission. Br J Sports Med 2013 Nov;47(16):1044-1053.

(5) Müller W, Maughan RJ. The need for a novel approach to measure body composition: is ultrasound an answer? Br J Sports Med 2013 Nov;47(16):1001-1002.

(6) Ackland TR, Lohman TG, Sundgot-Borgen J, Maughan RJ, Meyer NL, Stewart AD, et al. Current status of body composition assessment in sport: review and position statement on behalf of the ad hoc research working group on body composition health and performance, under the auspices of the I.O.C. Medical Commission. Sports Med 2012 Mar 1;42(3):227-249.

(7) Dennis SC, Noakes TD. Advantages of a smaller bodymass in humans when distance-running in warm, humid conditions. Eur J Appl Physiol Occup Physiol 1999;79(3):280-284.

(8) Larsen HB. Kenyan dominance in distance running. Comparative Biochemistry and Physiology Part A: Molecular & Integrative Physiology 2003;136(1):161-170.

(9) Reale R, Cox GR, Slater G, Burke LM. Regain in body mass after weigh-in is linked to success in real life judo competition. Int J Sport Nutr Exerc Metab 2016;26(6):525-530.

(10) Wroble RR, Moxley DP. Acute weight gain and its relationship to success in high school wrestlers. Med Sci Sports Exerc 1998 Jun;30(6):949-951.

(11) Kazemi M, Rahman A, De Ciantis M. Weight cycling in adolescent Taekwondo athletes. J Can Chiropr Assoc 2011 Dec;55(4):318-324.

(12) Reale R, Cox GR, Slater G, Burke LM. Weight Regain: No Link to Success in a Real-Life Multiday Boxing Tournament. Int J Sports Physiol Perform 2017 Aug;12(7):856-863.

(13) Horswill CA, Scott JR, Dick RW, Hayes J. Influence of rapid weight gain after the weigh-in on success in collegiate wrestlers. Med Sci Sports Exerc 1994 Oct;26(10):1290-1294.

(14) Claessens A, Lefevre J, Beunen G, Malina R. The contribution of anthropometric characteristics to performance scores in elite female gymnasts. J Sports Med Phys Fitness 1999;39(4):355.

(15) Di Cagno A, Baldari C, Battaglia C, Monteiro MD, Pappalardo A, Piazza M, et al. Factors influencing performance of competitive and amateur rhythmic gymnastics--gender differences. J Sci Med Sport 2009 May;12(3):411-416.

(16) Douda HT, Toubekis AG, Avloniti AA, Tokmakidis SP. Physiological and anthropometric determinants of rhythmic gymnastics performance. International Journal of Sports Physiology and Performance 2008;3(1):41-54.

(17) Benardot D, Zimmermann W, Cox GR, Marks S. Nutritional recommendations for divers. Int J Sport Nutr Exerc Metab 2014;24(4):392-403.

(18) O'Connor H, Caterson I. Weight loss and the athlete. In: Burke L, Deakin V, editors. Clinical Sports Nutrition. 4th ed. North Ryde: Mcgraw-Hill Professional; 2010. p. 116-148.

(19) Müller W. Towards research-based approaches for solving body composition problems in sports: ski jumping as a heuristic example. Br J Sports Med 2009 Dec;43(13):1013-1019.

(20) Sundgot-Borgen J, Meyer NL, Lohman TG, Ackland TR, Maughan RJ, Stewart AD, et al. How to minimise the health risks to athletes who compete in weight-sensitive sports review and position statement on behalf of the Ad Hoc Research Working Group on Body Composition, Health and Performance, under the auspices of the IOC Medical Commission. Br J Sports Med 2013 Nov;47(16):1012-1022.

(21) Artioli GG, Gualano B, Franchini E, Scagliusi FB, Takesian M, Fuchs M, et al. Prevalence, magnitude, and methods of rapid weight loss among judo competitors. Medicine & Science in Sports & Exercise 2010;42(3):436-442.

(22) Sundgot-Borgen J, Garthe I. Elite athletes in aesthetic and Olympic weight-class sports and the challenge of body weight and body compositions. J Sports Sci 2011;29(sup1):S101-S114.

(23) Sundgot-Borgen J, Torstveit M. Aspects of disordered eating continuum in elite high-intensity sports. Scand J Med Sci Sports 2010;20(s2):112-121.

(24) Rosendahl J, Bormann B, Aschenbrenner K, Aschenbrenner F, Strauss B. Dieting and disordered eating in German high school athletes and non-athletes. Scand J Med Sci Sports 2009;19(5):731-739.

(25) Byrne S, McLean N. Eating disorders in athletes: a review of the literature. Journal of science and medicine in sport 2001;4(2):145-159.

(26) Byrne S, McLean N. Elite athletes: effects of the pressure to be thin. J Sci Med Sport 2002 Jun;5(2):80-94.

(27) World Health Organization. Constitution of the world health organization. Basic documents. 45th ed. New York; 2006.

(28) Kagawa M. Anthropometry and Health for Sport. In: Hume P, Kerr D, Ackland T, editors. Best Practice Protocols for Physique Assessment in Sport. 1st ed.: Springer Singapore; 2017. p. 32-41.

(29) World Health Organization. GLOBAL STATUS REPORT on noncommunicable diseases 2014. Geneva: World Health Organization; 2014.

(30) Lim SS, Vos T, Flaxman AD, Danaei G, Shibuya K, Adair-Rohani H, et al. A comparative risk assessment of burden of disease and injury attributable to 67 risk factors and risk factor clusters in 21 regions, 1990-2010: a systematic analysis for the Global Burden of Disease Study 2010. Lancet 2012 Dec 15;380(9859):2224-2260.

(31) Arcelus J, Mitchell AJ, Wales J, Nielsen S. Mortality rates in patients with anorexia nervosa and other eating disorders: a meta-analysis of 36 studies. Arch Gen Psychiatry 2011;68(7):724-731.

(32) Smink FR, van Hoeken D, Hoek HW. Epidemiology of eating disorders: incidence, prevalence and mortality rates. Curr Psychiatry Rep 2012 Aug;14(4):406-414.

(33) Treasure J, Claudino AM, Zucker N. Eating disorders. Lancet 2010 Feb 13;375(9714):583-593.

(34) Becker AE, Grinspoon SK, Klibanski A, Herzog DB. Eating disorders. N Engl J Med 1999 Apr 8;340(14):1092-1098.

(35) Sullivan PF. Mortality in anorexia nervosa. Am J Psychiatry 1995;152(7):1073-1074.

(36) Lackner S, Mörkl S, Müller W, Fürhapter-Rieger A, Oberascher A, Lehofer M, et al. Novel approaches for the assessment of relative body weight and body fat in diagnosis and treatment of anorexia nervosa: A cross-sectional study. Clinical Nutrition 2019.

(37) Mallinson RJ, De Souza MJ. Current perspectives on the etiology and manifestation of the "silent" component of the Female Athlete Triad. Int J Womens Health 2014 May 3;6:451-467.

(38) Müller W, Platzer D, Schmölzer B. Scientific approach to ski safety. Nature 1995;375:455.

(39) Müller W, Platzer D, Schmölzer B. Dynamics of human flight on skis: improvements in safety and fairness in ski jumping. J Biomech 1996;29(8):1061-1068.

(40) Müller W. Determinants of ski-jump performance and implications for health, safety and fairness. Sports medicine 2009;39(2):85-106.

(41) Müller W, Gröschl W, Müller R, Sudi K. Underweight in ski jumping: the solution of the problem. Int J Sports Med 2006;27(11):926-934.

(42) Schmölzer B, Müller W. The importance of being light: aerodynamic forces and weight in ski jumping. J Biomech 2002 Aug;35(8):1059-1069.

(43) Schmölzer B, Müller W. Individual flight styles in ski jumping: results obtained during Olympic Games competitions. J Biomech 2005;38(5):1055-1065.

(44) International Olympic Comittee. IOC Concerned about Body Composition, Health and Performance of Athletes. 2010; Available at: http://www.olympic.org/en/content/The-IOC/Commissions/Medical/?articleNewsGroup=-1&articleId=104170.

(45) Müller W, Fürhapter-Rieger A, Ahammer H, Lohman T, Meyer NL, Sardinha L, et al. Relative body weight and standardised ultrasound measurement of subcutaneous fat in athletes: an international multicentre reliability study, under the auspices of the IOC Medical Commission. Sports medicine 2019;Epub ahead of print.

(46) Slater G, Shaw G, Kerr A. Athlete Considerations For Physique Measurement. In: Hume P, Kerr D, Ackland T, editors. Best Practice Protocols for Physique Assessment in Sport. 1st ed.: Springer Singapore; 2017. p. 54-63.

(47) Lohman T, Milliken L, Sardinha L. Introduction to Body Composition and Assessment. In: ACSM., Lohman T, Milliken L, editors. ACSM´s Body Composition Assessment. 1st ed. Champaign IL: Human Kinetics; 2019. p. 1-16.

(48) Aragon AA, Schoenfeld BJ, Wildman R, Kleiner S, VanDusseldorp T, Taylor L, et al. International society of sports nutrition position stand: diets and body composition. J Int Soc Sports Nutr 2017 Jun 14;14:16-017-0174-y. eCollection 2017.

(49) Hawes MR, Martin AD. Human body composition. Kinanthropometry and exercise physiology laboratory manual: tests, procedures and data 2001;1:7-46.

(50) Lohman T, Milliken L. ACSM´s Body Composition Assessment. 1st ed. Champaign IL: Human Kinetics; 2019.

(51) Heymsfield S, Lohman T, Wang Z, Going S. Human Body Composition: 2nd ed. 2nd ed.: Human kinetics; 2005.

(52) Wang Z, Pierson Jr RN, Heymsfield SB. The five-level model: a new approach to organizing body-composition research. Am J Clin Nutr 1992;56(1):19-28.

(53) Lee SY, Gallagher D. Assessment methods in human body composition. Curr Opin Clin Nutr Metab Care 2008 Sep;11(5):566-572.

(54) Bea J, Cureton K, Lee V, Milliken L, Sardinha L. Body Composition Models and Reference Methods. In: ACSM., Lohman T, Milliken L, editors. ACSM´s Body Composition Assessment. 1st ed. Champaign IL: Human Kinetics; 2019. p. 17-30.

(55) Siri WE. Body composition from fluid spaces and density: analysis of methods. Techniques for measuring body composition 1961;61:223-244.

(56) Brožek J, Grande F, Anderson JT, Keys A. Densitometric analysis of body composition: revision of some quantitative assumptions. Ann N Y Acad Sci 1963;110(1):113-140.

(57) Visser M, Gallagher D, Deurenberg P, Wang J, Pierson RN,Jr, Heymsfield SB. Density of fat-free body mass: relationship with race, age, and level of body fatness. Am J Physiol 1997 May;272(5 Pt 1):E781-7.

(58) Roemmich JN, Clark PA, Weltman A, Rogol AD. Alterations in growth and body composition during puberty. I. Comparing multicompartment body composition models. J Appl Physiol 1997;83(3):927-935.

(59) Streat S, Beddoe A, Hill G. Measurement of body fat and hydration of the fat-free body in health and disease. Metab Clin Exp 1985;34(6):509-518.

(60) Modlesky CM, Cureton KJ, Lewis RD, Prior BM, Sloniger MA, Rowe DA. Density of the fat-free mass and estimates of body composition in male weight trainers. J Appl Physiol (1985) 1996 Jun;80(6):2085-2096.

(61) Prior BM, Modlesky CM, Evans EM, Sloniger MA, Saunders MJ, Lewis RD, et al. Muscularity and the density of the fat-free mass in athletes. J Appl Physiol 2001;90(4):1523-1531.

(62) Toomey CM, McCormack WG, Jakeman P. The effect of hydration status on the measurement of lean tissue mass by dual-energy X-ray absorptiometry. Eur J Appl Physiol 2017;117(3):567-574.

(63) Bone JL, Ross ML, Tomcik KA, Jeacocke NA, Hopkins WG, Burke LM. Manipulation of muscle creatine and glycogen changes dual X-ray absorptiometry estimates of body composition. Medicine & Science in Sports & Exercise 2017;49(5):1029-1035.

(64) Withers RT, Laforgia J, Heymsfield S. Critical appraisal of the estimation of body composition via two-, three-, and four-compartment models. American Journal of Human Biology: The Official Journal of the Human Biology Association 1999;11(2):175-185.

(65) Lohman T. Advance in body composition assessment. 2nd ed. Champaign, IL: Human Kinetics; 1992.

(66) Streat S, Beddoe A, Hill G. Measurement of body fat and hydration of the fat-free body in health and disease. Metab Clin Exp 1985;34(6):509-518.

(67) Heymsfield SB, Waki M, Kehayias J, Lichtman S, Dilmanian FA, Kamen Y, et al. Chemical and elemental analysis of humans in vivo using improved body composition models. Am J Physiol 1991 Aug;261(2 Pt 1):E190-8.

(68) Wang Z, Zhang J, Ying Z, Heymsfield SB. New insights into scaling of fat-free mass to height across children and adults. Am J Hum Biol 2012;24(5):648-653.

(69) Fuller NJ, Jebb SA, Laskey MA, Coward WA, Elia M. Four-component model for the assessment of body composition in humans: comparison with alternative methods, and evaluation of the density and hydration of fat-free mass. Clin Sci (Lond) 1992 Jun;82(6):687-693.

(70) Wang Z, Shen W, Withers R, Heymsfield S. Multicomponent molecular-level models of body composition analysis. In: Heymsfield S, Lohman T, Wang Z, Going S, editors. Human Body Composition: 2nd ed.
. 2nd ed. Champaign (IL): Human Kinetics; 2005. p. 163-176.

(71) Shen W, Wang Z, Punyanita M, Lei J, Sinav A, Kral JG, et al. Adipose tissue quantification by imaging methods: a proposed classification. Obes Res 2003;11(1):5-16.

(72) MacKenzie-Shalders K. Imaging Method: Computed Tomography And Magnetic Resonance Imaging. In: Hume P, Kerr D, Ackland T, editors. Best Practice Protocols for Physique Assessment in Sport. 1st ed.: Springer Singapore; 2017. p. 116-122.

(73) B. Heymsfield S, Wang Z, Baumgartner RN, Ross R. Human body composition: advances in models and methods. Annu Rev Nutr 1997;17(1):527-558.

(74) Runge V, Nitz W, Heverhagen J. The physics of clinical MR taught through images. 4th ed. New York: Thieme Publishers; 2018.

(75) Liang Z, Lauterbur PC. Principles of magnetic resonance imaging: a signal processing perspective. : SPIE Optical Engineering Press; 2000.

(76) Ross R, Goodpaster B, Kelley D, Boada F. Magnetic resonance imaging in human body composition research: from quantitative to qualitative tissue measurement. Ann N Y Acad Sci 2000;904(1):12-17.

(77) Kvist H, Sjostrom L, Tylen U. Adipose tissue volume determinations in women by computed tomography: technical considerations. Int J Obes 1986;10(1):53-67.

(78) Silver HJ, Welch EB, Avison MJ, Niswender KD. Imaging body composition in obesity and weight loss: challenges and opportunities. Diabetes Metab Syndr Obes 2010 Sep 28;3:337-347.

(79) Prado CM, Heymsfield SB. Lean tissue imaging: a new era for nutritional assessment and intervention. J Parenter Enteral Nutr 2014;38(8):940-953.

(80) Clarys J, Martin At, Drinkwater D. Gross tissue weights in the human body by cadaver dissection. Human biology 1984:459-473.

(81) Clarys JP, Martin AD, Marfell-Jones MJ, Janssens V, Caboor D, Drinkwater DT. Human body composition: A review of adult dissection data. American Journal of Human Biology: The Official Journal of the Human Biology Association 1999;11(2):167-174.

(82) Martin AD, Ross WD, Drinkwater DT, Clarys JP. Prediction of body fat by skinfold caliper: assumptions and cadaver evidence. Int J Obes 1985;9 Suppl 1:31-39.

(83) Clarys J, Provyn S, Marfell-Jones M. Cadaver studies and their impact on the understanding of human adiposity. Ergonomics 2005;48(11-14):1445-1461.

(84) Shepherd JA, Ng BK, Sommer MJ, Heymsfield SB. Body composition by DXA. Bone 2017;104:101-105.

(85) Lewiecki EM. Clinical applications of bone density testing for osteoporosis. Minerva Med 2005 Oct;96(5):317-330.

(86) Blake GM, Fogelman I. The clinical role of dual energy X-ray absorptiometry. Eur J Radiol 2009;71(3):406-414.

(87) Slater G, Nana A, Kerr A. Imaging Method: Dual-Energy X-Ray Absorptiometry. In: Hume P, Kerr D, Ackland T, editors. Best Practice Protocols for Physique Assessment in Sport. 1st ed.: Springer Singapore; 2017. p. 123-133.

(88) Neeland I, Grundy S, Li X, Adams-Huet B, Vega G. Comparison of visceral fat mass measurement by dual-X-ray absorptiometry and magnetic resonance imaging in a multiethnic cohort: the Dallas Heart Study. Nutrition & diabetes 2016;6(7):e221.

(89) Pietrobelli A, Formica C, Wang Z, Heymsfield SB. Dual-energy X-ray absorptiometry body composition model: review of physical concepts. Am J Physiol 1996 Dec;271(6 Pt 1):E941-51.

(90) Lands LC, Hornby L, Hohenkerk JM, Glorieux FH. Accuracy of measurements of small changes in soft-tissue mass by dual-energy x-ray absorptiometry. Clin Invest Med 1996 Aug;19(4):279-285.

(91) Roubenoff R, Kehayias JJ, Dawson-Hughes B, Heymsfield SB. Use of dual-energy x-ray absorptiometry in body-composition studies: not yet a “gold standard”. Am J Clin Nutr 1993;58(5):589-591.

(92) Tothill P, Hannan W, Wilkinson S. Comparisons between a pencil beam and two fan beam dual energy X-ray absorptiometers used for measuring total body bone and soft tissue. Br J Radiol 2001;74(878):166-176.

(93) Cross TM, Smart RC, Thomson JE. Exposure to diagnostic ionizing radiation in sports medicine: assessing and monitoring the risk. Clinical Journal of Sport Medicine 2003;13(3):164-170.

(94) Orchard JW, Read JW, Anderson I(F. 2. The use of diagnostic imaging in sports medicine. Med J Aust 2005;183(9):482-486.

(95) Deurenberg-Yap M, Schmidt G, van Staveren WA, Hautvast JG, Deurenberg P. Body fat measurement among Singaporean Chinese, Malays and Indians: a comparative study using a four-compartment model and different two-compartment models. Br J Nutr 2001;85(4):491-498.

(96) Withers RT, LaForgia J, Pillans R, Shipp N, Chatterton B, Schultz C, et al. Comparisons of two-, three-, and four-compartment models of body composition analysis in men and women. J Appl Physiol 1998;85(1):238-245.

(97) Van der Ploeg G, Withers R, Laforgia J. Percent body fat via DEXA: comparison with a four-compartment model. J Appl Physiol 2003;94(2):499-506.

(98) Stewart A, Hannan W. Prediction of fat and fat-free mass in male athletes using dual X-ray absorptiometry as the reference method. J Sports Sci 2000;18(4):263-274.

(99) Wang W, Wang Z, Faith MS, Kotler D, Shih R, Heymsfield SB. Regional skeletal muscle measurement: evaluation of new dual-energy X-ray absorptiometry model. J Appl Physiol 1999;87(3):1163-1171.

(100) Kim J, Wang Z, Heymsfield SB, Baumgartner RN, Gallagher D. Total-body skeletal muscle mass: estimation by a new dual-energy X-ray absorptiometry method. Am J Clin Nutr 2002;76(2):378-383.

(101) Going S. Hydrodensitometry and air displacement plethysmography. Human body composition 2005:17-33.

(102) Siri WE. The gross composition of the body. Advances in biological and medical physics: Elsevier; 1956. p. 239-280.

(103) Shaw G, Kerr A. Non-Imaging Method: Air Displacement Plethysmography (Bod Pod). In: Hume P, Kerr D, Ackland T, editors. Best Practice Protocols for Physique Assessment in Sport. 1st ed.: Springer Singapore; 2017. p. 79-87.

(104) Gnaedinger R, Reineke E, Pearson A, Van Huss W, Wessel JA, Montoye H. Determination of body density by air displacement, helium dilution, and underwater weighing. Ann N Y Acad Sci 1963;110(1):96-108.

(105) Dempster P, Aitkens S. A new air displacement method for the determination of human body composition. Med Sci Sports Exerc 1995 Dec;27(12):1692-1697.

(106) Peeters M, Claessens A. Effect of deviating clothing schemes on the accuracy of body composition measurements by air-displacement plethysmography. International Journal of Body Composition Research 2009;7(4).

(107) Anderson DE. Reliability of air displacement plethysmography. Journal of Strength and Conditioning Research 2007;21(1):169.

(108) Collins A, McCarthy H. Evaluation of factors determining the precision of body composition measurements by air displacement plethysmography. Eur J Clin Nutr 2003;57(6):770.

(109) Collins MA, Millard-Stafford ML, Evans EM, Snow TK, Cureton KJ, Rosskopf LB. Effect of race and musculoskeletal development on the accuracy of air plethysmography. Med Sci Sports Exerc 2004 Jun;36(6):1070-1077.

(110) Noreen EE, Lemon PW. Reliability of air displacement plethysmography in a large, heterogeneous sample. Med Sci Sports Exerc 2006 Aug;38(8):1505-1509.

(111) Tucker LA, Lecheminant JD, Bailey BW. Test-retest reliability of the Bod Pod: the effect of multiple assessments. Percept Mot Skills 2014;118(2):563-570.

(112) Vescovi JD, Zimmerman SL, Miller WC, Hildebrandt L, Hammer RL, Fernhall B. Evaluation of the BOD POD for estimating percentage body fat in a heterogeneous group of adult humans. Eur J Appl Physiol 2001;85(3-4):326-332.

(113) Wells J, Fuller N. Precision of measurement and body size in whole-body air-displacement plethysmography. Int J Obes 2001;25(8):1161.

(114) Ludwig UA, Klausmann F, Baumann S, Honal M, Hövener J, König D, et al. Whole-body MRI-based fat quantification: A comparison to air displacement plethysmography. Journal of Magnetic Resonance Imaging 2014;40(6):1437-1444.

(115) Collins MA, Millard-Stafford ML, Sparling PB, Snow TK, Rosskopf LB, Webb SA, et al. Evaluation of the BOD POD for assessing body fat in collegiate football players. Med Sci Sports Exerc 1999 Sep;31(9):1350-1356.

(116) Fields DA, Wilson GD, Gladden LB, Hunter GR, Pascoe DD, Goran MI. Comparison of the BOD POD with the four-compartment model in adult females. Medicine & Science in Sports & Exercise 2001;33(9):1605-1610.

(117) Millard-Stafford ML, Collins MA, Evans EM, Snow TK, Cureton KJ, Rosskopf LB. Use of air displacement plethysmography for estimating body fat in a four-component model. Med Sci Sports Exerc 2001 Aug;33(8):1311-1317.

(118) Biaggi RR, Vollman MW, Nies MA, Brener CE, Flakoll PJ, Levenhagen DK, et al. Comparison of air-displacement plethysmography with hydrostatic weighing and bioelectrical impedance analysis for the assessment of body composition in healthy adults. Am J Clin Nutr 1999;69(5):898-903.

(119) Vescovi JD, Hildebrandt L, Miller W, Hammer R, Spiller A. Evaluation of the BOD POD for estimating percent fat in female college athletes. The Journal of Strength & Conditioning Research 2002;16(4):599-605.

(120) Claros G, Hull HR, Fields DA. Comparison of air displacement plethysmography to hydrostatic weighing for estimating total body density in children. BMC pediatrics 2005;5(1):37.

(121) Davis JA, Dorado S, Keays KA, Reigel KA, Valencia KS, Pham PH. Reliability and validity of the lung volume measurement made by the BOD POD body composition system. Clinical physiology and functional imaging 2007;27(1):42-46.

(122) Blew R, Sardinha L, Milliken LA:. Body Composition Laboratory Methods. In: ACSM., Lohman T, Milliken L, editors. ACSM´s Body Composition Assessment. 1st ed. Champaign IL: Human Kinetics; 2019. p. 31-58.

(123) Bender DA, Bender AE. Nutrition: a reference handbook. : Oxford university press; 1997.

(124) Institute of Medicine (US). Panel on Dietary Reference Intakes for Electrolytes, Water. DRI, dietary reference intakes for water, potassium, sodium, chloride, and sulfate. : National Academy Press; 2005.

(125) Rush E. Non-Imaging Method: Doubly-Labelled Water. In: Hume P, Kerr D, Ackland T, editors. Best Practice Protocols for Physique Assessment in Sport. 1st ed.: Springer Singapore; 2017. p. 100-107.

(126) Ellis KJ. Human body composition: in vivo methods. Physiol Rev 2000;80(2):649-680.

(127) Schoeller A. Hydrometry. In: Heymsfield S, Lohman T, Wang Z, Going S, editors. Human Body Composition: 2nd ed.
. 2nd ed. Champaign (IL): Human Kinetics; 2005. p. 35-49.

(128) Measurement of total body water: isotope dilution techniques. Ross Conference on Medical Research; 1985.

(129) Speakman JR, Nair KS, Goran MI. Revised equations for calculating CO2 production from doubly labeled water in humans. Am J Physiol 1993 Jun;264(6 Pt 1):E912-7.

(130) Racette SB, Schoeller DA, Luke AH, Shay K, Hnilicka J, Kushner RF. Relative dilution spaces of 2H- and 18O-labeled water in humans. Am J Physiol 1994 Oct;267(4 Pt 1):E585-90.

(131) Njoku C, Stewart A, Hume P, Kolose S. Non Imaging Method: 3D Scanning. In: Hume P, Kerr D, Ackland T, editors. Best Practice Protocols for Physique Assessment in Sport. 1st ed.: Springer Singapore; 2017. p. 70-78.

(132) Rogers M, Olds T. 3D anthropometry-applications to health and exercise science. Sport Health 2004;22(3):21.

(133) Wells JC, Treleaven P, Cole TJ. BMI compared with 3-dimensional body shape: the UK National Sizing Survey. Am J Clin Nutr 2007;85(2):419-425.

(134) Wells JC, Cole TJ, Treleaven P. Age-variability in body shape associated with excess weight: the UK National Sizing Survey. Obesity 2008;16(2):435-441.

(135) Wells J, Cole T, Bruner D, Treleaven P. Body shape in American and British adults: between-country and inter-ethnic comparisons. Int J Obes 2008;32(1):152.

(136) Wang J, Gallagher D, Thornton JC, Yu W, Horlick M, Pi-Sunyer FX. Validation of a 3-dimensional photonic scanner for the measurement of body volumes, dimensions, and percentage body fat. Am J Clin Nutr 2006;83(4):809-816.

(137) Ryder J, Ball S. Three-dimensional body scanning as a novel technique for body composition assessment: A preliminary investigation. Journal of Exercise Physiologyonline 2012;15(1).

(138) Matiegka J. The testing of physical efficiency. Am J Phys Anthropol 1921;4(3):223-230.

(139) Lohman TG, Roche AF, Martorell R. Anthropometric standardization reference manual. : Human kinetics books; 1988.

(140) Brandon L, Milliken L, Blew R, Lohman T. Body Composition Field Methods. In: ACSM., Lohman T, Milliken L, editors. ACSM´s Body Composition Assessment. 1st ed. Champaign IL: Human Kinetics; 2019. p. 59-89.

(141) Marfell-Jones MJ, Stewart A, De Ridder J. International standards for anthropometric assessment. ; 2012.

(142) Hume P, Sheerin K, Hans de Ridder J. Non Imaging Method: Surface Anthropometry. In: Hume P, Kerr D, Ackland T, editors. Best Practice Protocols for Physique Assessment in Sport. 1st ed.: Springer Singapore; 2017. p. 64-69.

(143) Hume P, Marfell-Jones M. The importance of accurate site location for skinfold measurement. J Sports Sci 2008;26(12):1333-1340.

(144) Lohman TG. Skinfolds and body density and their relation to body fatness: a review. Human biology 1981;53(2):181.

(145) Sinning WE, Wilson JR. Validity of “generalized” equations for body composition analysis in women athletes. Res Q Exerc Sport 1984;55(2):153-160.

(146) Sinning WE, Dolny DG, Little KD, Cunningham LN, Racaniello A, Siconolfi SF, et al. Validity of "generalized" equations for body composition analysis in male athletes. Med Sci Sports Exerc 1985 Feb;17(1):124-130.

(147) Durnin JV, Womersley J. Body fat assessed from total body density and its estimation from skinfold thickness: measurements on 481 men and women aged from 16 to 72 years. Br J Nutr 1974;32(1):77-97.

(148) Jackson AS, Pollock ML. Generalized equations for predicting body density of men. Br J Nutr 1978;40(3):497-504.

(149) Jackson AS, Pollock ML, Ward A. Generalized equations for predicting body density of women. Med Sci Sports Exerc 1980;12(3):175-181.

(150) Kerr D, Stewart A. Body composition in sport. Applied Anatomy and Biomechanics in Sports.Edit: Ackland TR., Elliott BC., Bloomfield, J 2009;2:67-81.

(151) Wang J, Thornton J, Kolesnik S, Pierson Jr R. Anthropometry in body composition: an overview. Ann N Y Acad Sci 2000;904(1):317-326.

(152) Lyra CO, Lima, Severina Carla Vieira Cunha, Lima KC, Arrais RF, Pedrosa LFC. Prediction equations for fat and fat-free body mass in adolescents, based on body circumferences. Ann Hum Biol 2012;39(4):275-280.

(153) Friedl KE, Westphal KA, Marchitelli LJ, Patton JF, Chumlea WC, Guo SS. Evaluation of anthropometric equations to assess body-composition changes in young women. Am J Clin Nutr 2001;73(2):268-275.

(154) Thorland WG, Tipton CM, Lohman TG, Bowers RW, Housh TJ, Johnson GO, et al. Midwest wrestling study: prediction of minimal weight for high school wrestlers. Med Sci Sports Exerc 1991 Sep;23(9):1102-1110.

(155) Brambilla P, Bedogni G, Moreno L, Goran M, Gutin B, Fox K, et al. Crossvalidation of anthropometry against magnetic resonance imaging for the assessment of visceral and subcutaneous adipose tissue in children. Int J Obes 2006;30(1):23.

(156) Bouchard C. BMI, fat mass, abdominal adiposity and visceral fat: where is the 'beef'? Int J Obes 2007;31(10):1552.

(157) Van Der Kooy K, Leenen R, Seidell JC, Deurenberg P, Visser M. Abdominal diameters as indicators of visceral fat: comparison between magnetic resonance imaging and anthropometry. Br J Nutr 1993;70(1):47-58.

(158) Valsamakis G, Chetty R, Anwar A, Banerjee A, Barnett A, Kumar S. Association of simple anthropometric measures of obesity with visceral fat and the metabolic syndrome in male Caucasian and Indo-Asian subjects. Diabetic Med 2004;21(12):1339-1345.

(159) Iribarren C, Darbinian JA, Lo JC, Fireman BH, Go AS. Value of the sagittal abdominal diameter in coronary heart disease risk assessment: cohort study in a large, multiethnic population. Am J Epidemiol 2006;164(12):1150-1159.

(160) Stewart A, Nevill A, Johnstone A. Shape change assessed by 3D laser scanning following weight loss in obese men. Kinanthropometry XI 2008:20-24.

(161) Kerr A, Hume P. Non Imaging Method: Bioelectrical Impedance Analysis. In: Hume P, Kerr D, Ackland T, editors. Best Practice Protocols for Physique Assessment in Sport. 1st ed.: Springer Singapore; 2017. p. 88-99.

(162) Chumlea W, Sun S. Bioelectrical impedance analysis. In: Heymsfield S, Lohman T, Wang Z, Going S, editors. Human Body Composition: 2nd ed.
. 2nd ed. Champaign (IL): Human Kinetics; 2005. p. 79-87.

(163) Kerr A, Slater G, Byrne N, Chaseling J. Validation of bioelectrical impedance spectroscopy to measure total body water in resistance-trained males. Int J Sport Nutr Exerc Metab 2015;25(5):494-503.

(164) Moon JR, Tobkin SE, Roberts MD, Dalbo VJ, Kerksick CM, Bemben MG, et al. Total body water estimations in healthy men and women using bioimpedance spectroscopy: a deuterium oxide comparison. Nutrition & Metabolism 2008;5(1):7.

(165) Rodriguez-Sanchez N, Galloway SD. Errors in dual energy x-ray absorptiometry estimation of body composition induced by hypohydration. Int J Sport Nutr Exerc Metab 2015;25(1):60-68.

(166) O'brien C, Young A, Sawka M. Bioelectrical impedance to estimate changes in hydration status. Int J Sports Med 2002;23(05):361-366.

(167) Heiss CJ, Gara N, Novotny D, Heberle H, Morgan L, Stufflebeam J, et al. EFFECT OF A 1 LITER FLUID LOAD ON BODY COMPOSITION MEASURED BY AIR DISPLACEMENT PLETHYSMOGRAPHY AND BIOELECTRICAL IMPEDANCE. Journal of Exercise Physiology Online 2009;12(2).

(168) Saunders MJ, Blevins JE, Broeder CE. Effects of hydration changes on bioelectrical impedance in endurance trained individuals. Med Sci Sports Exerc 1998 Jun;30(6):885-892.

(169) Kyle UG, Bosaeus I, De Lorenzo AD, Deurenberg P, Elia M, Gómez JM, et al. Bioelectrical impedance analysis—part II: utilization in clinical practice. Clinical nutrition 2004;23(6):1430-1453.

(170) Bosy-Westphal A, Later W, Hitze B, Sato T, Kossel E, Gluer CC, et al. Accuracy of bioelectrical impedance consumer devices for measurement of body composition in comparison to whole body magnetic resonance imaging and dual X-ray absorptiometry. Obes Facts 2008;1(6):319-324.

(171) Buchholz AC, Bartok C, Schoeller DA. The validity of bioelectrical impedance models in clinical populations. Nutrition in clinical practice 2004;19(5):433-446.

(172) World Health Organization. Physical status: the use and interpretation of anthropometry. Report of a WHO Expert Committee. World Health Organ Tech Rep Ser 1995;854:1-452.

(173) Nevill AM, Winter EM, Ingham S, Watts A, Metsios GS, Stewart AD. Adjusting athletes' body mass index to better reflect adiposity in epidemiological research. J Sports Sci 2010;28(9):1009-1016.

(174) Müller W. Determinants of ski-jump performance and implications for health, safety and fairness. Sports medicine 2009;39(2):85-106.

(175) Sengeis M, Müller W, Störchle P, Fürhapter-Rieger A. Body weight and subcutaneous fat patterning in elite judokas. Scand J Sports Med. 2019;29(11):1774-1788.

(176) Bullen BA, Quaade F, Olessen E, Lund SA. Ultrasonic reflections used for measuring subcutaneous fat in humans. Hum Biol 1965 Dec;37(4):375-384.

(177) Booth RA, Goddard BA, Paton A. Measurement of fat thickness in man: a comparison of ultrasound, Harpenden calipers and electrical conductivity. Br J Nutr 1966;20(4):719-725.

(178) Bellisari A, Roche AF. Anthropometry and ultrasound. In: Heymsfield S, Lohman T, Wang Z, Going S, editors. Human Body Composition: 2nd ed.
. 2nd ed. Champaign (IL): Human Kinetics; 2005. p. 109-127.

(179) Hawes S, Albert A, Healy M, Garrow J. A comparison of soft-tissue radiography, reflected ultrasound, skinfold calipers and thigh circumference for estimating the thickness of fat overlying the lliac crest and grater trochanter. Proc Nutr Soc 1972;31:91-92.

(180) Pineau J, Filliard JR, Bocquet M. Ultrasound techniques applied to body fat measurement in male and female athletes. Journal of athletic training 2009;44(2):142-147.

(181) Pineau JC, Guihard-Costa AM, Bocquet M. Validation of ultrasound techniques applied to body fat measurement. A comparison between ultrasound techniques, air displacement plethysmography and bioelectrical impedance vs. dual-energy X-ray absorptiometry. Ann Nutr Metab 2007;51(5):421-427.

(182) Stolk R, Wink O, Zelissen P, Meijer R, Van Gils A, Grobbee D. Validity and reproducibility of ultrasonography for the measurement of intra-abdominal adipose tissue. Int J Obes 2001;25(9):1346.

(183) Wagner DR. Ultrasound as a tool to assess body fat. Journal of obesity 2013;2013.

(184) Weiss LW, Clark FC. The use of B-mode ultrasound for measuring subcutaneous fat thickness on the upper arms. Res Q Exerc Sport 1985;56(1):77-81.

(185) Johnson KE, Miller B, Juvancic-Heltzel JA, Agnor SE, Kiger DL, Kappler RM, et al. Agreement between ultrasound and dual-energy X-ray absorptiometry in assessing percentage body fat in college-aged adults. Clinical physiology and functional imaging 2014;34(6):493-496.

(186) Loenneke JP, Barnes JT, Wagganer JD, Wilson JM, Lowery RP, Green CE, et al. Validity and reliability of an ultrasound system for estimating adipose tissue. Clinical physiology and functional imaging 2014;34(2):159-162.

(187) Selkow NM, Pietrosimone BG, Saliba SA. Subcutaneous thigh fat assessment: a comparison of skinfold calipers and ultrasound imaging. Journal of athletic training 2011;46(1):50-54.

(188) Smith-Ryan AE, Fultz SN, Melvin MN, Wingfield HL, Woessner MN. Reproducibility and validity of A-mode ultrasound for body composition measurement and classification in overweight and obese men and women. PloS one 2014;9(3):e91750.

(189) Wagner DR, Cain DL, Clark NW. Validity and reliability of A-mode ultrasound for body composition assessment of NCAA division I athletes. PloS one 2016;11(4):e0153146.

(190) Ackland T, Müller W. Imaging Method: Ultrasound. In: Hume P, Kerr D, Ackland T, editors. Best Practice Protocols for Physique Assessment in Sport. 1st ed.: Springer Singapore; 2017. p. 108-115.

(191) Müller W, Horn M, Fürhapter-Rieger A, Kainz P, Kröpfl JM, Ackland TR, et al. Body composition in sport: interobserver reliability of a novel ultrasound measure of subcutaneous fat tissue. Br J Sports Med 2013 Nov;47(16):1036-1043.

(192) Müller W, Lohman TG, Stewart AD, Maughan RJ, Meyer NL, Sardinha LB, et al. Subcutaneous fat patterning in athletes: selection of appropriate sites and standardisation of a novel ultrasound measurement technique: ad hoc working group on body composition, health and performance, under the auspices of the IOC Medical Commission. Br J Sports Med 2016 Jan;50(1):45-54.

(193) Toomey C, McCreesh K, Leahy S, Jakeman P. Technical considerations for accurate measurement of subcutaneous adipose tissue thickness using B-mode ultrasound. Ultrasound 2011;19(2):91-96.

(194) Müller W, Horn M, Fürhapter-Rieger A, Kainz P, Kröpfl JM, Maughan RJ, et al. Body composition in sport: a comparison of a novel ultrasound imaging technique to measure subcutaneous fat tissue compared with skinfold measurement. Br J Sports Med 2013 Nov;47(16):1028-1035.

(195) Towards an accurate determination of subcutaneous adipose tissue by means of ultrasound. 6th World Congress of Biomechanics. Singapore; 2010.

(196) Kelso A, Vogel K, Steinacker JM. Ultrasound measurements of subcutaneous adipose tissue thickness show sexual dimorphism in children of three to five years of age. Acta Paediatrica 2019;108(3):514-521.

(197) Kelso A, Müller W, Sengeis M, Fürhapter-Rieger A. Inter-observer reliability in standardised ultrasound measurements of subcutaneous adipose tissue in children. submitted.

(198) Kelso A, Trájer E, Machus K, Treff G, Müller W, Steinacker JM. Assessment of subcutaneous adipose tissue using ultrasound in highly trained junior rowers. European journal of sport science 2017;17(5):576-585.

(199) Sengeis M, Müller W, Störchle P, Fürhapter-Rieger A. Ultrasound technique: A new approach for measuring subcutaneous adipose tissue in endurance athletes. Sports Orthopaedics and Traumatology 2018;34(2):165-166.

(200) Störchle P, Sengeis M, Müller W. Differences in fat patterning between lean and overweight persons. Ernährung aktuell Informationsdienst der Österreichischen Gesellschaft für Ernährung. 2016;4:28.

(201) Ashwell M, Gunn P, Gibson S. Waist-to-height ratio is a better screening tool than waist circumference and BMI for adult cardiometabolic risk factors: systematic review and meta-analysis. Obesity reviews 2012;13(3):275-286.

(202) Stewart A, Marfell-Jones M, Olds T, De Ridder J. International standards for anthropometric assessment. Lower Hutt, New Zealand; 2011.

(203) Sumner EE, Whitacre J. Some Factors affecting accuracy in the collection of data on the Growth in Weight of School Children. J Nutr 1931;4(1):15-23.

(204) Circadian variation in effects of weight-training on spinal shrinkage. Proc Brit Assoc Sport Med Ann Conf; 1985.

(205) Reilly T, Tyrrell A, Troup J. Orcadian variation in human stature. Chronobiol Int 1984;1(2):121-126.

(206) Herman IP. Physics of the Human Body. 1st ed. Berlin: Springer Science & Business Media; 2007.

(207) Lund CC, Browder NC. The estimation of areas of burns. Surg Gynecol Obstet 1944;79:352-358.

(208) Bland JM, Altman D. Statistical methods for assessing agreement between two methods of clinical measurement. The lancet 1986;327(8476):307-310.

(209) Cohen J. Statistical power analysis for the behavioral sciences. : Routledge; 2013.

(210) Du Bois D, Du Bois EF. A formula to estimate the approximate surface area if height and weight are known. Arch Intern Med 1916(17):863-871.

(211) Haycock GB, Schwartz GJ, Wisotsky DH. Geometric method for measuring body surface area: a height-weight formula validated in infants, children, and adults. J Pediatr 1978;93(1):62-66.

(212) Mosteller RD. Simplified calculation of body-surface area. N Engl J Med 1987 Oct 22;317(17):1098.

(213) Thomas DM, Bredlau C, Bosy-Westphal A, Mueller M, Shen W, Gallagher D, et al. Relationships between body roundness with body fat and visceral adipose tissue emerging from a new geometrical model. Obesity 2013;21(11):2264-2271.

(214) Störchle P, Sengeis M, Müller W. FAT patterning differences in male and female persons: Application of a highly accurate and precise ultrasound technique. . Book of Abstracts of the 21th Annual Congress of the European College of Sport Science 2016:540.

(215) Marfell-Jones M, Nevill A, Stewart AD. Anthropometric surrogates for fatness and health. Body composition in sport, exercise and health 2012:124-146.

(216) Van Mulder T, de Koeijer M, Theeten H, Willems D, Van Damme P, Demolder M, et al. High frequency ultrasound to assess skin thickness in healthy adults. Vaccine 2017;35(14):1810-1815.

(217) Gibney MA, Arce CH, Byron KJ, Hirsch LJ. Skin and subcutaneous adipose layer thickness in adults with diabetes at sites used for insulin injections: implications for needle length recommendations. Curr Med Res Opin 2010;26(6):1519-1530.

(218) Laurent A, Mistretta F, Bottigioli D, Dahel K, Goujon C, Nicolas JF, et al. Echographic measurement of skin thickness in adults by high frequency ultrasound to assess the appropriate microneedle length for intradermal delivery of vaccines. Vaccine 2007;25(34):6423-6430.

(219) Escoffier C, de Rigal J, Rochefort A, Vasselet R, Léveˆque J, Agache PG. Age-related mechanical properties of human skin: an in vivo study. J Invest Dermatol 1989;93(3):353-357.

(220) Derraik JG, Rademaker M, Cutfield WS, Pinto TE, Tregurtha S, Faherty A, et al. Effects of age, gender, BMI, and anatomical site on skin thickness in children and adults with diabetes. PLoS One 2014;9(1):e86637.

(221) Nattiv A, Loucks A, Manore M, Sanborn C, Sundgot-Borgen J, Warren M. American College of Sports Medicine position stand: The female athlete triad. Med Sci Sports Exerc 2007;39(10):1867-1882.

(222) Ibrahim MM. Subcutaneous and visceral adipose tissue: structural and functional differences. Obes Rev 2010 Jan;11(1):11-18.

(223) Sengeis M, Müller W, Störchle P, Fürhapter-Rieger A. Competitive performance of Kenyan long-distance runners compared to their relative body weight and subcutaneous fat. in review.

(224) Vague J. The degree of masculine differentiation of obesities: a factor determining predisposition to diabetes, atherosclerosis, gout, and uric calculous disease. Am J Clin Nutr 1956;4(1):20-34.

(225) Shen W, Punyanitya M, Silva AM, Chen J, Gallagher D, Sardinha LB, et al. Sexual dimorphism of adipose tissue distribution across the lifespan: a cross-sectional whole-body magnetic resonance imaging study. Nutrition & metabolism 2009;6(1):17.

(226) Ashwell M, Gunn P, Gibson S. Waist-to-height ratio is a better screening tool than waist circumference and BMI for adult cardiometabolic risk factors: systematic review and meta-analysis. Obes Rev 2012 Mar;13(3):275-286.

(227) Arner P. Regional adipocity in man. J Endocrinol 1997 Nov;155(2):191-192.

(228) Stoner L, Chinn V, Cornwall J, Meikle G, Page R, Lambrick D, et al. Reliability tests and guidelines for B-mode ultrasound assessment of central adiposity. Eur J Clin Invest 2015 Nov;45(11):1200-1208.

(229) Wajchenberg BL. Subcutaneous and visceral adipose tissue: their relation to the metabolic syndrome. Endocr Rev 2000 Dec;21(6):697-738.